Pan-European flood hazard and damage assessment;

evaluation of a new If-SAR Digital Terrain Model for flood depth and flood extent calculation

Marco Rusmini

March, 2009

Pan-European flood hazard and damage assessment; evaluation of a new If-SAR Digital Terrain Model for flood depth and flood extent calculation

by

Marco Rusmini

Thesis submitted to the International Institute for Geo-information Science and Earth Observation in partial fulfilment of the requirements for the degree of Master of Science in Geo-information Science and Earth Observation, Specialisation: Geo-hazards

Thesis Assessment Board

Prof. Dr. V. G. Jetten (Chair and 2nd Supervisor)
Dr. T. W. J. van Asch (External Examiner)
Dr. D. Alkema (1st Supervisor)
Observer: Drs. T. Loran (Course Director)

INTERNATIONAL INSTITUTE FOR GEO-INFORMATION SCIENCE AND EARTH OBSERVATION
ENSCHEDE, THE NETHERLANDS

"Volli, e sempre volli,

e fortissimamente volli"

Disclaimer

This document describes work undertaken as part of a programme of study at the International Institute for Geo-information Science and Earth Observation. All views and opinions expressed therein remain the sole responsibility of the author, and do not necessarily represent those of the institute.

Abstract

The European Flood Alert System (EFAS) aims at increasing preparedness of river floods in trans-national European catchments, by providing local water authorities with medium range probabilistic forecasting information three to ten days in advance. The flood simulation is performed by LISFLOOD, a hybrid between a conceptual and physical rainfall‐runoff model.

Within the EFAS Project, rivers discharges for a 100 years return period flood event have been calculated with this model based on historical rainfall data, in order to provide the European Commission with a potential flood damage assessment at a European scale.

The aim of this study is to assess and improve the accuracy in calculating the water extent and depth in flooded areas.

In the study area, the Po river catchment in Italy, the planar approximation approach was applied in extracting flood extent and depth: the discharges were translated into water levels; the flood wave was considered as a plane, and it was intersected with a 100m resolution SRTM DEM. A comparison with a local detailed flood modeling study (Mike 11 model) showed significantly different estimations of the flooded areas, due to the low accuracy of the DEM itself, and the absence of information about the defense measures. Therefore the results were corrected with: 1) the introduction of protection structures, 2) the overall planar approximation method implementation with a new 5m resolution IF-SAR digital terrain model.

The introduction of the defences improved the results based on the SRTM DEM and pointed out new sources of inaccuracy in other input maps, like the CCM (Catchments Characterization and Modelling) river network dataset used in the calculation.

The new DTM showed reasonable results compared to the local hazard assessment (coincidence higher than 80%); moreover it well represents the defence measures, so that there is no need to include them separately in the procedure. The damage assessment was performed based on stage damage functions and the CORINE land use dataset, to better evaluate the improvement obtained. The potential damage calculation showed more precise estimations for the most critical areas.

Finally the results achieved with the SRTM DEM can't be deemed as satisfactory, even considering the large scale of application; but it still represents the only available elevation dataset at pan-European level so far. Hence, the acquisition of more accurate terrain models seems to be essential in the calculation of pan-European damage assessment.

Acknowledgements

My thanks go firstly to the supervisor of this thesis, Dr. Dinand Alkema, for having put all his effort in the organization of this research, and moreover for the help in the scientific field and not only.
A special acknowledgment goes to Dr. Ad de Roo, NaHa (Natural Hazard) action leader (Institute for Environment and Sustainability, JRC) for having accepted me in his team. He assisted me in the fulfilment of the study by providing data and support. He drove me in understanding the subject and he supervised both the writing and the analysis part. Thanks also to his entire staff: Josè Barredo for his patience and the knowledge in the field of loss estimation; Peter Salamon for the assistance in PCRaster procedures; Rugter Dankers I wish him all the best in his new adventure; Hadewij Sint for the funny times during lunches, Jutta Theilen, Katalin Bodis, Mauro del Medico, Davaide Muraro and all the others.
Thanks to the entire staff of the "*Autorità di Bacino del Fiume Po"* for the provision of the project on hazard assessment used as reference in this study; in particular I want to mention Ing. Piero Tabellini, and Ing. Luciano Chionna.
I want to acknowledge all the AES staff and in general the entire ITC family for this wonderful and unique experience. I want to thank them for having had the possibility to be part of the SAB in the last year.
Thank to all the new friend I found here, for the support during the long study days and the nights...

...ma il ringraziamento più grande va a voi, Mamma Andrea e Silvia.
Mamma mi hai sopportato sempre, anche in questi ultimi giorni in cui ero intrattabile, sapevi prima di me che ce l'avrei fatta un giorno; spero tu sia felice e spero che tu continui ad esserlo per lungo tempo; sei la donna più forte che abbia mai incontrato. Penso che tutto questo sia proprio merito tuo.
Andrea è anche grazie a te che sono riuscito a realizzare un sogno, non ti ringrazierò mai a sufficienza. Ti auguro di essere felice e di avere tutto il successo che ti meriti. Hai fatto cose che pochi riescono solo a pensare; voglio che tu ne sia consapevole.
Silvia, compagna mia, sei stata la mia spalla per tutta questa strada, e finalmente ce l'ho fatta, grazie per avermelo fatto notare quando non ci credevo. Spero di restitutirti un po' della forza che mi hai dato, spero di essere alla tua altezza.

In fine il mio pensiero va sempre a te, che non ci sei più. Non sai quanto mi fa male non poterti consegnare tra le mani questi fogli imbrattati di inchiostro; mi consolo con il fatto che saresti stato più felice di me. Ti voglio bene, sempre.

Table of contents

List of figures

List of tables

List of Abbreviations

ADBPO: Autorità di Bacino del fiume Po (Po Basin Authority)
CCM: Catchment Characterization and Modelling, Rivers and Catchments database v.1 2003
CCM2: Catchment Characterization and Modelling, Rivers and Catchments database v.1 2007
CMRWF: Centre of Medium Range Weather Forecasts
CLC: CORINE Land Cover
DEM: Digital Elevation Model
DSM: Digital Surface Model
DTM: Digital Terrain Model
DSM: Digital Surface Model
DWD: Deutche Wetterdienst
EFAS: European Flood Alert System
EFFS: European Flood Forecast System
ETRS-LAEA: European Terrestrial Reference System – Lambert Azimuthal Equal Area
IES: Institute for Environment and Sustainability
LMNH: Land Management and Natural Hazards (unit)
NUTS/LAU: Nomenclature of Territorial Units for Statistics/Land Administrative Units
PPP: Purchasing Power Parity
SRTM: Shuttle Radar Tomography Mission
JRC: Join Research Centre
JRC-MARS: Meteorological Archival and Retrieval System

1. Introduction

1.1. Floods in Europe

Every year floods cause enormous damage all over the world. In the last decade of the 20th century, floods killed about 100,000 persons and affected over 1.4 billion people (Jonkman, 2005). Considering only Europe, river flooding has been recently recognized as a major hazard, in particular after the 1997 Odra /Oder flood, the 1994 and 2002 Po floods, the 2001 Vistula flood, and the most destructive 2002 inundation on the Labe/Elbe. According to the report of Munich-Re (2003), the series of floods in August of 2002, alone, caused in Europe damage at the level exceeding 15 billion Euro (9.2 in Germany, and 3 each in Austria and in the Czech Republic) (Kundzewicz et al., 2005). It has been observed that flood risk and vulnerability is likely to have grown in many areas. The triggering factors have to be found into the direct or indirect impact of the increasing human activities. Kundzewicz suggests three possible sources of the increase in flood risk and vulnerability in Europe:

1. Changes in terrestrial systems (hydrological systems and ecosystems; land-cover change, river regulation, channel straightening, embankments, changes of conditions of transformation of precipitation into runoff leading to a higher peak and shorter time to peak).
2. Changes in socio-economic systems (increasing exposure and damage potential: floodplain development, growing wealth in flood-prone areas, land-use change like urbanization, deforestation, elimination of natural inundation areas (wetlands, floodplains causing land-cover changes in terrestrial systems), changing risk perception).
3. Changes in climate (holding capacity of the atmosphere, intense precipitation, seasonality, circulation patterns).

The term flood includes different events. The primary differences among flood types are established considering the size of the affected areas, the duration and intensity of the triggering precipitations. Based on these, three main different flooding events are generally recognized (Barredo, 2007; Jonkman, 2005; Perry, 2000):

1. River floods are the result of intense and/or persistent rain for several days or even weeks over large areas. River floods are usually the combination of several factors in a given region i.e. weather and soils conditions, measures for flood protection, land use, etc. In Europe, this type of flood can also be related to seasonal regimes. The warning time is higher and the water rising time is lower than flash floods; the flood extent and duration are related to the morphological parameters of the area.

2. Flash floods are mostly local events and scattered in time and space. They are the result of intense rainfall over a small area within a short period of time, usually less than 6 h, causing water to rise and fall quite rapidly. ‘‘Severe rainfall on the flood location may be used as indicator for this type of flood’’ (Jonkman, 2005). They mainly affect areas with moderate to high slope gradient.
3. Storm/surge coastal floods are rare events, but they do have huge loss potential for lives and properties. This type of flood is water that is pushed onto dry land by onshore winds/ storms. It can occur on the coast of seas and big lakes (Perry, 2000). The triggering factors of this event are slightly different from the ones previously described; more important are atmospheric conditions like the wind speed and direction or the sea currents rather than the precipitation pattern. Nowadays the coastal floods are studied in the prospective of the sea level rise, as it will enormously increase the population affected (Nicholls, 2002).

Not included into this classification, others events with different characteristics belong to the definition of flood; e.g. ice-jam floods; dam and levee failure floods; debris, landslide, and mudflow floods (Perry, 2000). The project described below refers only to river floods at a continental scale.

A need of more effort in prevention and mitigation against inundations is enhanced by the future scenarios regarding the two main triggering factors: the increase of the population and the change in the distribution and intensity of meteorological events. The present world population of 6.5 billion is projected by the United Nations to increase to 9 billion and may eventually reach as many as 11 billion by 2050 (Pimentel and Pimentel, 2006); the new comers will occupy the land still available, which are more likely to be prone to natural hazards. On the other hand, the climate change will have strong impact on flood hazard in the following decades. The dependency of rainfall intensity and frequency, hence floods, from climate change has been proved after several debates in the last years (Axel, 2003; Mitchell, 2003; Muzik, 2002). Higher intensity rainfall events will probably occur also in areas that show a tendency toward drier conditions, as rainfalls will be distributed into more intense events separated by longer dry periods (Christensen and Christensen, 2004). Simulations at global and regional scale revealed an increase in annual precipitation in the northern Europe, and a decrease in the Mediterranean regions; in Central Europe the precipitation is expected to be higher in winter and lower in summer (Christensen and Christensen, 2007). Extreme events are expected to increase either in frequency and intensity especially in the North and also in the southern Europe, in winter months. Simulations driven by both A2 and B2 SRES (Special Report on Emission Scenarios) scenarios show that, in many rivers in Europe extreme discharge events are likely to increase in intensity and frequency, while the variation of discharge of other rivers will decrease the flood hazard. Especially in Eastern Europe, an event with a return period of 100 years will most likely double the occurrence probability, becoming a 50 years return period flood event (Dankers and Feyen, 2008).

1.2. History of EFAS

Due to the increase of floods risk and vulnerability, more tools to study and predict occurrence and behaviour of these phenomena are needed. As mentioned before, floods are triggered by precipitation with exceptional intensity and/or duration; therefore the first critical aspect in flood forecasting is the availability of reliable weather forecasting information. During the last 20 years many advances in weather prediction added new input data for flood forecast, like probabilistic weather forecasts based on ensemble prediction systems (Kimura, 2002; Leutbecher and Palmer, 2008). The first flood prediction project started in United States in the Eighties, developed by the National Weather Service (NWS) of the National Oceanic and Atmospheric Administration (NOAA). The project called Advanced Hydrologic Prediction Service (AHPS) provides flood forecasting punctual information at more than 7000 measurement stations spread all over the country, based on real-time observations of the rivers' hydrologic conditions in the stations themselves, combined with weather predictions based on remote sensed data from radar and thermal infrared sensors (AHPS, 2006; Austin, 2002).

The disasters that occurred during the last decades in Europe drove the European Union to invest funding in developing the first European Flood Forecasting System (EFFS, 1999-2003); a research project under the 5th Framework Programme of the European Commission developed by the team of the Land Management and Natural Hazards unit of the Institute for Environment and Sustainability (IES–Join Research Centre, Ispra Italy: http://ies.jrc.ec.europa.eu/index.php?page=home) with the help of 19 partners from meteorological and hydrological services, research institutes and operational services (De Roo et al., 2003; Kwadijk, 2003). The EFFS prototype consisted of the following four components integrated in a generic modelling framework based on the LISFLOOD suite of raster-based hydrology and hydraulic codes (De Roo et al., 2000):

1. global Numerical Weather Prediction models;
2. optional downscaling of global precipitation using a regional Numerical Weather Prediction model;
3. a catchment hydrology model comprising a soil water balance model with daily time step and a flood simulation model with hourly time step;
4. a high-resolution flood inundation model.

The EFFS project was the basis for a more advanced prototype. In 2003 The European Commission Join Research Centre (JRC) delivered founding for the development of the European Flood Alert System (EFAS) with the aim of simulating hydrological processes in trans-national river basins, and providing harmonized flood information across Europe. The first objective of EFAS is to complement Member States activities on flood preparedness, and provide National hydrological services with medium-range flood forecasting information, earlier than the local monitoring systems which are mostly based on short-range forecasts (Thielen et al., 2006). The probabilistic flood forecasting information with a lead-time up to 10 days represents for the end users a pre-alert for their forecast

systems; moreover EFAS aims at giving downstream National and local authorities an overview of the current and forecasted flood situation in upstream and neighboring countries. In this scenario, catchment-based data, beyond administrative boundaries, resulting from EFAS model can be useful for comparison with local simulations. Secondly, EFAS aims to provide the European Commission with an overview of ongoing and expected floods in Europe, useful for crisis management in case of large trans-national flood events that might need intervention on an international scale (Thielen et al., 2008). Finally, at the state of the art of hydrological modeling, EFAS represents the only hydrologic simulation at pan-European scale, therefore, secondary outputs, like simulations of flood events with different occurrence probability, acted as input for scenario studies on the following topics:

- climate change impact on flood hazard at European scale (Dankers and Feyen, 2008): the EFAS model outputs have been applied to assess the changes in flood occurrence based on different scenarios from HICRAM climate change model within the framework of PRUDENCE project (Christensen and Christensen, 2007)
- flood damage potential in Europe based on the simulation of a general flood event with a probability of 1 into 100 years; the spatial distribution of potential damage due to floods represents a fundamental aspect in actions of prevention and mitigation for decision makers (Barredo et al., 2008).

1.3. Problem Statement

The good results and the improvements provided by the validation studies of De Roo et al. (2006) and Kalas et al. (2008) respectively on 2005 alpine floods and 2006 Moravia River flood, allowed the EFAS team in widening the initial horizons of its research objectives. EFAS is the first flood forecast project set up at such large scale; therefore, for the first time, homogeneous data about flood hazard were available at a pan-European scale. For this aim, JRC created a series of networks for data collection and storage able to provide the basis for more advanced applications of the system. The availability of a well performing hydrological model for all the Europe suggested its applications on further research fields, as mentioned in section 1.2. IES team evaluated the possibility to extract information regarding potential flood damage assessment for the entire European Continent. The main aim was to provide the European Commission with estimates of the economic impact of floods in such a way that comparisons among different States could be possible. The team developed a strategy to extract from EFAS model the essential hydrologic parameters. The damage assessment is based on the application of depth-damage functions related to the CORINE (De Lima, 2005) landuse classes (see chapter 3). The team published in 2008 a first draft of flood potential damage assessment (Fig. 1.1) based on the simulation of a general event with an occurrence of 1 into 100 years for all Europe (Barredo et al., 2008); With the term potential damage, the authors aimed at estimating the maximum loss in a scenario without protection measures. This decision was dictated by the impossibility to

introduce the defence structures in the hazard assessment. The map shows potential damages expressed in million Euros in purchasing power parities (PPT) among the States Members.

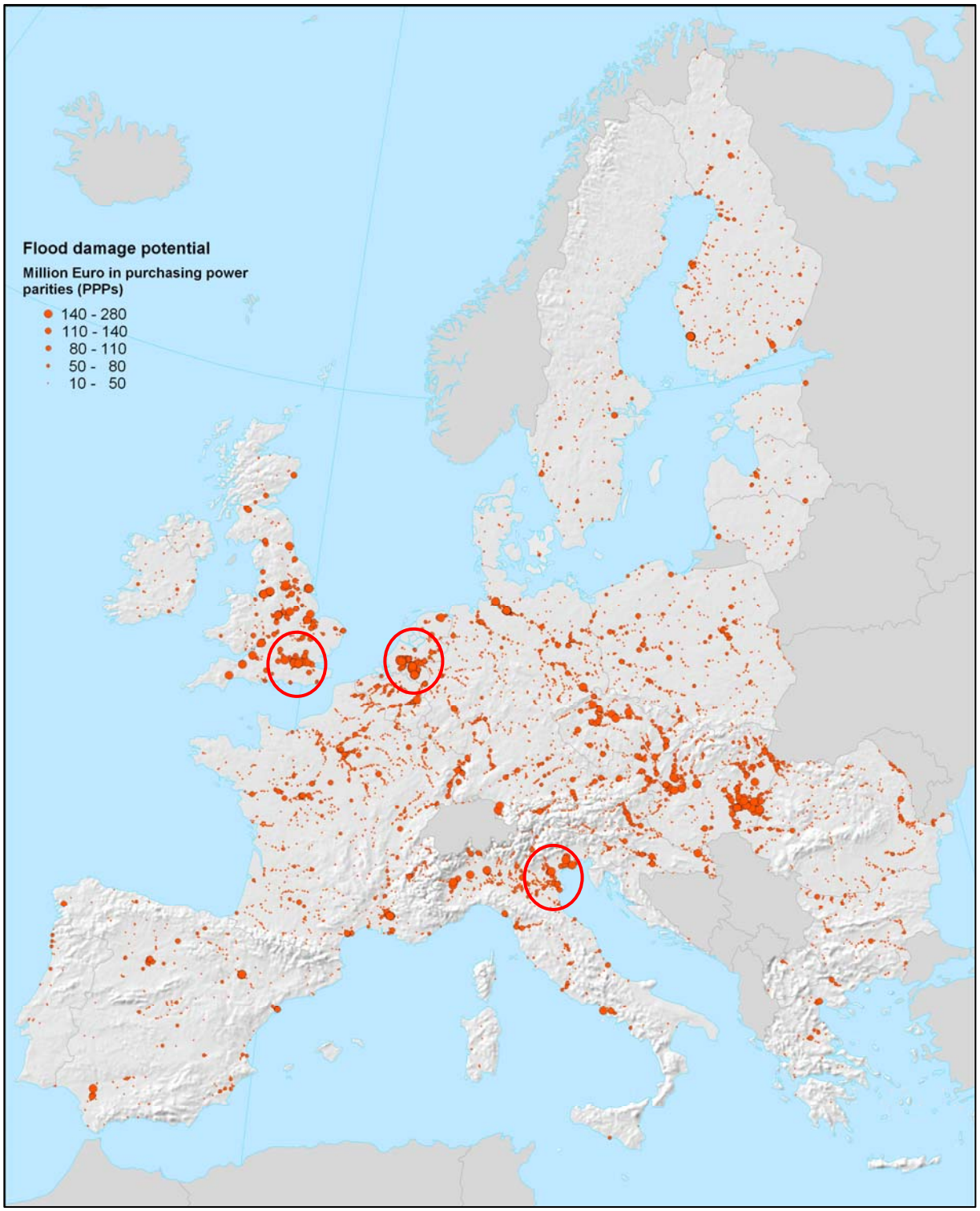

Fig. 1.1: 100 years return period flood potential damage assessment map for Europe from (Barredo et al., 2008); the red circles highlight the areas in which the potential damage assessment seems to exaggerate the loss.

The map has the benefit to show for the first time the impact, in monetary terms, of direct damage caused by flood events for the European countries in a homogenous way; which allows the comparison among different states. Information about economic impact of floods is essential for flood hazard

prevention and mitigation activities at inter-National scale. In the map in Fig 1.1, some areas are pointed out through red circles where the damage of the 100 years return period flood event seem to be exaggerated due to the omission of the protection measures. The highlighted areas correspond to the Po delta in Italy, the western Netherlands and the area surrounding the London metropolis in England; these areas present severe damage rates due to their very high population density and, therefore, the presence of elements at risk with elevated value. At the same time, the above mentioned areas are largely protected from flood events through advanced defence structures and flood prevention and mitigation systems (ADBPO, 2006; Hall et al., 2005). This fact clearly points out the most affecting inaccuracy of the damage assessment methodology which is related to the hazard evaluation. Due to the resolution at which the flood extent and depth is carried out (100m), the effect of defence measures, lakes, polders are not taken into account in the calculation. The heavier weight on the accuracy of the results is certainly referred to the absence of information about defence structures. At the moment no strategy is planned to include them in the flood extent calculation. Furthermore, in order to include them, a full and homogeneous database at European scale should be available. The data collection regarding defence structures is a difficult task because such information does not exist for all the State Members and whenever surveys exist, it is likely that they differs in the classification and the description of the structures themselves. Moreover it has been noticed during the data collection for this research that the information provided by local authorities (Po Basin Authority in this case) were in some cases out of date and therefore not entirely reliable.

Regarding the evaluation of the damage, at the moment it is focused on the calculation of the direct damages caused by flood events, through the application of depth-damage functions, therefore the methodology does not take into account different aspects like the rate of the population affected or the evaluation of possible causalities.

1.4. Objectives and Research Questions

Due to the inaccuracies pointed out in the previous section, the general aims of this study are to define if the overall methodology still provides reasonable results despite of the above mentioned inaccuracies, and where it is likely to be improved.

The first part of the work is focused on the evaluation of the hazard assessment. The study area chosen in this research is the Po catchment in Italy. An initial investigation focused on finding previous researches related to the same topic in the same area was carried out: a detailed flood modelling study was available in the organization “Autorita’ di Bacino del Fiume Po” (ADBPO http://www.adbpo.it/on-line/ADBPO/Home.html in Parma, Italy), which represents the most important water management Authority for the Po basin at inter-regional level.

Firstly the original technique from JRC was followed to extract the flood extent and water level. Secondly, the effects produced by the absence of defence measurements in the calculations were evaluated.

As main objective, *this research aims at improving the overall damage assessment methodology developed by EFAS team*. In order to achieve this result, four sub-objectives were defined; the first two are related to the calculation of the flood extent and depth map, while the last two regard the evaluation of the evaluation of the damage.

1.4.1. Sub-Objective 1: Simulation of Defence Measures

Through the spatial comparison between the hazard map from JRC and the map from the local detailed study mentioned above (called "Sottoprogetto: SP1.1: Piene e naturalità degli alvei") this research aimed to quantitatively assess the flood extent produced. The comparison wanted to point out which were the sources of inaccuracies that affect the overall procedure applied in the EFAS hazard assessment methodology. The damage assessment produced by EFAS team is based on the simulation of LISFLOOD model; but the effects of the presence of lakes, reservoirs, polders and longitudinal or transversal defence measurements were not taken into account in the calculation of water level and extent.

From the ADBPO project, the database of longitudinal defence measurements was extracted; therefore, the first sub-objective is *the introduction of protection measures in the methodology and the assessment of the improvements achieved.*

The research questions to be addressed are the following:

1. Which kinds of information are available about defence structures and which ones are needed to consider the structure in the methodology?
2. What could be an adequate strategy to calculate the effect of the structures in the flood extent simulation?
3. Once the structures have been introduced, is there any significant improvement on the outputs compared with the originals?

1.4.2. Sub-Objective 2: Use of High Res. Digital Terrain Model in Hazard Assessment

The water level and extent calculation are extracted by combining a planar approximation of the flood wave with a high resolution Raster Digital Elevation Model - DEM (Bates and De Roo, 2000) described in section 3.4.1. Due to the data availability at the operational scale, the research team opted for a 100 m horizontal resolution DEM. It is likely to believe that the main source of errors in flood extent and depth calculation is the DEM itself and its derivatives like the flow direction map and the river network. New 5m resolution elevation datasets were available for two subsets of the main study area. The second sub-objective of the study is *the application and the feasibility study of the methodology developed by EFAS team on a new high resolution elevation dataset.* Three main questions follow the aim:

1. Is the same methodology applicable to the new datasets? In detail, can the derived input maps be obtained from the new datasets?
2. Can the vertical accuracy of the new datasets replace the absence of information on defence measures?
3. Do the results justify the acquisition of those elevation maps?

1.4.3. Sub-Objective 3: Potential damage evaluation with improved hazard maps

After having applied the improvements on the hazard calculation, the successive step was to translate that information into a flood damage assessment. EFAS team opted for a semi-quantitative method to calculate the potential damage assessment. The parameters available form the hazard assessment were the flood extent and depth; therefore a methodology based on stage-damage functions (Huizinga, 2007) was applied. These are functions based on the relation between water level and damage (Dutta et al., 2003; Krzysztofowicz and Davis, 1983) expressed in monetary terms through the use of Purchasing Power Parities indices (Van Vuuren and Alfsen, 2006). See section 5.2.2 for in-depth description.

The goal of this section of the research is *the application of the potential damage assessment to the new hazard data* calculated for the study area in the former part of the work: the flood extent map for the Po Area with defence measurements at 100m resolution and the flood extent for the subsets from the new elevation models at 5m resolution. The potential damage assessment cannot be validated due to the absence of existing data at such large scale. Potential damage calculation for the original and the improved hazard data aims to add further terms of comparison and evaluation on the introduction of improvements described above, that can help in answering the research questions related to this sub-objective:

1. Are the improvements of the hazard map corresponding to more reliable results of the potential damage evaluation? Moreover, which effects have the improvements introduced on the damage assessment?
2. How to best combine the resolution of CORINE (100m) and the resolution of the new elevation models (5m)?

1.4.4. Sub-Objective 4: Life Loss Estimation Approach

Due to the complexity of the subject, life loss estimation is still not included in the EFAS. *An adjunctive sub-objective of this work is to find an applicable method for life loss estimation.* This part wants to be a brief overview of the problem and a feasibility evaluation of the methodologies available in literature in order to provide starting points for further studies on the topic. The related research questions are:

1. Which is the information available for life loss estimation? Which are needed?

2. Which are the suitable methodologies in literature to estimate life losses? Are they applicable in this case?

1.5. Thesis Organization

The first part of the work (Chapter 1) contains a brief description of the flood events in Europe. Then the historical background that preceded EFAS project was illustrated; the second part of the chapter describes the objectives of the research, and points out the main research questions that have to be answered.

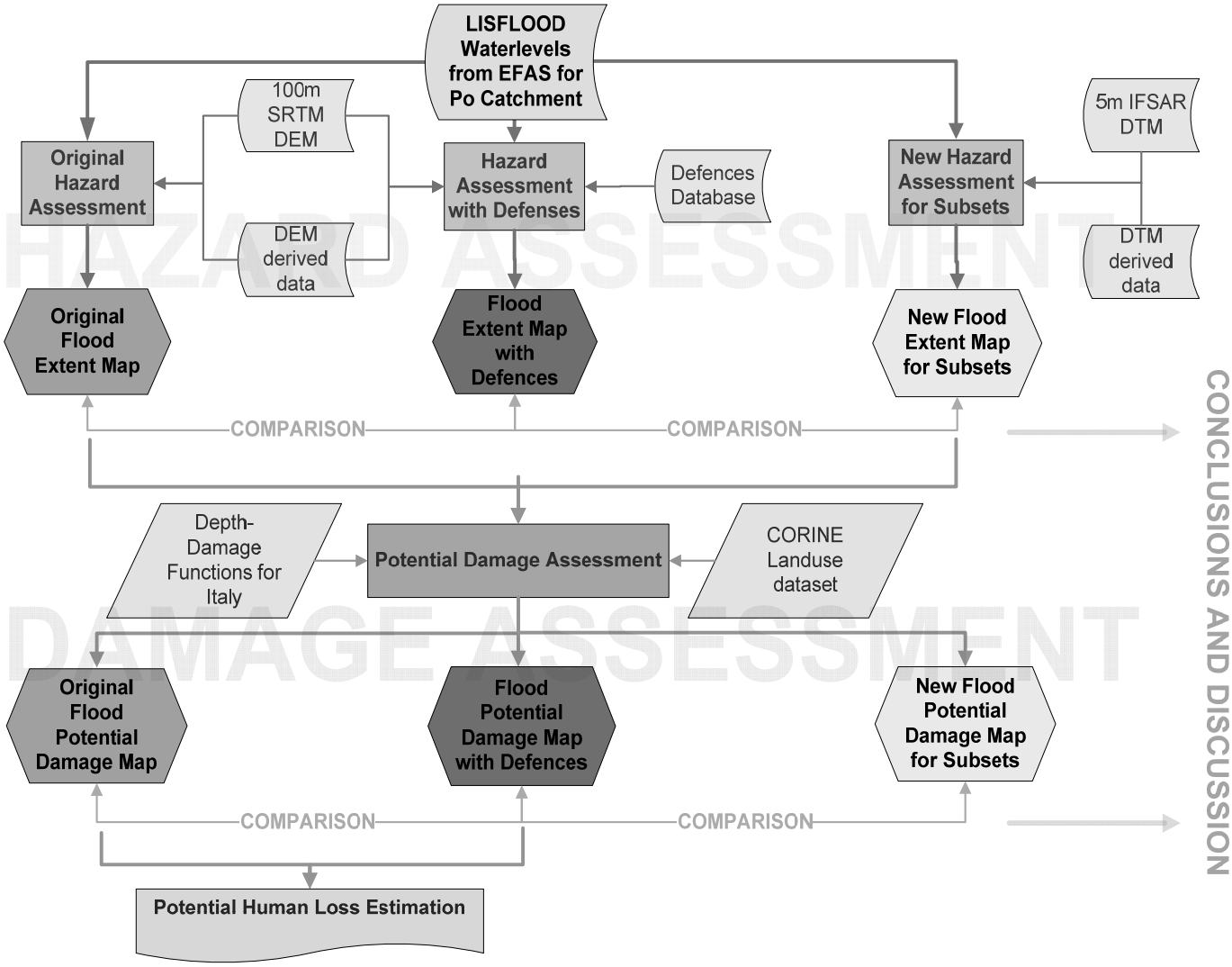

Fig. 1.2: Thesis Flowchart

Chapter 2 opens with a description of EFAS project. The second part of the chapter describes under different aspects the selected study area and the reasons why this case study has been chosen. The chapter 2 closes with the description of the hazard assessment study provided by the local authority. With chapter three, the research enters in the core of the methodology related to hazard assessment. The first part of the chapter explains the methodology structure and the input data. This section wants to provide a theoretical background on the problem and the suggested solutions that will be applied. The calculations of the flood extent maps are shown and widely described. 1) The EFAS flood extent based on the 100m SRTM DEM, 2) the EFAS-SRTM 100m flood extent corrected through the simulation of defence measures, 3) the introduction of the new Digital Terrain Model and calculation of flood extent for the selected subsets are the main part in which the chapter is organized.

In chapter four, the results from the hazard assessment are shown, together with the results of the comparison with the local study from "Autorità di Bacino del Fiume Po" and the conclusions achieved.

In chapter five, the technique of the flood potential damage assessment are applied to the flood extent maps for the Po catchment obtained in chapter three: EFAS-SRTM 100m flood extent map, the EFAS-SRTM 100m map calculated with the introduction of the defence measures, and the subsets maps obtained through the application of the new elevation datasets. The differences in the damages evaluated for each input maps are highlighted.

Chapter six is a brief review of life loss estimations methodologies available in literature. The different methodologies are evaluated to assess their applicability in this case study. The chapter closes with a review and a statistic description of historic events in Europe that have been collected through the open source databases available nowadays.

Finally chapter seven illustrates the conclusions related to the initial research questions. The results from the comparison of the different hazard maps with the reference local hazard study are integrated with the information from the comparison of the different damage calculations.

Fig. 1.2 shows the flowchart of the thesis: the first part (blue) of the graph illustrates the overall methodology related to chapter three. In the second part in red, the damage assessment (chapter 5) is schematized, while from the outputs related to the entire Po area the considerations on lives loss estimation are carried out (chapter 6). The comparison of the outputs from hazard and damage assessment represents the basis for the conclusions of the research (chapter 6).

2. EFAS and Case Study description

This chapter includes a description in detail of the European Flood Alert System. In the second part, the selected study area is illustrated, while the final part briefly describes the hazard assessment study used as comparison in this research.

2.1. EFAS

The European Flood Alert System aims at providing flood forecast information through the acquisition of different weather forecast sources. The EFAS project is a research activity developed by the Land Management and Natural Hazard (LMNH) unit of the Institute for Environment and Sustainability (IES) located at the European Join Research Centre (JRC) in Ispra, Italy.

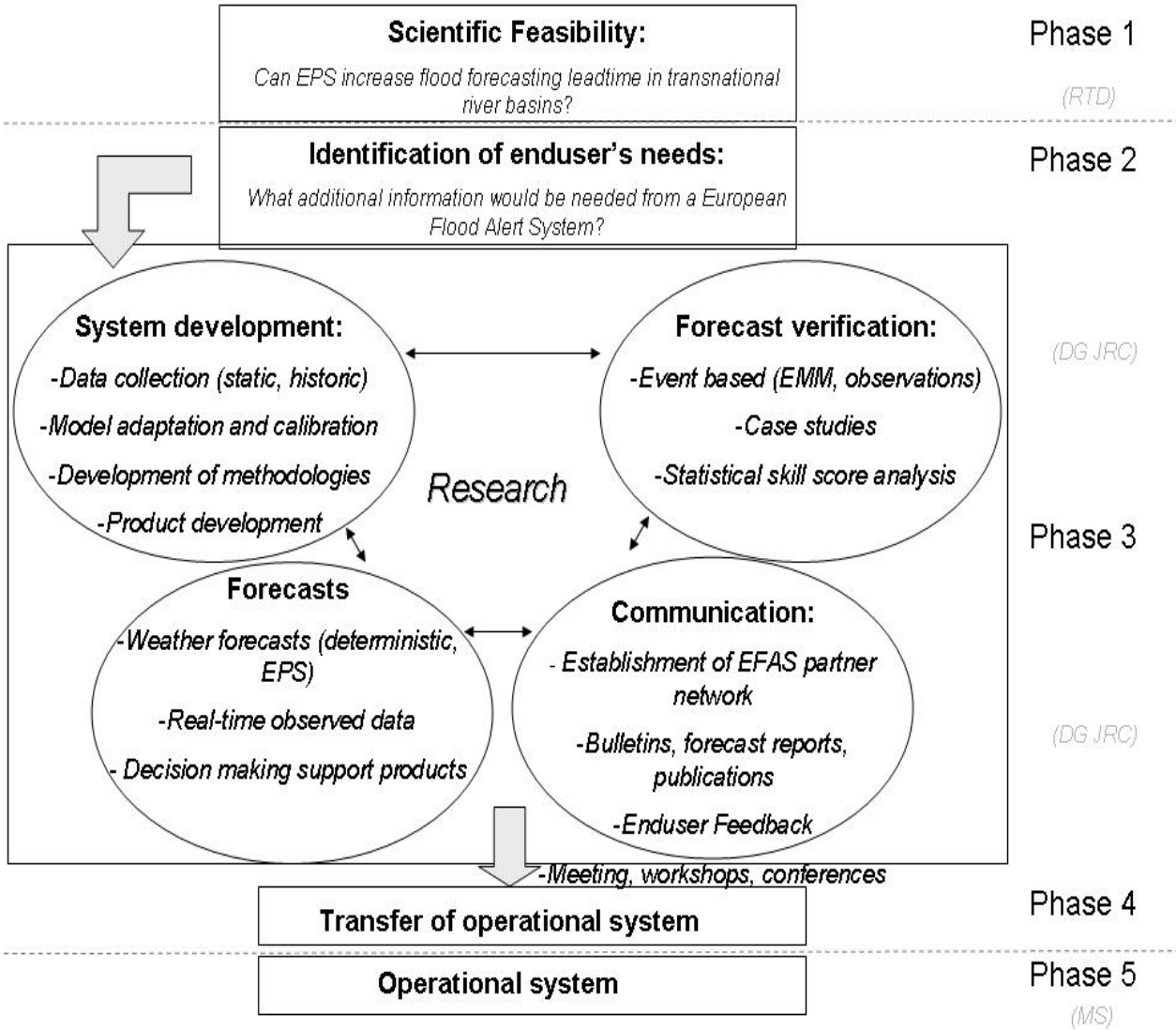

Fig. 2.1: General framework of the European Flood Alert System (Thielen et al., 2008).

It is based on the discharge simulation from hydrological LISFLOOD model that runs daily at an operational scale of 5 Km cell size. The input information described below has been collected and

stored in a series of databases by the EFAS team. The overall framework of EFAS includes the following five parts resumed in Fig 2.1 and briefly described here below. At the state of the art, the first three parts have been completed, while the remaining two are expected to be ended by the end of 2010.

1. Assessment of scientific feasibility: EFFS research project and its results in the cases of Meuse flood in 1995 and the Po flood in 1994 proved that the probabilistic forecasts provided early warning of 6 to 8 days (Bartholmes and Todini, 2005; Gouweleeuw et al., 2005); representing the scientific base for EFAS development.
2. Identification of End-users requirements. From surveys based on questionnaires (Thielen et al., 2003), EFAS resulted to provide improvements in: extension of lead-times, interpretation of probabilistic weather and flood information, provision of flood situation in upstream and neighbouring areas, sharing information and data.
3. Prototype development: input data collection, model adaptation and calibration; implementation of forecast methodology based on threshold exceedance; events based forecasts verification; communication to the partners network through bulletins and end-users feedback.
4. Definition of an easy running and stable configuration of the system.
5. Transfer of the operational system to a European organization that will run and disseminate the forecasts to Member States.

2.1.1. Observed data and Weather Forecasting data

Observed input data were necessary to set-up calibrate and validate the model; The observed data related to precipitations, temperature, evaporation, transpiration, are updated daily and collected in the meteorological database called JRC-MARS Meteorological Archival and Retrieval System (Baudouin, 2003) with data from 1975 from about 200 stations across Europe. Currently EFAS receives data from the database, with a 1-2 days delay, as daily values for a 24 hours period. Real-time hydrological information is not fully available at European scale; therefore discharge data are collected through the database of the Global Data Runoff Centre (GRCD, 1988). Approximately 800 measurement stations records are available from 1990 up to now.

The most important data for flood prediction activity is the input weather forecast information. The quality of the flood alerts is directly depending on the accuracy of weather forecasting (De Roo and Maurer, 2006); therefore EFAS receives daily weather forecasts from different sources. One of the aims of the activity of EFAS in the pre-operational period is to assess the reliability of the different sources of weather forecasting data.

Probabilistic and deterministic meteorological forecasting data are provided directly by the European Centre for Medium-Range Weather Forecasts (ECMWF). The Deutche Wetterdienst (DWD) instead provides deterministic forecast information hourly. The characteristics of observed meteorological data and the forecast data are listed in table 2.1. The Ensemble Prediction System (EPS) applied in

ECMWF forecasts is a probabilistic weather forecast technique based on the idea that small analysis errors, may affect the large scale flow during the forecast period: different analysis produce considerably different forecast. To represent the uncertainty of the initial conditions small amplitude selected perturbations are added to the analysis, creating a range of slightly different initial conditions. The EPS provides as added value a degree of uncertainty in weather forecasting (Persson and Grazzini, 2007). Moreover, (Demeritt et al., 2007) stated in their studies that, without the regular contribution of the EPS, flood forecasts are unlikely to express their full skills and confidence rates.

Tab. 2.1: EFAS input data in the period 2005\2006. Abbreviations: P = total precipitation; T = temperature; E = evaporation; E0 = potential evaporation of water; ES0 = potential evaporation of bare soil; ET0 = potential evapotranspiration.

	DWD	ECMWF Deterministic	ECMWF EPS	Observed meteorological data (JRC MARS)
Temporal resolution	1 h (1–3 days) 3 h (4–7 days)	3 h (1–3 days) 6 h (4–10 days)	6 h (1–10 days)	Daily
Spatial resolution	7km (1–3 days) & 40 km	(~40 km)	(~80 km)	Gridded 50×50 km
Times provided	12:00; 00:00	12:00; 00;00	12:00; 00:00	Irregular, typically at 23:00
Input fields	P, T, E	P, T, E	P , T , E	P , T , E0, ES0, ET0
Bias removal	None	None	None	None

2.1.2. Hydrological Model

The Hydrological model used in EFAS is LISFLOOD (Van Der Knijff and De Roo, 2008), a hybrid between a conceptual and physical rainfall-runoff model combined with a routing module in the river channel. It is based on the Kinematic wave function and it is built using the PC Raster Dynamic Modelling Language (De Roo et al., 2000). This model has been designed for large river channels; in particular its aim in EFAS is to monitor all the European basins larger than 2000 Km^2 (Thielen et al., 2008). In EFAS LISFLOOD model is set on a 5x5 Km regular grid structure for operational activities; while it runs with a 1x1 Km grid in the pilot projects in the Elbe and Danube catchments for research purposes. The input parameters consist in the meteorological forecasts datasets described above and in a series of static and dynamic maps listed in table 2.2. The calculation of initial conditions is performed on a daily time step based on observed input data from JRC-MARS. The time-steps for forecasting operations are different, depending on the inputs: for the forecast calculations based on the deterministic weather forecasts (DWD and ECMWF) are run hourly; and the ones based on EPS with a 24 hours time-step. Precipitation is assumed to be snow if the average temperature is below 1°C; snowmelt is simulated using a simple degree-day factor method. Infiltration and runoff are calculated with the Xinanjiang simulation approach (Zhao and Liu, 1995); while in the simulation of preferential flow, the contribution of water on surface is assumed to be a non linear function of the relative

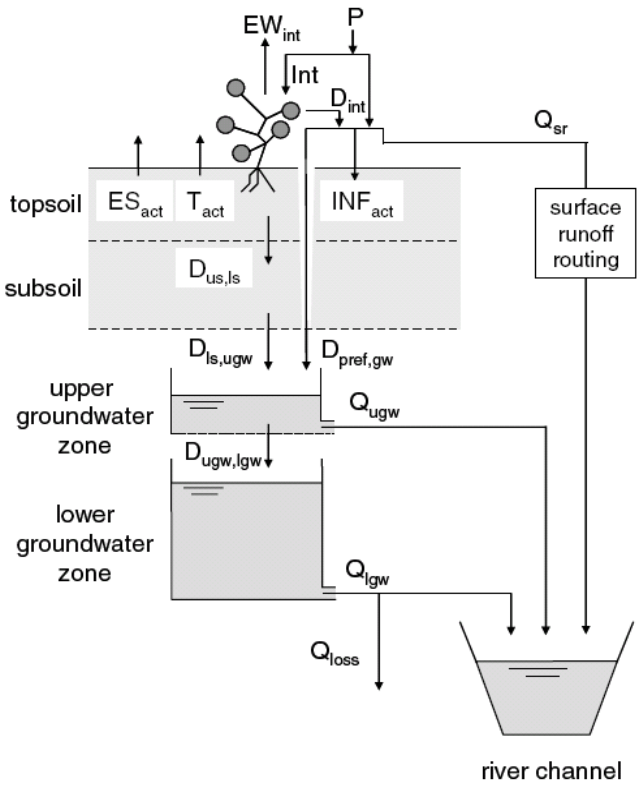

Fig. 2.2: Schematic overview of LISFLOOD model (Feyen et al., 2007). P = precipitation; Int = interception; EWint = evaporation of intercepted water; Dint = leaf drainage; ESact = evaporation from soil surface; Tact = transpiration (water uptake by plant roots); INFact = infiltration; Qsr = surface runoff; Dus,ls = drainage from upper to lower soil zone; Dls,ugw = drainage from lower soil zone to upper groundwater zone; Dpref,gw = preferential flow to upper groundwater zone; Dugw,lgw = drainage from upper to lower groundwater zone; Qugw = outflow from upper groundwater zone; Qlgw = outflow from lower groundwater zone; Qloss = loss from lower groundwater zone. (Note that snowmelt is not included in the figure, even though it is simulated by the model.)

saturation of the topsoil. The moisture fluxes are assumed to be entirely gravity driven.The groundwater system is described using two parallel linear reservoirs. Surface runoff is routed to the nearest downstream channel using a 4-point implicit finite difference solution (Van Der Knijff and De Roo, 2008) of the kinematic wave equation (Chow et al., 1988).The kinematic wave technique is a simplified version of the dynamic wave technique. The full dynamic wave consists of two partial differential equations on conservation of mass (continuity) momentum (dynamic): the Saint-Venant equations. The kinematic wave treats part of the physical processes as negligible. Kinematic wave models are based on the continuity equation and a simplified form of the momentum equation used for the full dynamic wave. The physical factors, which the kinematic wave technique is based on, are gravitational forces and frictional forces only (Shultz et al., 2008). The limited amount of hydrological data is the problem that most affects the goodness of LISFLOODS outputs; to provide EFAS with high-density historic and real-time hydrologic and meteorological data, two projects have been promoted by JRC: EU-FLOOD GIS and European Terrestrial Network for River Discharge ETN-R (De Roo and Maurer, 2006).

2.1.3. Flood Forecasting and validation

After the calculation of hydrographs with LISFLOOD from weather forecasts, the successive task for EFAS staff was to transform this information into a proper flood forecast. A methodology based on critical thresholds was created. The lack of information about reservoirs, lakes, polders and defence measures, combined with the limited amount of meteorological observations, avoided any quantitative comparison between simulated discharges and observed thresholds.

Tab. 2.2: LISFLOOD input parameters; (Van Der Knijff and De Roo, 2008).

Map	Description
	GENERAL
Mask Map	Boolean map that defines model boundaries
	TOPOGRAPHY
Ldd	Local drain direction map (with value 1-9); this file contains flow directions from each cell to its steepest downslope neighbor. Ldd directions are coded according a specific diagram that resembles the numeric key pad of a PC's keyboard, except for the value 5, which defines a cell without local drain direction (pit). The pit cell at the end of the path is the outlet point of a catchment.
Grad	Slope gradient [m m-1], i.e. value of 0.5 indicates a 26.5 degree angle (gradient equals tangent of slope in degrees)
Elevation Range	Elevation range, i.e. difference between maximum and minimum elevation within pixel (m)
	LAND USE
Land Use	Map with land use classes (CORINE land cover, CEC 1993)
Forest	Forest fraction for each cell. Values range from 0 (no forest at all) to 1 (pixel is 100% forest)
Direct Runoff Fraction	Fraction urban area for each cell. Values range from 0 (no urban area at all) to 1 (pixel is 100% urban)
	SOIL
Texture1	Soil texture class layer 1 (upper layer)
Texture2	Soil texture class layer 2 (lower layer)
Soil Depth	Soil depth [cm]: depth to bedrock or groundwater
	CHANNEL GEOMETRY
Channels	Map with Boolean 1 for all channel pixels, and Boolean 0 for all other pixels on Mask Map
Chan Grad	Channel gradient [m m-1]
Chan Man	Manning's roughness coefficient for channels
Chan Length	Channel length [m] (can exceed grid size, to account for meandering rivers)
Chan SdXdY	Channel side slope [m m-1]
Chan Depth Threshold	Bankfull channel depth [m]
	DEVELOPMENT OF VEGETATION OVER TIME
LAI Maps	Pixel-average Leaf Area Index [m2 m-2]
	DEFINITION OF INPUT/OUTPUT TIMESERIES
Gauges	Nominal map with locations at which discharge time series are reported
Sites	Nominal map with locations (individual pixels or areas) at which time series of intermediate state and rate variables are reported

Therefore a method based on quantiles was applied: LISFLOOD was run based on observed data and produced, for each river cell, a series of discharge data; those data have been ranked and the thresholds have been selected. A four alert levels scale was introduced and to each level an identification colour was assigned. The four classes represent a qualitative description of the magnitude of the event for each river pixel (Fig. 1.2).For the severe threshold cut-off, the discharge of a 14 years return period was chosen; the high threshold is represented by the 99th percentile, which corresponds to a return period of 1-2 years. The main focus of EFAS predictions is on riverine floods. Such events are

triggered by atmospheric conditions that last for several days; to include this aspect, EFAS was based on the so called "temporal persistence" principle: each river pixel is classified as flooded if it exceeds the thresholds for at least three consecutive 12 hours step forecasts. Finally, EFAS forecasts information is delivered to States Members through real-time reports using the web interface created on purpose (http://efas-is.jrc.ec.europa.eu/).

EFAS Thresholds	Colour	Description
Severe (S)		Very high possibility of flooding, potentially severe flooding expected
High (H)		High possibility of flooding, bank-full conditions or higher expected.
Medium (M)		Water levels high but no flooding expected
Low (L)		Water levels higher than normal but no flooding is expected

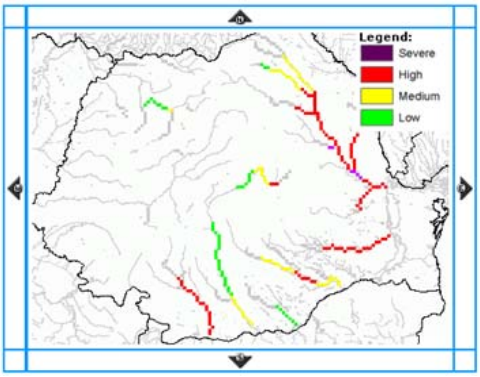

Fig. 2.3: EFAS Thresholds with corresponding hazard zones descriptions and an example of a EFAS forecast output; (Thielen et al., 2008)

Since the system started its activity, survey operations collected information on flood events, so that the EFAS team could perform validations on forecasts outputs. EFAS result for 2005 and 2006 were cross-checked using floods records collected in the same period: in the 80% of the events forecasted by EFAS, the flood happened. More detailed studies were carried out on specific events by using observations. De Roo (2006) verified the forecasts of the 2005 alpine floods. Between the 22nd and the 27th of August 2005, flood events with high magnitude occurred in tributaries of the Rhine River in Switzerland and Austria and in several tributaries of the Danube River in Germany, and Hungary. An EFAS flood alert report was sent on 21st.

"…The EFAS alert proved to match very well the observed flooding. EFAS forecasts indicated well the overall region of severe flood problems … EFAS forecasted very well the extreme floods that happened in the Iller where floods were associated with return periods of more than 100 years, and Upper Isar River. The 50- to 100-year return period floods in the middle part of the Isar and the downstream part of the Lech were also well predicted by EFAS with a Severe Alert Level…" from De Roo et al, 2006. Analysis on the spring floods of Morava River in 2006 were performed by Kalas M. et al. (2008). The LISFLOOD model was run with deterministic and in turn probabilistic weather forecasts; the results were validated against observed data. Kalas (2008) highlighted in his work the potential advantage of hydrologic forecasts based on ensemble weather predictions.

2.2. Study Area

The choice fell on the Po Basin for different reasons. First of all the IES-JRC institute is located in Ispra, 80 Km from Milan, next to Varese Lake. Secondly, the Po represents a medium basin size compared to the dimensions in Europe, with approximately 40% of the territory covered by flat areas and the remaining part divided by hilly land and mountainous terrains; so that it covers a wide variety of morphologically different flood prone areas. Moreover, through the local authorities, a flood hazard assessment study for the entire basin catchment was available in Italian language, and it was comparable with the EFAS one regarding the methodologies applied. The state of the art regarding flood disaster management in Italy is likely to be considered an average of the European level. The situation about the structural defence measurements (see Tab. 3.1) could fall in between the basins with high level of protection in the Netherlands or England (Hall et al., 2005) and other catchments less protected. Finally the landcover in the basin is various and it includes a mix of agricultural land, urban areas and special structures like wide industrial sites, airports and important transport networks, so that a potential damage assessment in the study area can be reasonably meaningful.

Tab. 2.3: Embankments length of Po River and tributaries.

River name	Embankments and Levees on the left bank (Km)	Embankments and Levees on the right bank (Km)	Total (Km)
Po watercourse	1342	796	2138
Po delta			154
Tributaries	924	350	1.274
Total			3466

2.2.1. Basin Characteristics

The Po Basin is situated in the Northern part of Italy (Fig. 3.1). It is the main river catchment in the country for river length (ca. 650 Km), and for discharge dimensions (in its final part during the 1951 flood event a discharge of 10.300 m^3/s was recorded). The basin area is ca. 72.000 Km^2 and it includes in total 3.210 municipalities located in the territory of 7 regions (Piemonte, Valle d'Aosta, Lombardia, Veneto, Emilia Romagna, Liguria, and Toscana) and in the independent province of Trento.

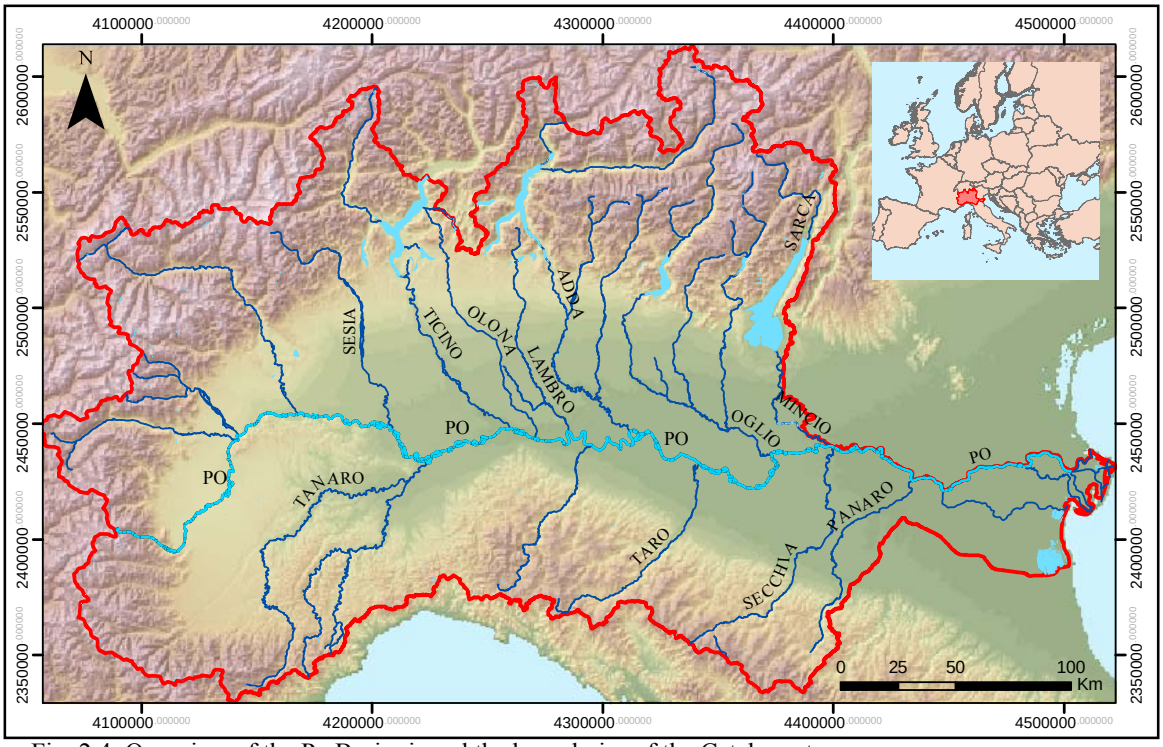

Fig. 2.4: Overview of the Po Basin; in red the boundaries of the Catchment.

The basin is located between two relatively young mountain ranges: the Alps in the North (first tectonic uplift in the Upper Cretaceous and a second in the Tertiary) and the Apennines in the Southern part. In between, the Po valley started its development in the Miocene. The basin was subject to high subsidence phenomena that contributed with a very high sedimentation velocity to the deposition of sedimentary layers raising a thickness of 8.000 m in various areas.

The climatic conditions of the basin are strongly influenced by the presence of the Alpine Chain that, on one hand affects the climatic conditions with its ca. 600 Km^2 of permanent glaciers coverage, on the other hand represents a barrier for the Northern cold winds. Other influencing factors are the proximity of the Ligurian and Adriatic Sea, and the presence of a series o natural water bodies that occupy 865 Km^2, in the Northern part of the basin, with a mitigation effect. The temperatures are extremely dominated by the quote: In the mountainous areas of the Alps and in the higher spots on the Apennines, values next to 5ºC are recorded as mean year temperatures. Mountainous areas of average quote have mean temperatures between 5 and 10 ºC in both the chains.

The majority of the areas fall in the interval of 10 to 15ºC, including the entire Po valley, the area of the lakes, and the valleys. The mean temperatures over 15ºC are proper to the coastal areas. The seasonal distribution of temperatures is homogeneous for the entire area, a low peak in January and a high peak in July.

The Lombardy region well represents the average of precipitation with an annual mean of ca. 1.200mm.

Tab. 2.4: Main Po Tributaries; Area = Basin Area; Length = River Length.

Name	Area Km^2	Length Km	Side	Name	Area Km^2	Length Km	Side
Adda	7.927		Left	Pellice	975	55	Left
Agogna	995		Left	Scrivia	1.237		Left
Lambro	1.980		Left	Sesia	3.075	141	Left
Sarca / Mincio	3000		Left	Stura	855	53	Left
Oglio	6.360	280	Left	Tanaro	8.080	238	Left
Olona	911	60	Left	Enza	890	100	Right
Terdoppio	515	86	Left	Nure	430	75	Right
Ticino	6.033	284	Left	Staffora	1.370		Right
Toce	1.778		Left	Panaro	1.775	165	Right
Dora Baltea	3.930	152	Left	Parma	815	100	Right
Dora Riparia	1.210		Left	Secchia	2.090	172	Right
Maira	1.210	105	Left	Taro	2.030	150	Right
				Trebbia	1.070	116	Right

Regarding the distribution, during spring, the maximum rainfalls are between 500 and 700mm in the area of Lago Maggiore and in the higher areas of the Apennine. In summer in the Po valley the range is 150 – 200mm. In autumn, the maximum values are recorded in the Alpine piedmont with a range between 600 and 700mm, while in the Po valley the precipitation varies from 200 and 250mm. The winter is the driest season with an average of less than 150mm; only in the lower part of Lombardy and Emilia rainfall around 200 350mm are likely to happen.

The Po River receives the contribution of 141 tributaries of different orders (see Tab. 2.1). The drainage pattern varies considerably, due to the different characteristics of the two mountainous ranges. Moreover, the behavior of the soil varies from the impermeable Alpine granitic bedrocks to the high permeability sedimentary layers in the Apennines. The Alpine watercourses receive the water mainly from the snow melting with a seasonal peak in late summer. In the Apennine side are the discharges are regulated by the runoff and the groundwater flow; therefore they have the seasonal minimum discharge in summer when in many cases they totally dry (ADBPO, 2006).

2.2.2. Socio-economic aspects

The Po Basin is, in numerous critical spots, highly urbanized. Especially in the left side several of the most productive Italian cities are located. Two metropolises (Milan and Turin) with more than a million of inhabitants and other four urban centers (Bergamo, Brescia, Parma and Modena) over 100 thousands inhabitants are located in the proximities of the main watercourses (Fig.2.2). The Po basin is the most strategic area in terms of national economy with a Gross Internal Product covering the 40% of the national amount. The population rose at 15.916.707 units according to 2001 ISTAT (Istituto Nazionale di Statistica http://www.istat.it/) census data. The employed in the Services are ca. 6, 2 millions while in the Industry they don't exceed 3, 3 millions; the workers in the Agriculture are ca. 282.000.

The main cities are located in the left land side of the river; Turin in particular is built on the junction between the Po River and the Dora Baltea River; Cremona and Piacenza are very close to the Po River; The Lambro River area in the southern part of Milan is the most critical of the basin regarding the population density (ADBPO, 2006).

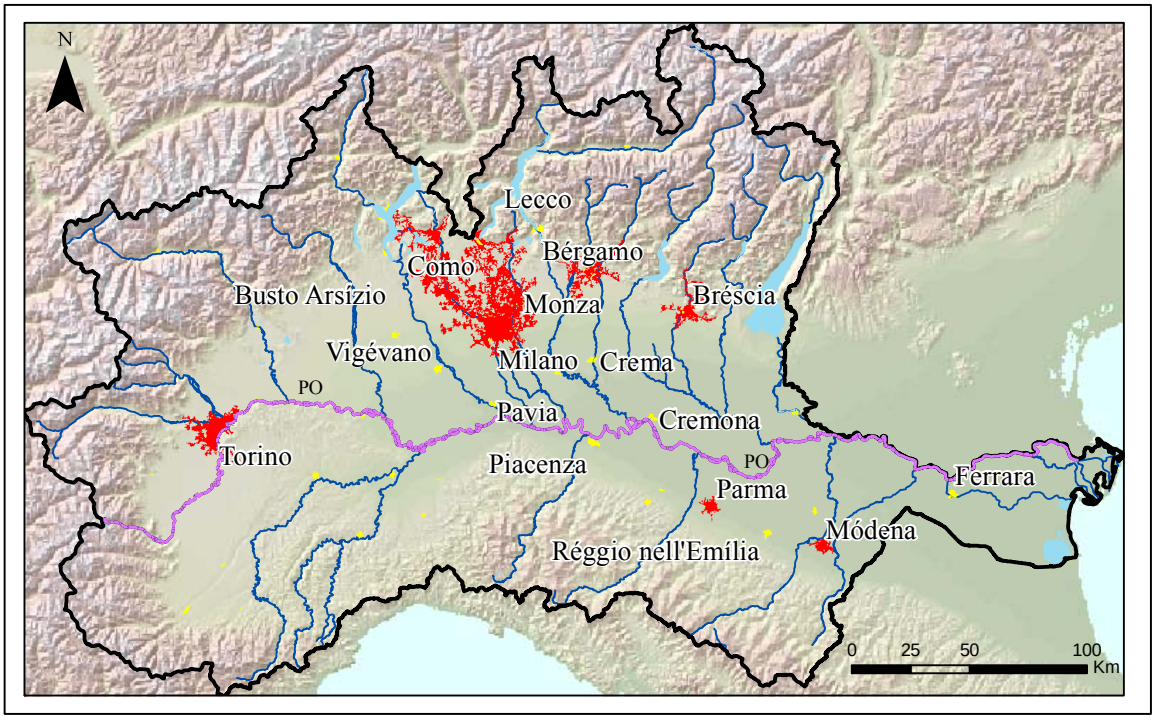

Fig. 2.5: Location of the main cities in the Po basin: in red the urban agglomerates with more than 100.000 inhabitants, in yellow the other main settlements.

2.2.3. Landcover

The landcover map showed in Fig. 3.3 is Po basin window of the CORINE (Coordination of Information on the Environment) dataset (version CLC2000), representing the European land -

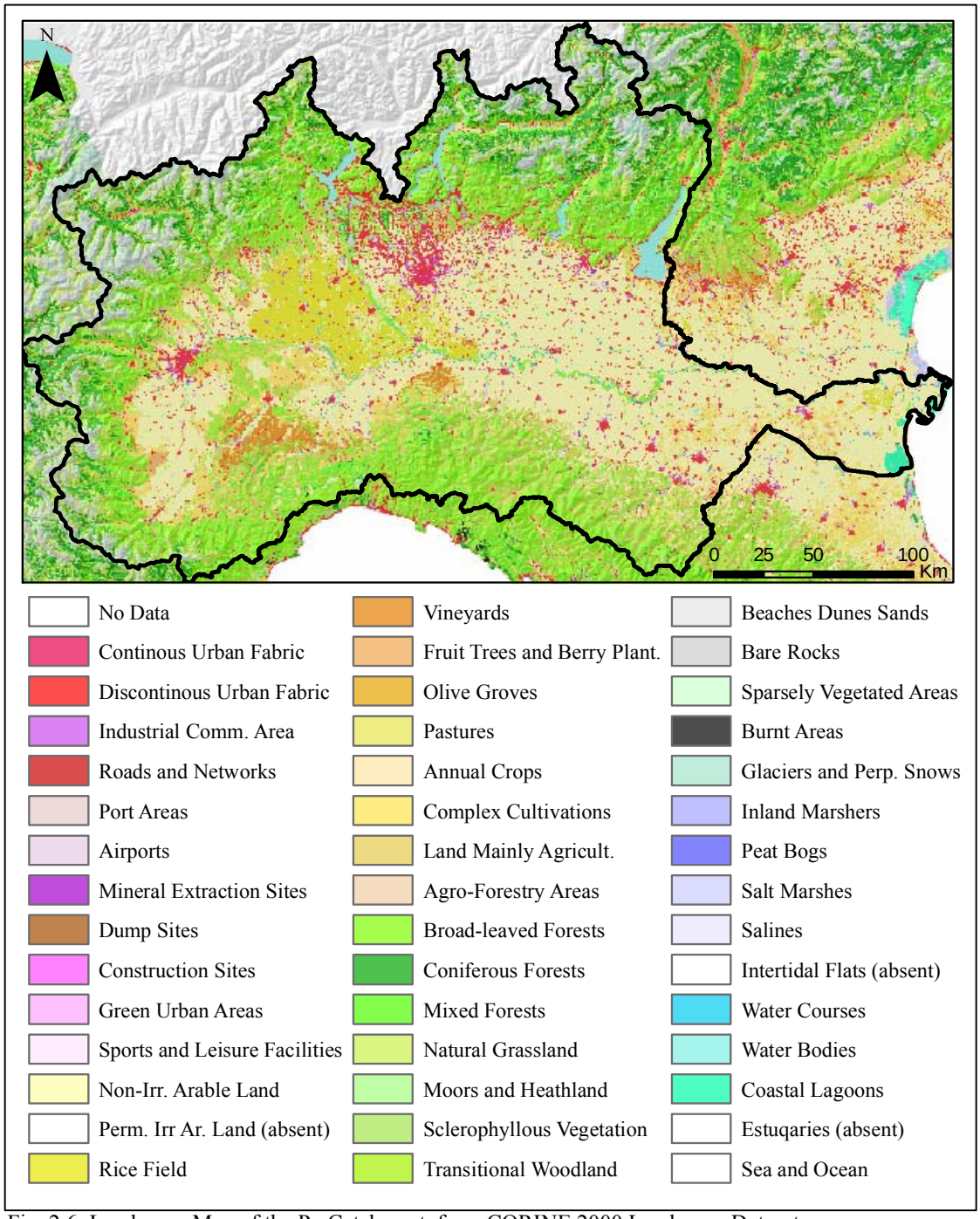

Fig. 2.6: Landcover Map of the Po Catchment, from CORINE 2000 Landcover Dataset.

cover dataset (De Lima, 2005); for more explanations on CORINE see section 5.3. The landcover is highly dependent on the height. In the Po valley, agricultural landcover is dominant: in the central and the Eastern part, non-arable land occupies the valley; settlements are frequent and small, and classified as discontinuous urban fabric. In the central part the urban area of Milan dominates over the agriculture. The areas next to the Po are cultivated mainly with rice fields. In the hilly areas, especially in the Southern ones that belong to the Apennine Range, the vineyards represent the main agricultural activity. As the quote rises over the 200m, the agriculture starts to leave the place to natural forests and grasslands, which draw a kind of green crown around the higher part of the basin. In the low lands the forested areas are frequent in the main river beds.

2.3. Local Hazard Assessment Study from Po Basin Authority

To reach the objectives of this research, a reference hazard study was required in order to allow a comparison with the outputs of EFAS. Due to the scale of observation, the identification of studies able to cover all the Po Basin area was difficult. The only project available was found through the help of the Po basin Authority. It consisted in a complete study on the hydrologic aspects of the Po catchment, and an exhaustive assessment of the damages caused by floods through the socio-economic characterization of the entire Po area. In the following part the study is described in details.

The Sub-project “SP 1.1 Piene e naturalità degli alvei fluviali” realized by the “Autoritá di Bacino del Fiume Po” (ADBPO) was subsequent to the series of floods in 1994 that affected vast areas in the Po catchment. The whole work, completed in January 1997 represents, still now, the only example of risk and damage assessment study for all the Po catchment area found in literature. The hazard assessment and the identification of the main parameters related to the flood hydrology have been realized on the whole Po catchment, including also the rainfall characterization of the basin. In addition, the evolution of the hydrographical network and the identification of monumental sites and naturalistic areas of regional and national importance have been defined. For all the possible flooded areas the socio-economic characteristics have been studied in order to calculate with a quantitative method the value of the elements at risk, therefore the potential damage related to different return period events. The final aim of the work was to evaluate the effectiveness of the flood prevention systems already present and to improve them with new defence strategies as structural and non structural measurements.

The Po River and other 44 tributaries have been considered. The study was mainly focused on the downstream areas, but in the cases of extreme damages after the ’94 flood the hazard evaluation

was extended also to the mountainous section of the catchments (especially for the rivers in the Piemonte region like Dora Baltea, Dora Riparia, Sesia, Elvo, Cervo). The river streams, with a total length of 3.300 Km, have been grouped in three different sub-projects, named "Sub-project-Tanaro" (including Tanaro, Belbo, Bormida, Orba); "Sub-project-Piemonte" (Po, Pellice, Chsione, Variata, Maira, Dora Riparia, Stura di Lanzo,Orco, Dora Blatea, Sesia, Cervo, Elvo); "Sub-project-Residuo" (Po, Scrivia, Agogna, Ticino, Toce, Tredoppio, Olona, Lambro, Trebbia, Nure, Chiavenna, Adda, Brembo, Serio, Arda, Ongina, Taro Stirone, Parma, Baganza, Enza, Crostolo, Oglio, Mella, Chiese, Mincio, Secchia, Panaro, Tiepido).

2.3.1. Study of the Flood Hydrology and Hydrologic Model

The characterization of the floods was carried out starting from rainfall analysis

The rainfall data considered in the study were provided by the SIMN (Servizio Idrologico Militare Nazionale) due to the wide historic series. The rain gauge stations considered were 324 for daily rainfall series and 224 for hourly series. The period between 1950 and 1986 was considered and values related to the floods of 1987, 1993 and 1994 were added successively.

The validation of the series was carried out through the calculation of linear regression curves for all the possible pairs of stations within each single area. The stations with low correlation due to local climate anomalies were excluded.

The aim of the analysis of the rainfall data was to define the heights of the precipitations of defined return periods. The maximum hourly (1,3,6,12,24 hours) and daily (1,2,3,4,5 days) rainfall measurements records for each year were considered, as they were published on the SIMN annual reports. The program used to determine the probability curves was HCH/PMAX; three different probabilistic distributions were applied to the historic series: Galton log-normal distribution, Pearson type III distribution, Fisher-Tippet distribution. The probabilistic law with the best adaptation was chosen in order to extract the rainfall height for the return periods of 10, 20, 50, 100, 200 and 500.

The model MIKE11 of DHI-Danish Hydraulic Institute consists of two different modules: the hydrologic module NAM that calculates the influxes-discharges and the hydrodynamic module HD for the movement of the flood wave.

The main parameters needed by the hydrologic module NAM were: non saturated soil storage capacity (LMax), runoff coefficient, time constants.

The storage capacity was defined as the maximum water content in the non saturated soil available for the evapo-transpiration, and it was described as height in mm. This parameter was dependant form the soil type and the depth of the root zone. The information regarding the root

zone was extracted from (Raghunath, 1987).The soil characteristics were derived from the "Carta Uso del Suolo" (soil map) and "Carta Geolitologica" (geolocic-lithologic map) of the Master Plan 1997.

The runoff coefficient was defined from the same sources using the method suggested by.(McCuen, 1982). The time constants are related to the concentration time expressed by the Giandotti Formula.

The hydrologic model NAM provided the hydrographs for 173 meaningful sections. These hydrographs were used as input in the sections of the simulated hydrographic network. The hydrodynamic module HD of the code MIKE11 solved the St. Venant equations calculating the movement of the flood wave along the stream. The outputs produced were the hydrographs of the discharges and the water levels in the check points.

The calibration/validation of the model was performed for each stream and the related catchment using historic flood records where available.

Finally with the MIKE11 model, flood events with return period of 20, 100, 200 years were simulated using constant intensity rainfall events with corresponding return periods. The final comparison with the results from statistical calculations and regionalization method confirmed the validity of the assumptions in the model.

2.3.2. Definition of the flooded areas extension

The hydrometric levels from the hydraulic model in each measure point were expressed in meters above the sea level (an example can be the Ticino River water level at the junction with the Po River: 61.56, 63.19, 63.70 m.s.l. for 20, 100, 200 years return period). On their basis, the boundaries of the different return period floods were drawn following the topology of the terrain by experts, taking into account the interactions with the structures like bridges, levees channels and embankments. The database contained the tables with descriptions of the structures and the conditions of the streams; the spatial information was stored in CAD files (AutoCAD12 poly-lines). The support was the "Carta Tecnica Regionale" (Regional Technical Map). It is a thematic map containing information regarding, topography, administrative boundaries, transportations network, settlements (building types, infrastructures, services), river network and water bodies, land use. The scale of the CTR maps used was 1:10.000 and the interval of the contour lines was 5 m. In the flat areas auxiliary lines at certain measured height were used to improve the accuracy of the terrain representation.

2.3.3. Database of engineering works and defence structures in general

The census of the defence measures had to provide a database of the major existing manmade structures: crossing structures, weirs and flood control measures, defence measures, which act as mitigation or represent a potential obstruction factor in the flood events. For each structure information was needed about, the degree of protection against floods, the effects on the hydrodynamic flow of the river, the conditions of preservation of the structure. The analysis included the acquisition of former studies, the interpretation aerial photographs at 1:2000 scale and field survey campaigns. Wide importance was given to the crossing structures (i.e. bridges), because of their big impact on flood propagation. The mitigation structures like levees, embankments were mapped without specifying the relative height in respect to the riverbed due to the amount of information. In the database they were described using vector files (AutoCAD12 files); the reports describe in details all the structures and their effects/functions. The effects of structures like bridges on the flood extend are clearly visible by overlapping the flood extends and the presence of structures crossing the river.

2.3.4. Data Extraction and Preparation

According to the purpose of this research, the main interesting aspects of the study were: the hazard assessment outputs represented by the different return periods floods extents, the database regarding the protection measures.

All the spatial elements in the SP1.1 were stored in vector files with .DWG extension using the software AUTOCAD 12. They were finally organized in geo-databases containing different features like points, lines, annotations, and labels. In separate text files and tables all the ancillary data were stored. To project the spatial information, the chosen system was ED 1950 UTM Zone 32N.

The .DWG vector files had only information related to the graphic, like colour code and length of the segments. No thematic information was found; hence they were extracted one by one, studied with the help of the metadata and manually labelled.

The flood extents were extracted for the 20, 100 and 200 years return periods. No information about water level was available. The selected format for the analysis was the .SHP (polylines shape-files) extension used by ESRI software ArcINFO9.2. The 20, 100, 200 years return period flood extents were originally represented through lines open at the extremities; those were converted into ArcGIS shape-files, manually closed at their ends and finally converted into polygons. The defence measures, originally represented by lines in AutoCAD files, were simply converted into shape-files. The files regarding both the flood extent and the protection structures

were finally projected using the reference coordinate system ETRS 1989 Lambert Azimuthal Equal Area (see section 3.1 for in-depth explanation on the adopted coordinate system).

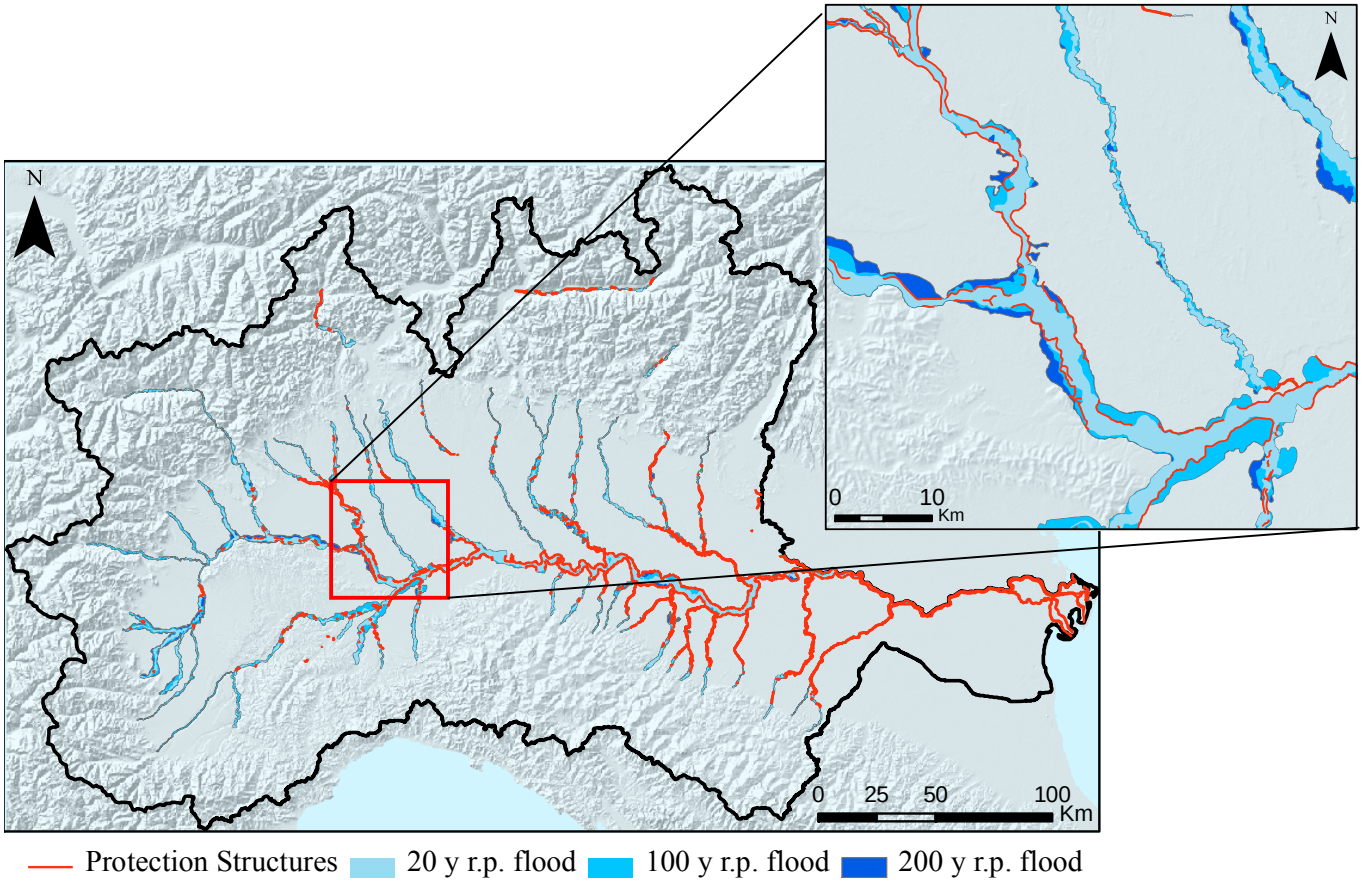

Fig. 2.7: vector layers extracted from the Po Basin Authority study hazard; y.r.p = years return period

3. Hazard Assessment

The methodology followed to evaluate the flood extent maps from EFAS outputs is resumed in Fig. 3.4. The starting input parameters were the waterlevels from LISFLOOD for 100y return period flood event for the entire Po area.

First step of the methodology was the calculation of flood extent and depth map for the entire basin using the original input data: 100m DEM and CCM2 (Catchment Characterization and Modeling database) river network (left side of the flowchart). In these sections the approach to calculate the flood extent and depth map is explained.

Successively the defense measurements from ADBPO were added to the flood extent and flood depth map calculated in the first step.

In the third step (right part) the new DTM subsets were introduced. The line drainage network and

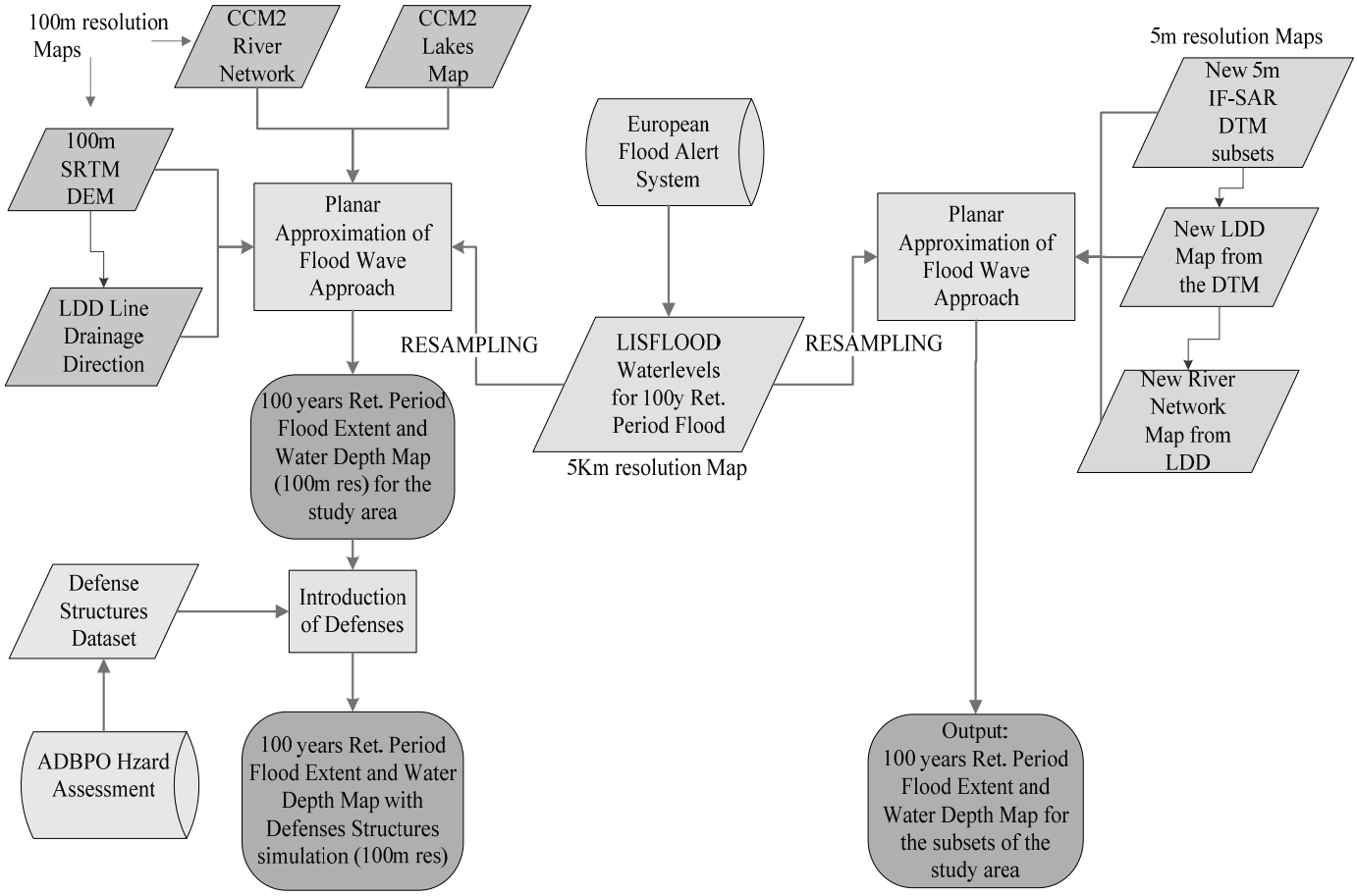

Fig. 3.1: flowchart of the flood extents and depths calculation.

the river network were extracted ex novo from the new DTMs and the flood extent and depth maps for the two available subsets were created.

The first part of the chapter describes the calculation of the original water extent map based on the 100m DEM and the simulation of the protection measures. The second part of the chapter shows the calculation of the flood extent and depth map based on the new DTM for two subsets of the Po area.

3.1. The Datasets Issue

Before the explanation in details of the procedure to extract the flood extent map, a description of input data is given. Due to the fact that the input data come from different sources, the first problem to be solved was the issue related to the Spatial Reference System.

When spatial data from different sources have to be analyzed, the first operations is to decide which coordinate system and projection has to be chosen among the different ones used in the different datasets. A brief introduction about the treatment of geographic data is needed. Among the geographic institutions of the European Commission the necessity of a common Spatial Reference System started to be discussed in December 1999 during the first workshop organized by JRC with the goal to ensure the compatibility of geographic data among Europe (Annoni et al., 2001). After the launch of the CORINE Landcover mission, the EUROSTAT (European Statistic Organization) started a new project called GISCO (Geographic Information System of the European Commission, EUROSTAT, 2005). Within the framework of the GISCO project, an extensive geo-referenced database has been developed. The database includes spatial information for Europe related to: topographic data (hydrography, altimetry, infrastructure data, administrative data), thematic data (land resources, environmental data, industrial themes) (Sadl, 2005). GISCO Project aimed at promoting the use of GIS and in becoming a reference centre in map production. On that basis the European Commission is preparing legislation able to improve the integration of spatial data in Europe. It is known with the name of INSPIRE (Infrastructure for Spatial Information in Europe, http://www.ec-gis.org/inspire). With this project European Commission set up the rules about: data collection and maintenance, data sharing, data understanding and interpretation (INSPIRE, 2007). When EFAS project started, the European Terrestrial Reference System 1989 Ellipsoidal Coordinate Reference System (ETRS89) was in use. Once the INSPIRE directive was available and in order to have consistency with other input

maps (like CORINE landcover map), EFAS team introduced the ETRS 1989 Lambert Azimuthal Equal Area Coordinate Reference System (ETRS-LAEA, see Tab. 3.1 for parameters).

Tab. 3.1: ETRS-LAEA definition parameters as they appear in ArcGIS 9.2.

Projection:	Lambert Azimuthal Equal Area	Angular Unit:	Deg. 0.0174532925199433299
False Easting:	4321000	Prime Meridian:	Greenwich (0.0)
False Northing:	3210000	Datum:	D_ETRS_1989
Central Meridian:	10.000000	Spheroid:	GRS_1980
Latitude of origin:	52	Semi major Axis:	6378137
Linear Unit:	Meter (1.000000)	Semi minor Axis:	6356752.3141403561
Coordinate System:	GCS ETRS 1989	Inverse Flattening:	298.25722210100002

Nowadays EFAS is still operating in ETRS89 coordinate system but, new projects, like the European Flood Potential Damage Assessment, are based on ETRS-LAEA Coordinate System. The input maps related to the present study have been re-projected in the ETRS-LAEA and all the outputs showed here follow the same specifications. In the Italian project SP1.1, spatial information represented by maps was originally created adopting the Universal Transverse Mercator Projection, zone 32N, referring to the European Datum 1950 based on the International ellipsoid of 1924 (Hayford).

3.2. Flood Extent and Depth Calculation

The first step in the hazard assessment section is the calculation o the flood extent map with the original input data as it was performed by the EFAS team.

The European flood potential damage assessment is carried out on the basis of the 100 years return period flood extent and water depth estimation with a horizontal resolution of 100m; therefore the flood parameters need to be extracted from the discharge calculations provided by LISFLOOD. Nowadays a wide variety of hydrologic model is available for flood simulation; from the one-dimensional finite difference solution of the full St. Venant equations, like the well known MIKE 11 (Liu et al., 2007), the TOPKAPI model (Bartholmes and Todini, 2005), to three-dimensional complex solutions of the Navier-Stokes equations (Li et al., 2005).Among these possibilities, the kinematic wave approach based on the 1-D solution of the St. Venant equations adopted in LISFLOOD 1D model is the simpler approach (see section 2.1.2). As already stated, LISFLOOD is one dimension model, the standard outputs are represented by discharge data; therefore to extract water extent and depth a further step is needed. In general, there are two main

possibilities: the application of a hydraulic two or three dimension model, or a geometric method based on the results of the 1-D models and a high resolution DEM. In the first case the previous codes are coupled with 2D models like MIKE 21 or other more complex models can be applied: an example is 1D-2D SOBEK (Usamah and Alkema, 2006). In the second case, the water depth values at each cross section location need to be integrated into a high resolution DEM and the inundation extent at the cross sections locations are linearly interpolated (Bates and De Roo, 2000). In this case the LISFLOOD model was applied with limited hydraulic parameters. Due to the operational scale the simulation with any 2D model was not allowed. Moreover, no cross sections were available to calculate flood extent based on high resolution DEM; therefore a methodology based on the planar approximation of the flood wave was used, in which the flood wave was considered as a plane and intersected with a 100 m resolution DEM. Bates and De Roo (2000) compared the results of the planar approximation approach with the results of 2D models and demonstrated that the geometric approach performed almost as well as the full two dimensional hydraulic model simulation. Starting from the work of Bates and De Roo, a methodology was developed to calculate flood extent and depth, applicable at European scale. The input parameters necessary to apply such technique are: 1) the water depth map representing the water level in the river channels for 100 years return period flood; 2) a high resolution DEM of the floodplain, the 100 m SRTM DEM; 3) the river network map and the flow direction map as secondary data extracted from the DEM; 4) the lakes mask map. The input maps (see Tab. 3.3) and the procedure are described in the following part.

Tab. 3.2: input maps for planar approximation approach.

Input map	Description	Spat. Res.	Source
wl.map	Water level for rivers cells in the Po basin	5Km	From LISFLOOD
dem.map	Digital Elevation Model of the Po area	100m	CCM2 database
ldd.map	Flow direction map of the Po area	100m	Calculated in PCRaster
river.map	River network of Po area	100m	CM2 database
Lake.map	Mask map with lakes larger than 1Km^2 in the Po area	100m	CCM2 database

3.2.1. 100 years return Period Flood Event Probability Estimation

In the study about the climate change impact on flood hazard in Europe, the simulations of temperature, precipitation, radiation, wind speed and humidity from HIRHAM Regional Climate Model were used by (Dankers and Feyen, 2008) to drive LISFLOOD model. To estimate the

probability of extreme discharge, the simulation consisted of a 30 years' time series corresponding to 1961-1990. They fitted a generalized extreme value (GEV) distribution (Coles, 2001) to the annual maximum values in each 5 Km pixel. GEV distribution is defined by the location, scale and shape parameters. Furthermore, a Gumbel distribution, a particular case of GEV with the shape parameter equal to zero, was applied. The validation was carried out by Dankers and Feyen (2008) by comparing the discharges with observations at 209 gauging stations across Europe in which daily time series of 30 years were available (covering the span 1960-1990 or 1970-2000). Finally, the discharge values for all the European rivers monitored by EFAS were extracted for the 20, 100, 200, 500 years return periods using the Gumbel distribution (Feyen et al., 2008). From the results of the above mentioned works, the 100 years discharges for the Po area were extracted in order to calculate the flood extent and depth.

3.2.2. Other Input maps

- **DEM, River Network Map, and Lakes Map**

The first version of the Rivers and Catchment Database for Europe (Vogt et al., 2003) was created in 2003, consisting in a database of river network and drainage basins including information about water bodies and catchment boundaries; it was based on a 250m DEM and homogeneous ancillary data covering the whole Europe from the northern Scandinavia to the

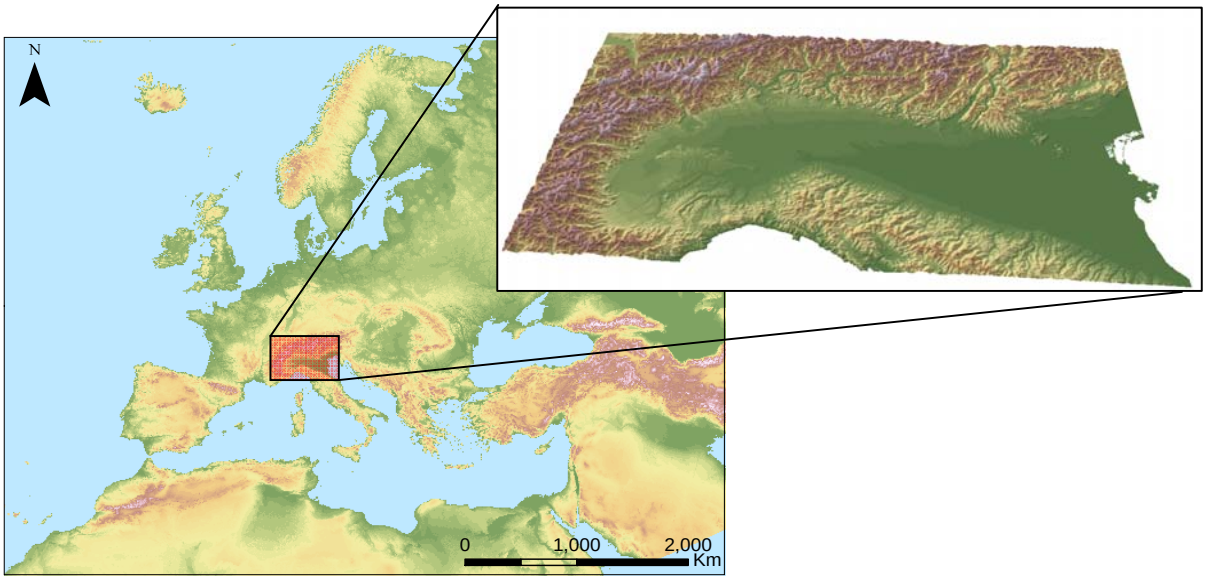

Fig. 3.2: 100m Mosaic DEM for Europe and Po area Subset.

Mediterranean Sea and from the Atlantic Coast to 38º Eastern longitude. In 2007 the second version of the database, CCM2, was created on the basis of a new 100m DEM and more adjunctive data, for a larger area including also Turkey and the Ural region (Vogt et al., 2007).

To create the CCM2 database, a new pan-European 100m DEM mosaic (see Fig 3.5) was generated on the basis of different elevation data: for Norway, Sweden and Finland, national elevation datasets with up to 100m spatial resolution or were used; USGS GTOPO 30 (USGS) with 30 arcsec spatial resolution for North-western Russia, Iceland and Shetland Islands; for western central and southern Europe, the SRTM (Shuttle Radar Tomography Mission) DEM with 3 arcsec spatial resolution (up to 60° 20′ Lat) was adopted. The cell size of the mosaic is 100m and the projection is the ERTS-LAEA according to the INSPIRE specifications.

The inland water body layer was created on the basis of the CORINE Landcover vector map: the classes corresponding to inland marshes, peat bogs, salt marshes, salines, intertidal flats, water courses, water bodies, coastal lagoons, estuaries, glaciers and perpetual snows were selected and integrated with the GISCO lakes layer and other databases. The final lakes map consisted in a representation of all the European water bodies with an area larger than 1 Km^2.

The river network was extracted from the DEM through the application of the algorithm suggested by (Soille, 2003). The errors in flat areas were corrected through the application of "adaptive drainage enforcement" and "forced burning" techniques: once detected the errors through comparisons of the results with validation data, consisting mainly of satellite images, the corresponding segments from the reference layers (local detailed drainage networks for instance) were selected as preferential or mandatory directions in the calculation of the new river network (Vogt et al., 2003).

From the CCM2 Database, the DEM, the European river network map and the lakes map were extracted for the Po basin at the resolution of 100m.

- **Local Drainage Direction Network Map (LDD)**

The flow direction map has been calculated in PC-Raster environment based on 100m DEM mosaic; the LDD (Local Drainage Direction) network is a derivative of the digital elevation model and represents for each pixel the downstream direction of flow over the elevation map, by a predefined code. This topological network is generated by an operator of the Dynamic Modeling language for models that incorporate transport of material. In PC-Raster environment, the flow direction is represented by a series of number-codes ranging from 1 to 9. Each of the nine numbers corresponds to the relative direction from the centre; number 5 represents pixels without flow direction, a pit (De Jong, 2005).

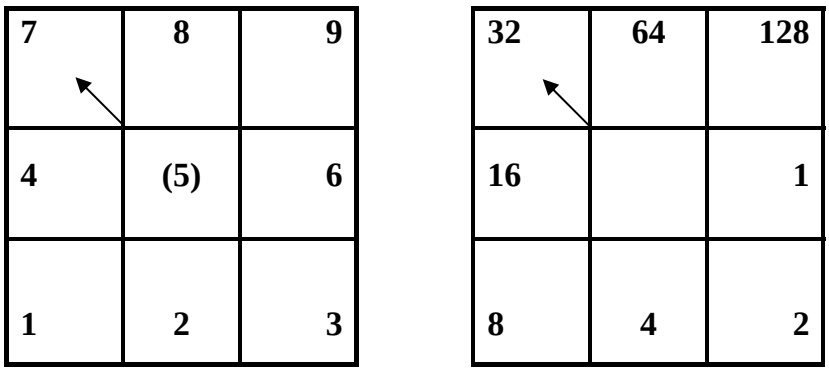

Fig. 3.3: Number codes for flow direction representation: PC-Raster (left side) ArcGIS (right side).

- **Water Level Map**

Finally the last input parameter is represented by the water level map. In the LISFLOOD model, an optional tool able to simulate the water levels in the channels is available (Van Der Knijff and De Roo, 2008). For simulations based on kinematic wave, only approximate water levels can be estimated from cross-sectional (wetted) channel area. The river cross section is described as a trapezoid and the flood plain as a rectangle; therefore water levels are dependent on channel width, side slope, and bankfull level. Once defined the geometry of the channel section and the floodplain (see Fig. 3.7), from discharge data, the area occupied by the water (cross sectional wetted channel area) at each time step is calculated. If the cross-sectional channel area exceeds the bankfull cross-sectional area (A_{bf}), the surplus is distributed over the floodplain (A_{fp}). From here, the water level on the floodplain is calculated and added to the channel depth to finally extract the final value of water depth ($D_{bf+}D_{fp}$ in Fig. 3.4).

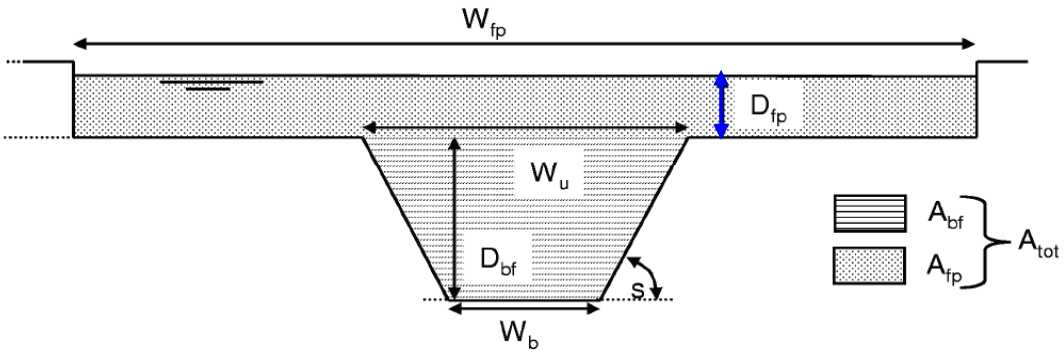

Fig.3.4:Channel geometry LISFLOOD waterdepth calculation (VanDer Knijff and De Roo, 2008)

In order to calculate water levels, the model needs information about bankfull channel depth (D_{bf}), channel width (W_u), side slope (S) and floodplain width (W_{fp}). Finally, in the output map, the value stored in each river cell is the theoretical water level in the channel (Van Der Knijff and

De Roo, 2008). Following this methodology, the waterdepth maps representing water levels for different return periods have been provided by EFAS team.

3.2.3. Planar Approximation Approach

The IES team studied a strategy, using the planar approximation approach of the flood wave, to extract flood extent and water level at 100m resolution from 5km cell size waterdepth map calculated by LISFLOOD. The following methodology has been developed in PC-Raster environment.

Because of the low spatial resolution of the SRTM-DEM, the rivers would not be fully visible in the DEM itself. Therefore the method is based on the assumption that the height in the SRTM at the location of the river represents the floodplain level. At the same time, the floodplain level which represents approximately the bankfull conditions (D_{bf} in fig.3.4), is assumed to be equal to 1 year return period flood waterdepth. According to this, the difference between the 100 years (Fig 3.5-1) and the 1 year return period (Fig. 3.5-2) waterlevels gives the approximation of the 100 years return period waterlevel exceeding the bankfull level (D_{fp}, blue arrow in Fig 3.4) that can be added, in the DEM, at the rivers location.

Following this line, the waterlevel exceeding the bankfull level for 100 years return period was provided for all the Europe. In the calculation of flood extent, only watercourses with a catchment larger than 500 Km^2 were considered (Fig. 3.5-3). Using as input the LDD network of the Po basin, all the catchments exceeding the threshold were extracted through the "*accuflux*" PC-Raster function. The waterdepth difference is masked with the river mask, and the final output is a map with 5km resolution representing the 100 years return period waterdepth exceeding the bankfull for rivers cells only (Fig. 3.5-4).

In order to combine the map of the previous step with the other input maps, it is resampled to 100m resolution. In this case a new LDD was created for the Po basin. The function LDD-repair was applied to create a sound-LDD; this operation changes the cell values of the unsound LDD in such a way that all downstream paths will end in a pit cell (De Jong, 2005) This function corrects problems due to sinks and connected cells with no output direction, and allows the LDD to be used in further analysis processes. The river catchments larger than 500 km^2 were extracted at 100m resolution using the river network from CCM2 database and the sound-LDD from the 100m DEM, with the same function described before.

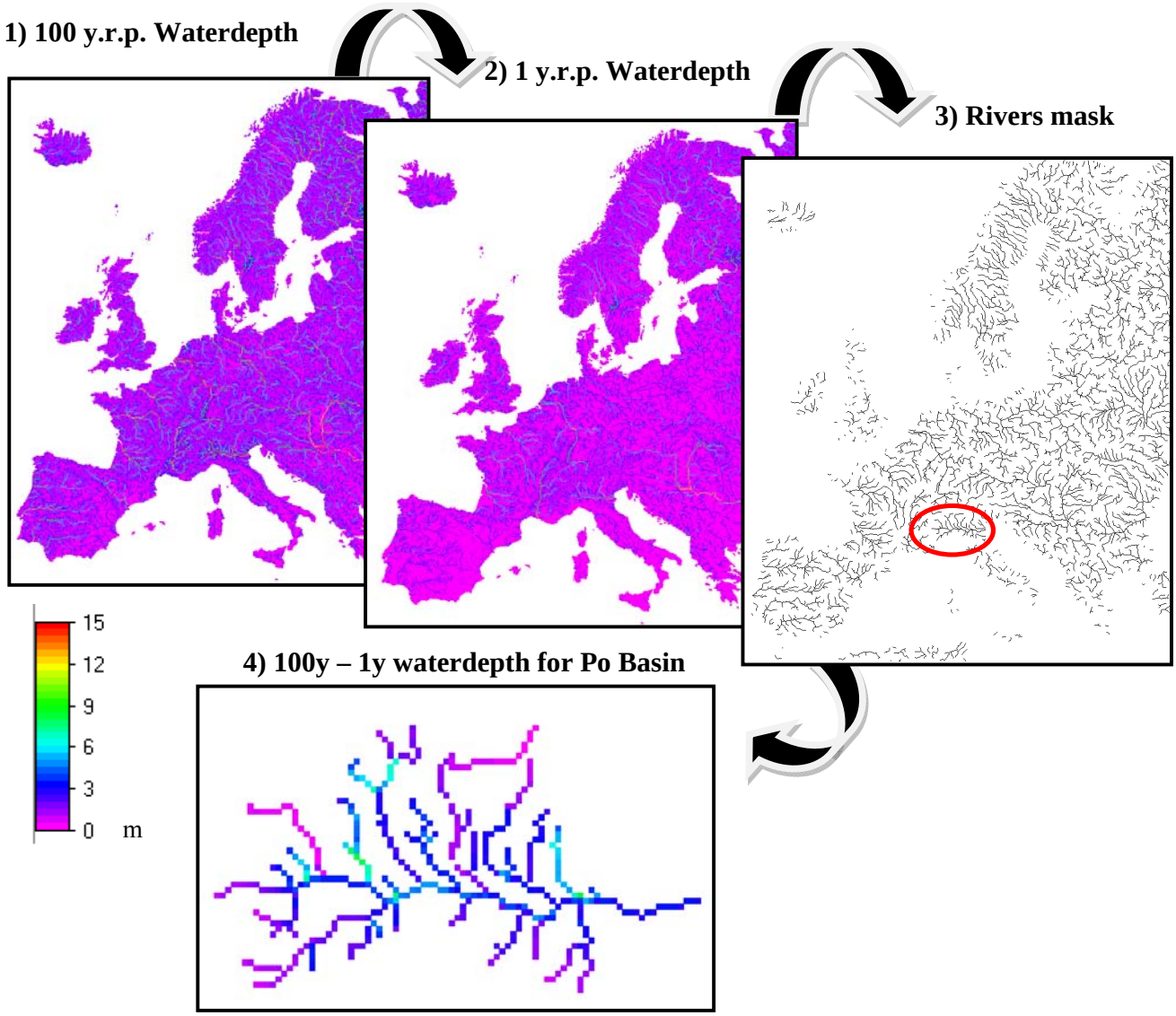

Fig. 3.5: Calculation of waterdepth for 100 years return period flood in Po catchment.

A modified LDD was produced by creating a pit in each river cell that belongs to the river network. The LDD can be easily modified by changing the number-code into 5 which represents a cell with no direction (see Fig.3.6). Due to the fact that the LDD has been modified with the introduction of the CCM2 river network, the pits (river pixels where the LDD values have been changed) sometimes are not located where exactly the river is. As a matter of facts, the CCM2 river network database, when overlapped with the 100m European SRTM based DEM, does not fit perfectly. In Fig 3.6 a subset of the Po area is shown where it is clear that the river bed is not

coincident with the drainage network. It means that the river channel is not located exactly where the topographic depression of the river is in the DEM.

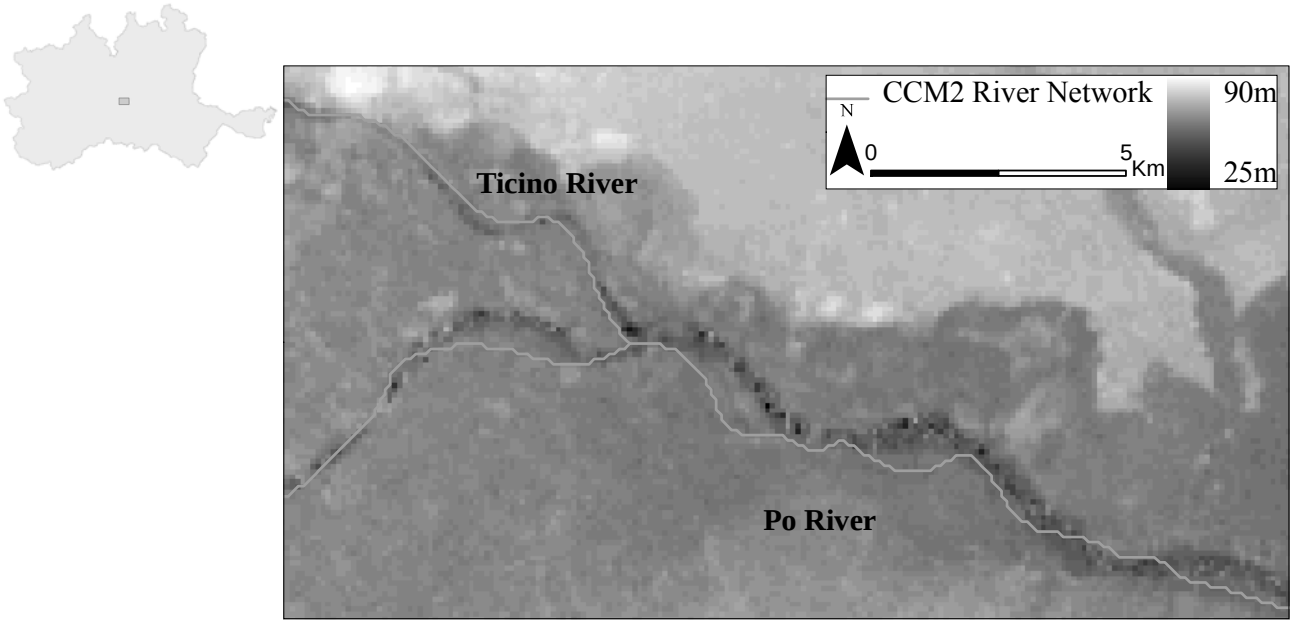

Fig. 3.6: Overlap of the CCM2 river network database (light gray line) on the 100m DEM.

The same problem is even enhanced in areas with high internal relief where the river channels from CCM2 are not in the valleys bottom; such imprecision can lead to wrong very high water levels. This fact was taken into account and corrected during the following steps of the procedure. For each river pixel, representing a pit in the LDD, the upstream area was calculated through the PCRaster function "*catchment*". A value representing the lowest point in each small catchment that belongs to each river cell has to be identified, in order to calculate the difference with the DEM. To avoid the problems mentioned before two maps were created: in the first one, the elevation of the lowest cell in each upstream area was assigned to the entire area itself; in the second one, the elevation of the river cell in the area was assigned to the entire upstream area. At this point, a threshold was fixed by the EFAS team: a floodplain which lies 5m below the river elevations was considered still acceptable; this is due to the presence, in wide European floodplains, of rivers with dikes systems higher than the surrounding floodplain, or due to the presence of back swamps that are morphologically lower than the river channel. If the value of the first map (lowest point in the catchment area belonging to the river cell) was more than 5 meters below the value of the second map then it was chosen; otherwise the value of the river cell was selected. Such value can be identified as the real water level in the DEM regarding that particular river cell upstream area. Once identified it, the difference between the DEM and the

value is calculated for each cell of the upstream area and a new map was created (for simplification the map will be called DEM-difference).

The successive step was to apply the water levels from LISFLOOD. The 5Km waterdepth map was re-projected from ETRS89 to ETRS-LAEA (see section 3.2.1) and then resampled to 100m resolution. Subsequently for each 100m river pixel the value of waterdepth was extracted from the 5Km waterdepth map. Due to the difference in the resolutions of the two, the 100m river network didn't match with the 5Km waterdepth cells datasets in the intermediate spots between two waterdepth cells (see Fig 3.7); hence the values had to be interpolated from the closest 5Km cell. The function "*spreadlddzone*" was applied. The expression identifies those cells from which the shortest friction-distance to every cell centre is calculated (De Jong, 2005); the expression has four main inputs: LDD, initial points map (representing the possible paths), initial friction distance (set at 0), and friction value (set at 1 = no friction in this case). Before to apply the expression, the map with only the values in the 100m river cells coincident with the 5km waterdepth cells is transformed into an ordinal map with value 0 instead of the no-data values where there is no river. This map is used as initial points map to drive the "*spreadlddzone*" expression. Once identified the closest value to the each river cell with no value, it was assigned to the cell in such way that all the 100m river cells had their waterdepth values. Afterwards, the values were extrapolated for all the upstream areas that belong to each 100m river cell. At this point, for each cell of those upstream areas, the difference between the height of the cell and the lowest height in the area corresponding to the river pit waterdepth in the river cell were known. (DEM-difference map, corrected as before), and the water depth in river cells were known.

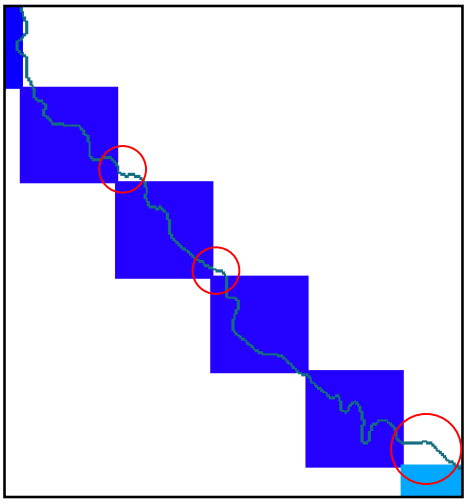

Fig. 3.7: Spatial relation between 100m CCM2 river network map and 5Km waterdepth map.

The flood extent was calculated by subtracting the DEM-difference map to the map with the extrapolated values. The result was a map with flooded areas represented by positive values; moreover the float values in the map indicate the waterdepth of the flood in meters. Further corrections were needed to refine the flood extent map: in the flooded areas, zones not connected with the river itself were included. To exclude those spots a map with equal identifier for the connected areas was created through the expression "*clump*" (boolean map with value "true" to the connected areas); with the expression "*areaarea*" the area value was assigned to each

connected area; finally all the areas under a certain threshold were excluded (the main flood area is the one that groups all the river network floods, obviously connected to each others). As explained before, the simulation of the flood events, carried out using LISFLOOD model, was not performed for the lakes and water bodies in general.

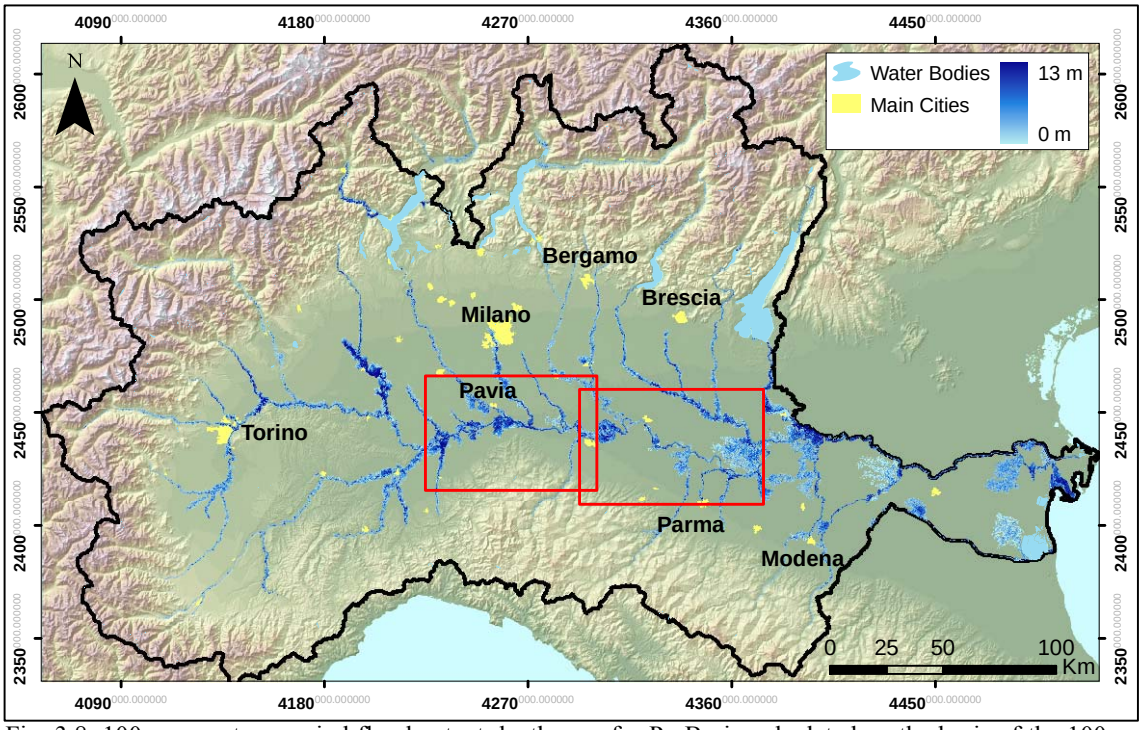

Fig. 3.8: 100 years return period flood extent-depth map for Po Basin calculated on the basis of the 100m resolution SRTM-DEM. In red the two subsets in Figs. 3.9 and 3.10.

The water bodies larger than 1Km^2 were therefore masked out using the dataset from CCM2 database. The flood extent was calculated for catchments larger than 500 Km^2. The rivers considered were, the Po River and 24 of its main and secondary, tributaries. On the left side: Pellice, Dora Riparia, Dora Baltea, Orco, Sesia, Cervo, Ticino, Lambro, Adda, Serio, Brembo, Oglio, Mella, Chiese, Mincio; on the right side: Maira, Stura di Lanzo, Scrivia, Treabbia, Taro, Parma, Enza, Secchia, Panaro. The total flooded area was estimated in 367,840 Ha. The water level exceeded the 13 meters in the deepest areas located on the Sesia watercourse, at the junction between the Po River and the Ticino River, at the junction between the Po and the Mincio River, and in other areas along the Po indicated in Fig. 3.8 through dark blue color. Two subsets of the main map are showed in Fig 3.9 and 3.10. Especially in the area next to the junction in fig 3.10, the large spread of the flood suggests that the calculation leads to inaccuracies if observed at detailed scale (see red circle).

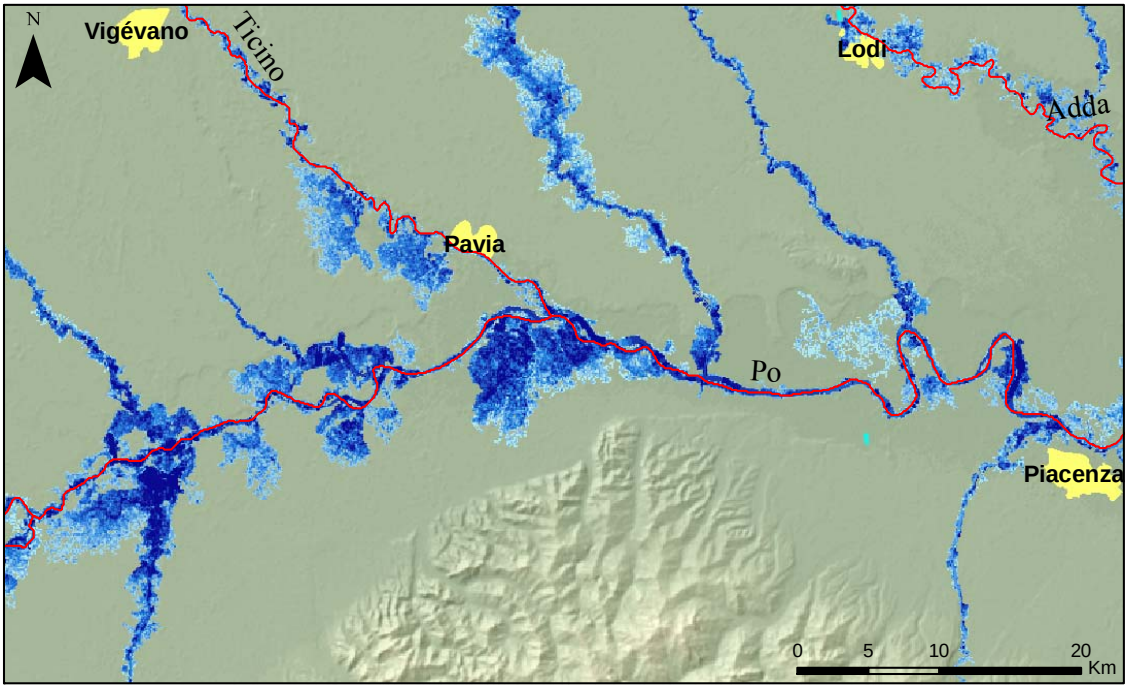

Fig. 3.9: Subset of the Flood Hazard Map illustrating the junction between the Po River and the Ticino River (in red, the river network)

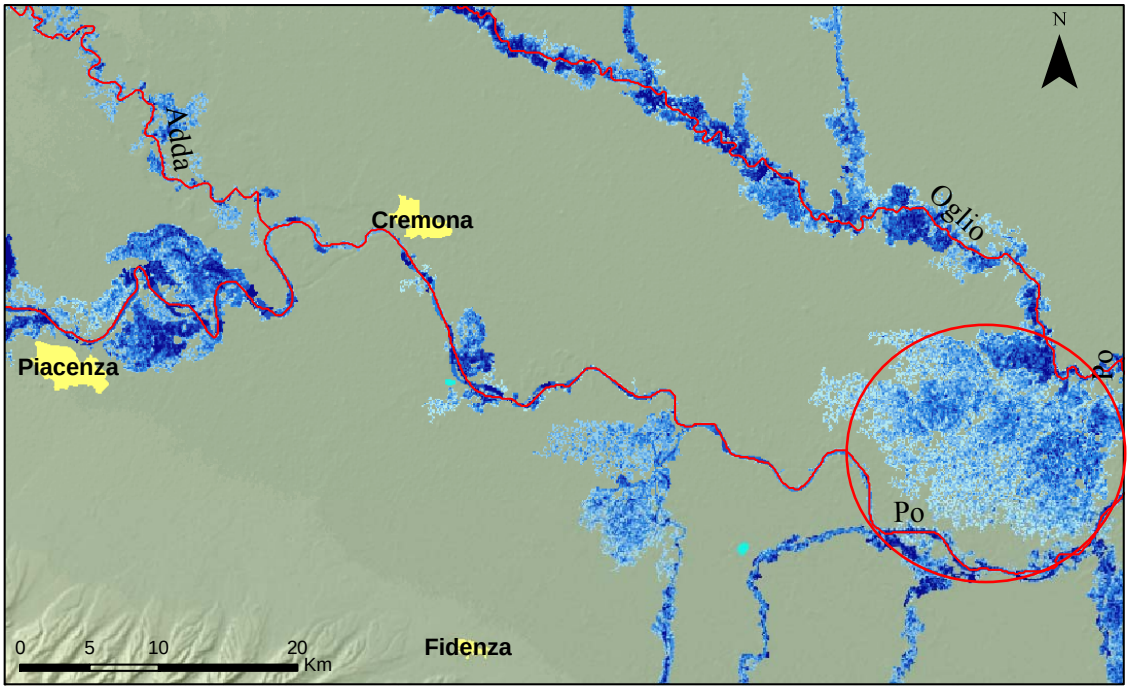

Fig. 3.10: Subset of the Flood Hazard Map illustrating the area of the Po river in between the cities of Piacenza and Cremona, and the junction between the Po River and the Oglio River River (in red, the river network; red circle: unexpected large flood spread).

The possible sources of errors will be treated in depth in the next chapters, after the comparison with the reference hazard study. But at this point, some steps in the methodology can be already commented. In the explanation of the planar approximation approach, in order to take into account the difference between the watercourse in the 100m DEM and the corresponding stream in the CCM2 river network, the correction was applied to those areas that were more than 5 meters below the river network. It means that, if the real river in the DEM does not fit with the CCM2 river network and the height difference between the real river elevation and the elevation at the nearest point of the CCM2 river network is less than 5 meters, for instance 4m, the waterlevel will be applied in a spot with an elevation 4m higher than the elevation in the river itself. Considering the fact that the difference between the 100 years and the 1 year return period water level ranges from 1m to 9 m in the highest points; inaccuracies up to 5 meters can lead to wrong flood extents estimations.

3.3. Simulation of Protection Measures

This section illustrates the overall methodology to reach the first research objective (see section 1.4.1) related to the introduction of the defense measures in the methodology for calculation of the flood extent developed by EFAS team.

Due to the 5Km horizontal resolution at which EFAS operates, the introduction of any data related to the protection structures in LISFLOOD model section was impossible; hence the data available were introduced in the flood extent and depth calculation through the strategy explained in this section. After having calculated the flood extent map through the methodology of EFAS team, the simulation of the effects of defense measures was carried out. The database containing the protection structures for the entire Po area was extracted from the reference hazard study of the Po basin Authority (ADBPO; section 2.6).

When we talk about river engineering measures, we consider a wide variety of structures that aim regulating the water flow and the sediment deposition of the water courses. According to (Mangelsdorf et al., 1990), the general category of river engineering measures can be divided into two main groups

- Flood alleviation works: traditional and environmental methods to limit the flood extent in the adjacent areas to the water courses in periods of high or extremely high discharge rates.
- Regional channel stabilization: including erosion control options and aggradation control options. Structures that aim at avoiding erosion/aggradation of the river channel, they act on

the normal river flow by modifying the morphometric properties of the channel, like the slope gradient or the shape of the vertical channel sections.

For the purpose of this research, only the first class of structures is described in details. Next to the traditional methods of increasing flood capacity, in the last years more advocated environmental options were taken into consideration. (Hey et al., 1990) evaluated the engineering and environmental performances on flood alleviation schemes in a case study in England and Wales.

TRADITIONAL METHODS

- Resectioning: it consists of dredging and/or widening the main channel to increase the in-bank discharge capacity, bed slope can be steepened to increase flow velocity with a consequent augment of flood capacity. In urban areas rectangular channels can be built due to limited space; to protect banks, vertical sheet piling, concrete or masonry walls are constructed to line the channel.
- Realignment: In association with restrictioning measures, the channel can be straightened to increase the longitudinal slope gradient; this increases the flow velocity and therefore the flood capacity.
- Adjacent flood banks: The construction of flood banks, dykes or levees is the most common solution for flood control; the can have different nature: natural materials (mainly clay, blocks or other impermeable materials covered by vegetation to increase the stability) or concrete and other artificial materials, especially in highly populated areas. These are placed close to the river; therefore they need to be higher than distant flood banks to ensure the same level of protection.

ENVIRONMENTAL METHODS

- Flood relief channels: this technique consists of constructing channels next to the main course to divert flow above a given stage away from the main channel; they can be dry in low flow periods. This structure has the advantage to leave intact the natural channel; it can be realized where enough space is available.
- Partial dredging: the dredging involves only a limited central section of the river to increase the cross sectional area. This solution is selected mainly in those river streams with shallow riffle sections.

- Two-stage channels: This system is created through the excavation of berms adjacent to the river channel; the berms can be as wide as the meander belt. The natural low-flow is preserved while the flood capacity is increased through the space created by the flood berms.
- Distant flood banks: In lowland areas without any space limitation, the flood banks (levees, embankments, dikes) can be placed at some distance from the main channel (often at the edge of the meander belt). They are mainly realized using natural materials and they are protected by vegetation. It is common the construction of a road on top of them. Their height and width can vary depending on the dimension of the river; usually they are lower than the adjacent flood banks.

In the present research, the considered protection measures consist of adjacent and distant flood banks. This is due to different reasons. The methodology to extract flood extent takes into consideration only the water level; therefore it does not have sense the introduction of such defense measures that act at directly changing parameters like flood velocity or sediment load. The data collected from the reference study only include a dataset regarding levees and embankments and a dataset of artificial channels. Due to the resolution at which the calculations were performed the second dataset was not taken into consideration. In this research the words: levee, dike, bank, and embankment have therefore the same meaning.

3.3.1. Classification of the Protection Measures

The levees database from ADBPO consisted in vector CAD files containing linear features representing single longitudinal structures: in the layer, artificial and natural levees, embankments and concrete dikes were included. Those files were not linked with any attribute table; information related to the nature of the structures, their effects on the flood propagation, and the conditions of preservation, were stored in a series of reports. The files were extracted and converted into ArcGIS shape-files without any ancillary data. The extraction of data related to the height of the levees was not possible, due to the lack of this information in the descriptive reports; moreover the descriptions in the reports were not judged reliable because related to the time period in which the study was carried out (1995-1997). From the same study, the flood extents for events with return periods of 20, 100, 200 years were available.

The structures layer as extracted by the reference study could not have been useful for the purpose of this research, due to the lack of information about the levees height. A further step was required: in order to have meaningful information from the available data, a classification of the structure based on the relations with the three flood extents was carried out. The three flood extents were overlapped on the structures layer. Three classes were detected based on the

protection of the defenses against the three different flood extents. The segments that were overlapped by all the flood extents were removed; the ones overlapped by the 100 and 200 years r.p. flood extents were classified as “active for 20 years r.p. flood”, and so on for the other two flood maps. Figs 3.11 and 3.12 show the final classification of the defense structures.

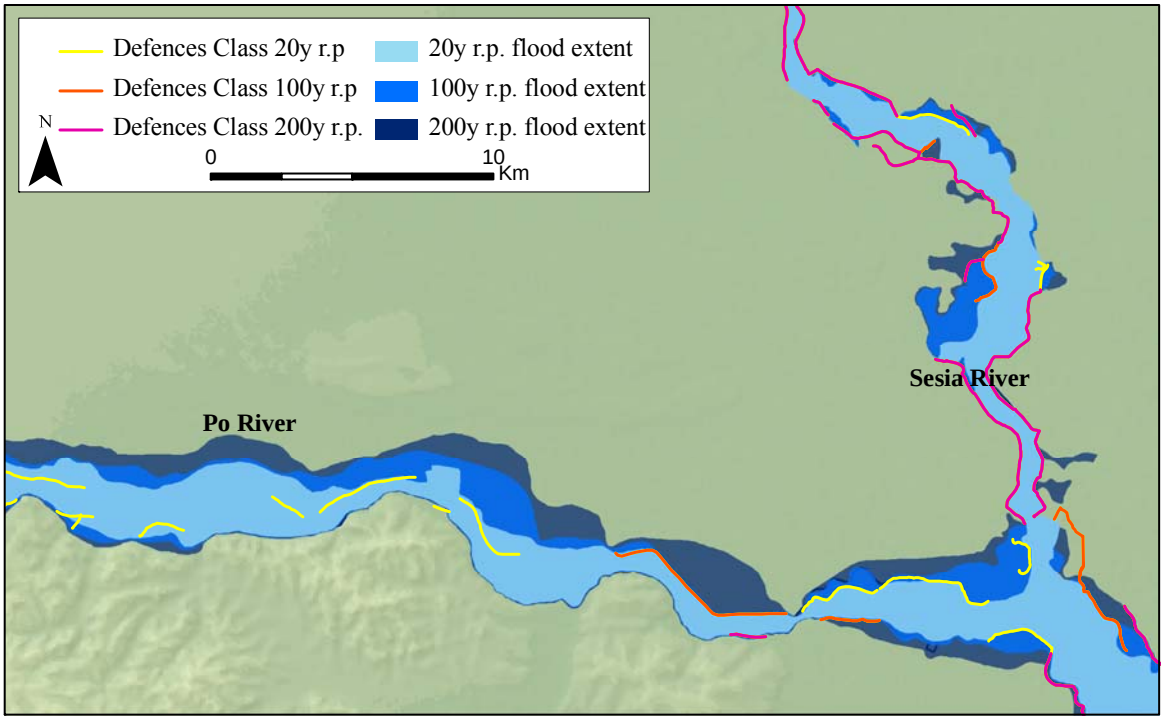

Fig. 3.11: Classification of the defence measures according to the relations to the flood extents.

This classification was performed ad hoc for the purpose of the research. It aimed at introducing the effect of the levees in the calculation of the extent related to the 100 year return period flood event through a geometric method based on the planar approximation approach of the flood wave explained in the previous sections. Therefore the use of this classification for different purposes is not possible. No others solutions were applicable in this situation.

Finally, the two classes 100 and 200 years r.p. were merged together. The resulting dataset represented the structures acting as protection against at least a flood event with a probability of 1 into 100 years.

The length of the protection structures for each class is listed in table 3.3; the comparison of this dataset with the data provided by the Po Basin Authority (ADBPO, 2006) gives a value of the goodness of the built dataset.

The official data published by the Po Basin Authority slightly differ from the dataset extracted; this is probably due to the different period of data collection: the hazard study was completed at the end of 1997, while the official data were published in 2006.

Tab. 3.3: summary of the defence measures dataset extracted from the reference hazard study and the comparison with the ADBPO official data.

Structures Class	Length in Kilometers
20 years return period	99.5
100 years return period	303.0
200 years return period	2989,8
Total	3492.3
From ADBPO	3466

3.3.2. DEM Correction and Flood Extent Calculation

As stated in section 3.2.3, the flood extent calculation is based on the relation between the height information from the DEM for the upstream area of each river network pixel and the waterlevel calculated by the LISFLOOD model. In order to simulate the defense measures, a certain elevation value was added directly in the DEM at the location of each feature.

The structures dataset was converted into a raster file with the same horizontal resolution of the SRTM-DEM (100m). This operation introduced inaccuracies in the water extent calculation; embankments and levees are unlikely to have sections with dimension of 100m, hence this operation overestimated in general the horizontal dimension of the structures. The maximum value in the map representing the difference between 100 years return period and the 1 year return period was 9.5 meters. In order to simulate the protections in the SRTM-DEM, a value higher than 9.5 meters (15m) was added in the DEM itself at the location of the defenses classified as safe for return period of 100 and 200 years.

With a simple GIS operation, at each 100m cell representing the protection structures, the elevation in the DEM was increased of 15 meters.

The result of the operation is illustrated in Fig. 3.12. The modified DEM was introduced in the final part of the procedure explained in section 3.2.3. When the waterdepth values were extrapolated from the river network cells to the upstream areas the difference between the height of each upstream cell and the waterdepth value was calculated using the modified DEM. The initial part of the calculation in which the LDD was modified and the upstream areas were calculated for each river network pixel was not changed; this expedient was necessary to avoid the fact that the original upstream areas would have been changed by the introduction of the

defense measures in between the areas themselves and the river network. The results of the operation were not satisfactory. The cause was certainly the difference in the resolution of the different datasets used: the procedure was carried out with a resolution of 100m, while the original dataset of the structures was realized by mapping the levees on the basis of a topographic map with a 1:10.000 scale.

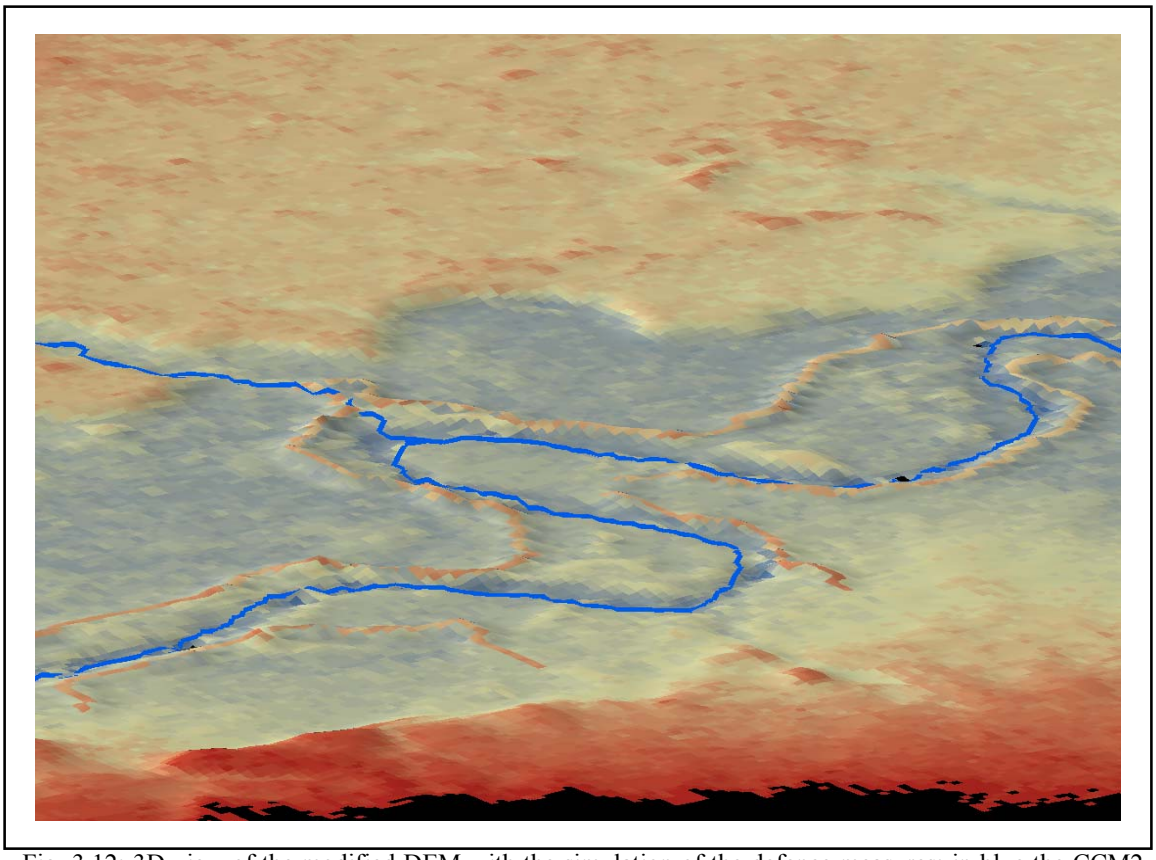

Fig. 3.12: 3D view of the modified DEM with the simulation of the defence measures; in blue the CCM2 river network. The view represents the junction between Po and Ticino Rivers.

The accuracy of the structures dataset and the fact that the levees were mapped using vector files allowed the engineers that realized the structure dataset to map each part of the features in detail; when the same dataset was rasterized at 100m resolution, it happened that many of the details of the structures were lost;

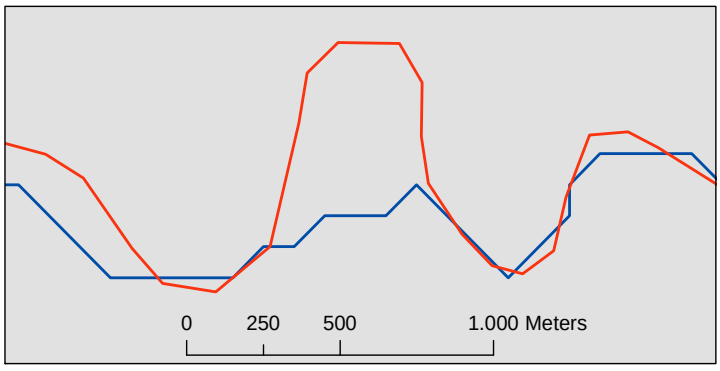

Fig. 3.13: Difference between CCM2 river network (blue) and ADBPO river network (red) for a particular of the Dora Riparia River in the city of Turin.

due to such loss, when the calculation was performed, some lowland areas under the protection of the levees were still connected to the main flooded areas in between the levees. No automatic correction was found for this problem; therefore the areas in which those errors happened were manually masked.

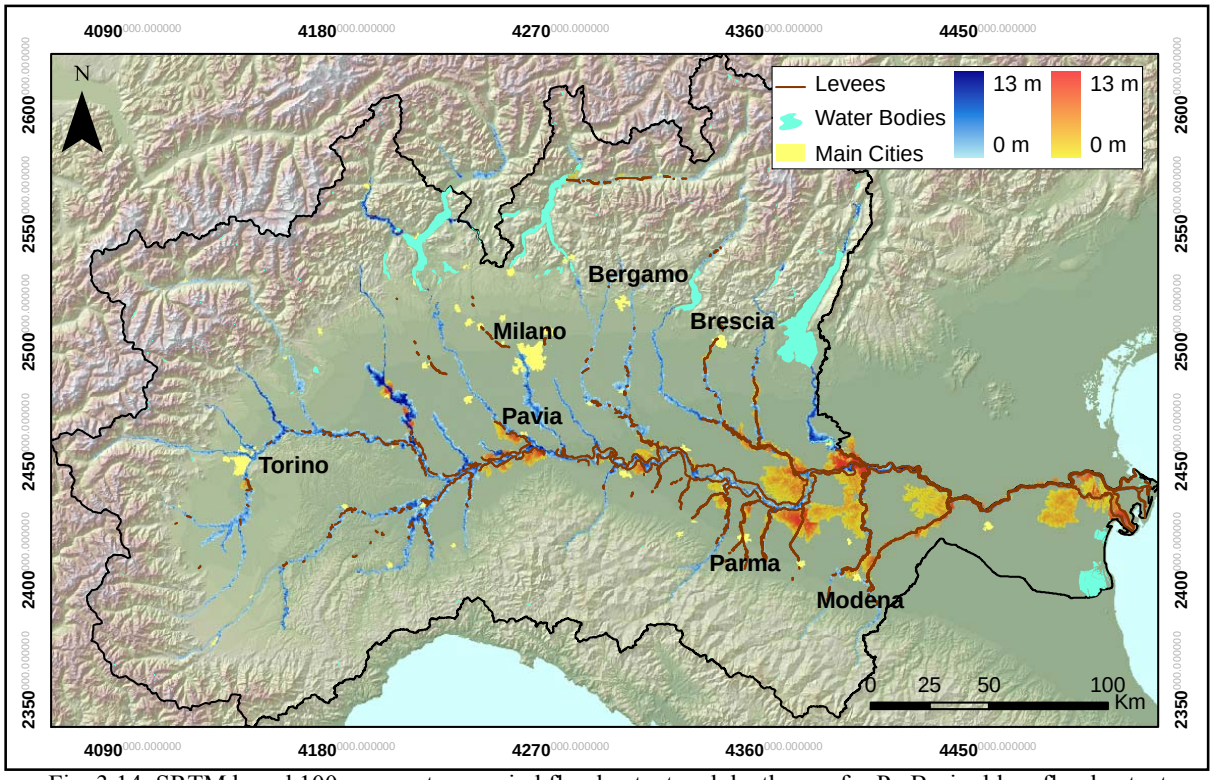

Fig. 3.14: SRTM based 100 years return period flood extent and depth map for Po Basin; blue: flood extent with simulation of defence measures; orange: flood extent without simulation of defences (fig. 3.8).

The final map is showed in Fig 3.14. The calculation of the water extent was performed using the river network from the CCM2 database; such database was realized on the basis of the 100m DEM described in section 3.2.2. The database of the protection structures was created on the basis of the ADBPO river network; if the two river network datasets are overlapped, they show differences in various areas (see Fig. 3.13). It is likely to consider the ADBPO river network more accurate, even if the statements cannot be verified. Such difference becomes significant in the upper areas of the catchments, where the water courses width, and the distance between the levees, where present, is comparable to the raster resolution at which the calculation was performed. In the dataset from ADBPO, protection structures mainly present in the lowland floodplain areas were mapped; hence the final result could be still considered reliable for the lowland flooded areas. Only in the case of the Sesia, Dora Baletea, and Dora Riparia rivers the high presence of mapped structures made the calculation not reliable.

3.4. Introduction of new Digital Terrain Model

This section of the research shows the application of the flood extent and depth calculation developed by EFAS team to the new high resolution elevation datasets regarding two subsets of the Po basin (objective 2, see section 1.4.2).

A brief introduction on the terminology is given, to better understand the data description. Different representations of elevation are nowadays available: from vector based data like contours maps or surface representation through triangular irregular networks (TINs), to raster based data like the common digital elevation models, in which the elevation value is stored in each cell of the raster grid. In this work only the last elevation data type was used. Among this category, three main acronyms are used to identify elevation models with different characteristics:

- DEM (Digital Elevation Model) represents a general grid of elevation data without any specifications on the nature of the represented relieves. It is mainly used for data with a medium-low horizontal resolution (> 30m) that does not allow the separation between the bare earth and other features like vegetation cover and buildings; examples are the 30 meters and 90 meters SRTM DEMs.
- DSM (Digital Surface Model) is used when elevation data correspond to a mixture of bare earth, vegetation, buildings and structures in general. In the case of If-SAR (Interferometric Synthetic Aperture Radar) or LiDAR (Light Detection And Ranging) sources, it represents the first object hit by the microwaves for radar or by the beam for LiDAR.
- DTM (Digital Terrain Model) means the elevation related to the bare earth; in the case of If-SAR it is extracted from the DSM through appropriate software.

Terrain information is usually the weakest part of flood models. In the term terrain information, both detailed information on land cover and terrain elevation data are included. The land cover provides information on the resistance to the water flow, while the elevation models allow calculating the downward flow of flood flux. (Sanders et al., 2005).

In the methodology developed by EFAS team, no data related to the land cover is involved; therefore the possible improvements should regard the two main input data: the waterdepth map from LISFLOOD and the elevation model which the extraction of the flood extent and depth is based on. The waterdepth map is outside the research field of the thesis; therefore the only improvement can derive from a higher quality in the elevation model. For this reason, a new elevation model was tested to calculate the flood extent and flood depth.

3.4.1. Data description

EFAS team evaluated the possibility to acquire more accurate elevation models for different purposes, including the flood hazard assessment. According to the scale of the EFAS project, the hypothetical dataset had to homogeneously cover the entire extent of Europe.

Intermap© Company (http://www.intermap.com/) is one of the worldwide most specialized providers of elevation models; during the last years it launched the NextMAP® Europe Program ending in 2009; the aim of this project was to provide a 3D high resolution digital mapping for the Western Europe from Iberian Peninsula till Ural Mountain range (http://www.intermap.com/uploads/1173138612.pdf). The technology adopted is the extraction of high resolution images and digital elevation models from airborne Interferometric Synthetic Aperture Radar (If-SAR). This technique has been widely tested for flood mapping purposes with excellent results (Sanders, 2007; Sanders et al., 2005). Intermap's IFSAR system, called STAR-*3i* is a 3cm wavelength, consists of X-band If-SAR operating on a Learjet commercial aircraft.

Fig. 3.15: Shaded relief of the new Intermap If-SAR DTM (on top) compared to the 100 DEM. Black

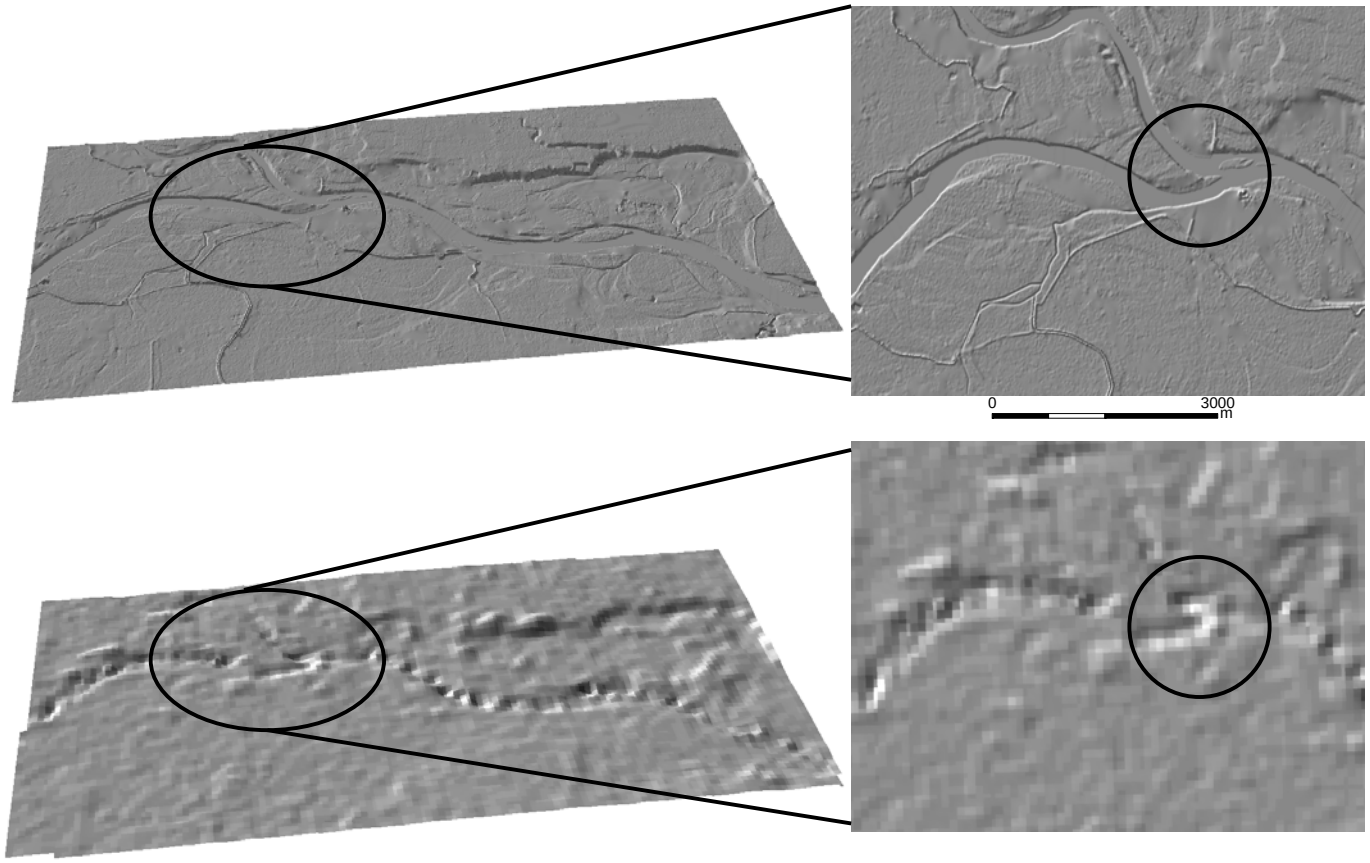

circles highlight features removal from DTM: a bridge visible in the DEM has been removed in the DTM.

This IFSAR sensor collects flight lines approximately 10 km in the across-track and 50-200 km along track at a coverage rate of 100 km2 every minute (Tighe, 2003). The IFSAR system generates an orthorectified radar image and an elevation model. The elevation model represents the elevation values from the first surface hit by the radar, for example tree tops and building tops. Therefore, this elevation data is referred to as DSM. Intermap has developed in-house software, called TerrainFit® that uses the first surface elevation values to derive a DTM from its STAR-3i system. This is an automated software package that uses a hierarchical pyramid surface fitting approach (Coleman, 2001). The DTMs derived from Intermap's NEXTMap European mapping program, have a horizontal resolution of 5 meters and a vertical accuracy RMSE of 1 meter (InterMAP©, 2008).

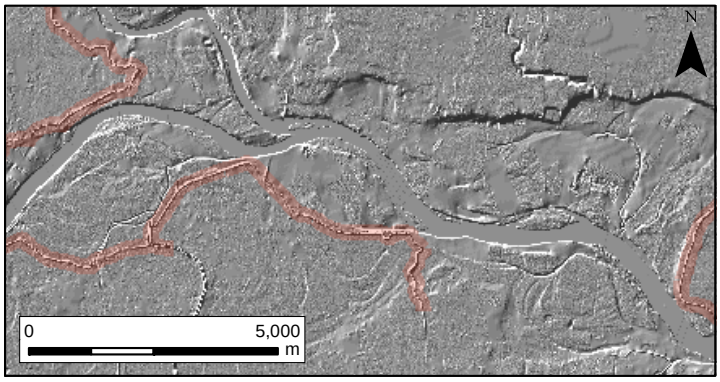

Fig. 3.16: Shaded relief of the new DTM; the levees are highlighted in red.

Intermap provided two subsets of the Po basin with a total area of 500 Km2. From the Intermap DTM, the vegetation and the buildings (including all kinds of structures like bridges, (see Fig. 3.13) were removed. This fact highly improved the use of such product for flood hazard evaluation. Another added value of the 5m DTM compared to the 100m DEM is that the levees next to the main rivers (Po and Ticino in the case) were well detected. This is due to the fact that the levees protecting main rivers are likely to be wider than the resolution of the DTM. In Fig. 3.16 the dykes' dataset from ADBPO was projected on the DTM subset; as clear from the image, the levees are well represented in the DTM and they perfectly fit with the ADBPO dataset.

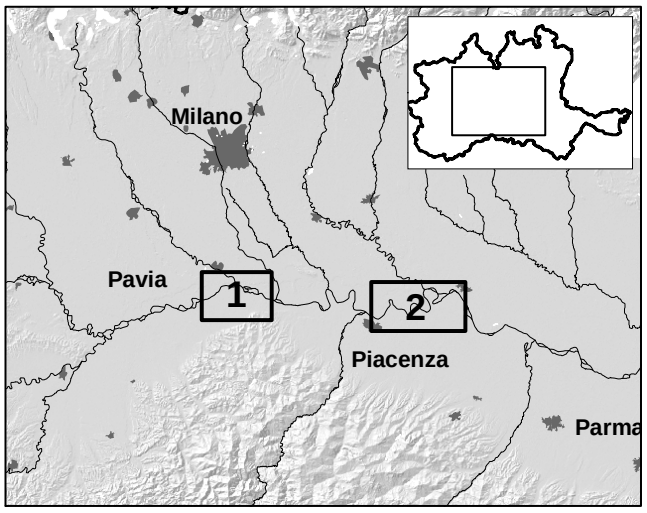

Fig. 3.17: location of the two subsets in the Po Basin.

Moreover, in the DTM the water level in the river channels is always clearly visible and homogeneous while in the 100m DEM, the streams are not carved out except for the

wider part of the Po and few other main rivers. Furthermore, where the river is visible, it often happens that waterlevels for contiguous pixels show unreal differences, due to the coarse resolution and to the sensor's limitations (100m DEM is derived from the 90m SRTM DEM through a space borne radar sensor, while the DTM comes from an airborne radar sensor).

Both the two subsets include the Po River; the first one (see Fig. 3.17) is at the junction between the Po River and the Ticino River, a 150 Km^2 natural flat area with different landcover classes including cultivated land, forests and discontinuous urban areas. This subset was chosen because it well represented the Po catchment river environment with a wide floodplain and a system of river terraces bordering it (visible in the northern part of the subset Fig. 3.15-16). The junction represented a good check point for the methodology; moreover the levees system located in the area (see Fig. 3.16) could represent a test for the improved hazard maps. The second subset represents the area between the cities of Piacenza and Cremona. The area was chosen for more reasons: the EFAS team has historical discharge data for the stations of the two cities and the DTM will be used to assess flood hazard with a 2D model in the coming months. A hydroelectric power plant is located in the river stream. The plant acts as a proper dam and drastically changes the hydrologic behavior of the river. Due to the operational scale (5Km), LISFLOOD model does not take into account the effect of such structures; therefore, by calculating the flood extent and depth in the area, the performance of the methodology applied to the new DTM could be evaluated when main structures exist on the river. As final remark about the choice of the subsets, the availability of data from Intermap was restricted to less than 500 Km^2 in total and not all the Po basin area was available.

3.4.2. Flow Direction Map and River Network Map Extraction

In order to apply the technique developed by EFAS team in calculating flood extent and depth, two products had to be derived from the DTM: the flow direction map and the river network map. The calculation of the maps was carried out in ArcGIS environment and then exported to PCRaster format.

The flow direction map is a derivative of DEMs in general; it represents for each pixel the downstream direction of flow over the elevation map; it is the equivalent to the LDD map in PCRaster language. The difference between the two maps consists of the coding of the directions through code numbers (see section 3.2.2 for details on the local drainage network and the direction codes). Afterwards the map was reclassified using PCRaster direction code numbers and exported into ASCII file. From this file the conversion into PCRaster format (.map) was possible through the PCRaster function "*asc2map*".

The river network map was calculated in ArcGIS environment. From the flow direction map the Flow Accumulation Map was extracted; this map represents the number of upstream cells that flow into each cell. In this map the stream cells have a number much higher than their upstream cells, due to the fact that all the water (in the case of river network calculation, it could be sediment or runoff or any other flowing material) coming from upstream areas flow to the downstream part of the DTM through them. Thresholds were defined to identify all the stream cells (above 10.000 due to the high number of cells in the DTMs: ca. 4000*2000 and 7500*3500 in the two subsets). The flow accumulation map was then transformed into a Boolean map with value 1 for the cells with a flow accumulation number higher than the predefined threshold (Tarboton et al., 1991). The river network map showed all the stream features in the DTMs; the majority of those features represented small irrigation channels and trenches that were detected in the DTMs due to the high horizontal resolution. Those features should not be included in the water extent calculation to avoid strange results. Therefore the features were converted into vectors through the application of the "Stream to Feature" function in ArcGIS' Spatial Analyst tool. This function converts into vectors the stream network segments on the basis of a stream raster map and a flow direction map, to optimize the process (Jenson and Domingue, 1988). From the vector file the stream order was extracted following the Strahler's Classification (Mourier et al., 2008), in which the stream order increases in the case of an intersection of streams with the same order. The minor streams where removed and only the main streams (the Po and the Ticino Rivers in the first subset and the Po and the Adda River in the second subset) were converted again to raster. Finally the DTM, the flow direction map and the river network map were converted into ASCII files and imported in PCRaster for flood extent calculation.

3.4.3. Flood Extent and Depth Calculation

To calculate the flood extent and depth from the new input maps the same methodology explained in section 3.2.3 was basically followed, with some corrections due to the different source of input data. A brief resume of the technique is provided: the upstream area for each pixel of the river network was calculated through the LDD map. The waterdepth from LISFLOOD was applied to the river network cells. The difference between the elevation of each pixel in the upstream areas and the waterlevel corresponding to the river pixel stated whether the pixel was flooded, the result gave also the water level in case it was flooded. The waterlevel used was the result of the difference between the 100 years return period flood waterlevel and the 1 year return period flood waterlevel, like in the original methodology.

With the new DTM many inaccuracies faced in the calculation with the original 100 DEM were solved. In the original methodology the main problem was produced by the fact that the CCM2 river network map, in a few spots, didn't fit exactly with the DEM (see section 3.2.3). In the case of the net DTM, the river network map was calculated ex novo directly from the DTM itself. No further corrections in the calculation were needed.

On the other hand, one of the problems encountered was related to the calculation of the upstream areas for the river network cells at the corners of the images. The river flowed from the left part to the right part of the area; therefore the outlet point of the LDD was on the right side of the DTMs; it happened that few areas in the corners of the DTMs were not connected to the main outlet point in the river network, because their "flow direction to the river" passed outside the area represented by the DTM. Therefore they were excluded from the calculation. To avoid that fact, the waterdepth value of the closest upstream area was given to those areas. The solution is somehow an assumption of the waterdepth, but those areas were located in the corners far from the river and mainly in higher positions in respect to the river hence not prone to floods. If the DTM had been available for the entire Po basin this problem would not have existed.

Finally the flood extent and depth map for 100 years return period flood event was calculated using original waterdepth map; the lakes mask map was not used because in the two subsets no water bodies were present. The result is shown in Fig 3.18, top map. In the figure the new map is overlaid on the 100 years return period flood hazard map from ADBPO (pink colour in transparency). The water extent calculated clearly underestimated the flood event according to the reference study. The main problem was found to be in the waterdepths from LISFLOOD. In fact, the assumption that the height at the river location corresponded to the floodplain in the SRTM-DEM stated that the waterdepth at the rivers locations was equal to 1 year return period in the SRTM-DEM; hence the difference between the 100 years and the 1 year return period water levels was used to calculate the flood extent and depth (see section 3.2.3). This solution was found well performing in the case of the 100m DEM, but it didn't provide acceptable results in the case of the new DTM. The main reason was that, in the 5m DTM, each stream is well carved out; the waterdepth in each channel represents the real waterlevel at the moment of the radar images acquisition. Furthermore the image seems to be acquired in a low-flow period; hence the waterdepth in the rivers is much lower than the 1 year return period. In order to find the best waterlevel representing the real waterdepth in the river at the moment of the acquisition, new waterdepth differences were calculated. During their studies on climate change impact of floods in Europe in 2008, Dankers and Feyen statistically calculated, through simulations with LISFLOOD model, the waterdepths for 1, 3, 5, 25, 35, 40, 45, 50, 60, 65, 75, 97, 98, 99

percentiles of waterdepths from the 30 years discharge records series (see section 3.2.1 for deeper explanation of the statistical calculations). The 50 percentile waterdepth means that such waterdepth is reached or exceeded 182.5 days of the year by the waterdepths calculated by LISFLOOD based on the 30 years discharges historic series; the 90 percentile waterdepths indicates that it is reached or exceeded 36.5 days every year and so on. Waterdepths differences calculated for the various percentiles were used to perform the flood extent and depth map for the two subsets of the Po basin.

The results were validated using the 100 years return period flood hazard map from the (ADBPO) reference study; the validation was carried out using a formula suggested by (Bates and De Roo, 2000).

$$Fit(\%) = \frac{IA_{ref} \cap IA_{calc}}{IA_{ref} \cup IA_{calc}} \times 100 = \frac{5233.4 Ha}{(5233.4 + 47.1 + 1131.7) Ha} \times 100 = 81.6\%$$

Where IA_{ref} is the inundated area of the reference study and IA_{calc} is the inundated area calculated with the technique based on the planar approximation of the flood wave. This formula calculates the accuracy of the flood extent map on the basis of the flood extent only, and it takes into account both overestimations and underestimations; the waterdepth could not be assessed because no reference information was available. The best results were achieved for both the subset areas using the difference between the 100 years return period waterdepth and the 50 percentile waterdepth (see section 4.2 for detailed description of the results). In Fig. 3.18 flood extent map calculated using the original waterdepths (100y – 1y return period waterdepth) and the map calculated from the new waterdepths (100y return period – 50perc waterdepth) are shown for the first subset; the flood extent map calculated with the new waterdepth gave a fit of ca. 82%. The calculation and the results will be widely discussed in the next chapter.

In annex A, the application of the same methodology on a different high resolution DTM (2.5m) is shown. The results will be evaluated by EFAS team in order to assess the validity of waterdepths calculated from LISFLOOD at European scale.

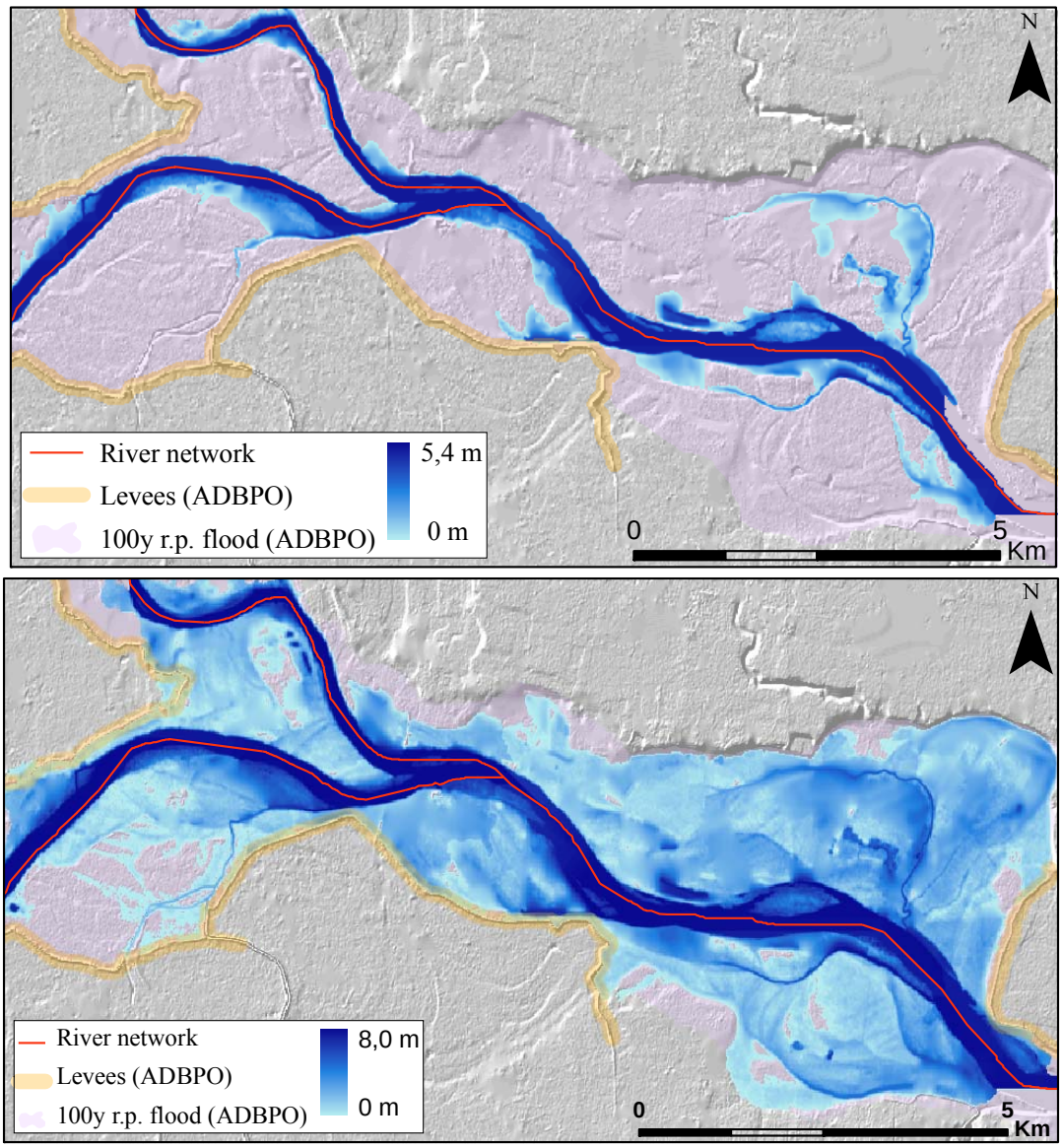

Fig. 3.18: Flood extent map calculated with original waterlevel (on top) and with new waterlevel (bottom).

4. Results from Hazard Assessment

In this chapter, the results regarding the hazard assessment improvements are evaluated trough the comparison with the maps realized in the previous steps and the reference hazard study from the Po Basin Authority (ADBPO). In the first part of the chapter, the original flood map calculated from EFAS' model waterdepths using the 100m DEM, and the flood map calculated from the same source with the introduction of protection measures using modified 100m DEM are, in turn, compared to the reference study from ADBPO. In the second part, the results from the comparison between the reference study (ADBPO) and the flood maps based on the new 5m DTM are described.

4.1. Assessment of 100m DEM based hazard maps

To assess the accuracy of the two maps produced (EFAS-SRTM DEM 100m flood water extent and depth map showed in fig 3.8, and the same map with the simulation of protection measures, fig. 3.12) were compared to the 100 years return period hazard map extracted from the reference study from Po Basin Authority (ADBPO). The comparisons were carried out only considering the water extent; no validation for water level information was available because the ADBPO hazard study did not include data related to waterdepth.

The two EFAS-SRTM DEM 100m flood extent and depth maps previously calculated cover all the Po basin area at a resolution of 100m, while the reference hazard map is represented by vector files digitized on a base map with a scale of 1:10.000; moreover not all the watercourses analyzed in the reference study were analyzed in the calculation of flood extent from EFAS outputs, and vice versa. This was mainly due to the fact that, for the maps calculated in this research, all the rivers with catchments larger than 500 Km^2 were considered; while for the reference hazard assessment by the Po Authority, a team of experts decided where to carry out the analysis on the basis of their knowledge of the area.

To make the comparison meaningful, the common areas for both the flood maps from EFAS and the reference flood map from ADBPO were identified. The first step was to convert the vector file of ADBPO hazard map to a raster file with the same resolution of the other maps (100m). The conversion obviously introduced some inaccuracies, but the resulting error was negligible, as shown in tab. 4.1.

The second preparatory step was the definition of the common areas. The map from ADBPO and the maps calculated during the research (see section 3.2) were overlapped and the areas not in common were excluded.

Tab. 4.1: conversion from vector to 100m raster of ADBPO flood extent map.

Flood extent map from ADBPO	Area in Ha
Vector Map	218.726,3
Conversion to 100m raster map	218.659
Error	0.03%

From the ADBPO 100 years return period flood extent map, the following watercourses were excluded: the Pellice Torrent, the Varaita Torrent, the Elvo Torrent, the Cervo Torrent, the initial stream of the Agogna torrent before the junction with the Maira trench, The initial part of Tredoppio torrent, the first part of the Olona Torrent until the junction with the Bozzente Torrent, the Torrents Nure, Chiavenna, Arda, and Stirone in the area of Parma and the Parma Torrent.
From the 100 years return period flood extent map (and the map with the introduction of the protection measures) the following water courses were excluded: the upstream section of the Sesia River (the first 23 Km ca.), the Olona Torrent, the upstream sector of the Trebbia River, the upstream area of the Bormida Torrent, the upstream area of the Taro river before the junction with the Ceno torrent; also the Po Delta area from the diversion of the river into two course (the Po and the "Po di Volano") to the mouth in the Adriatic Sea was not included in the analysis of Po Basin Authority; therefore it was masked from the EFAS map. Tab. 4.2 shows how much for each map was masked.

Tab. 4.2: comparable area between ADBPO and EFAS 100m flood extent maps in Ha.

(Ha)	Total	Considered in the Comparison	% Excluded
ADBPO Map	218659	197434	9,7%
EFAS Map	367840	323427	12,1%

4.1.1. Comparisons with the reference hazard study

The comparison was initially carried out at municipally level: the dataset of the municipalities was extracted from the NUTS/LAU (Nomenclature of Territorial Units for Statistics/Land Administrative Units) European database; it consists in a database of the European territory based on the hierarchical classification of regions in different levels (Luck and Knors, 2007). For Italy the classification is: (NUTS-0) Italy, (NUTS-1) Groups of Regions, (NUTS-2) Regions, (NUTS-3) Provinces, (LAU-1) null, (LAU-2) Municipalities, as it appears in the official EUROSTAT website. The Italian LAU-2 dataset was provided by EFAS team in vector files. The number of municipalities affected by flood (the common flooded areas to be compared) was 979 (see annex 1 for more details). For each municipality the flooded area from each map was calculated. The municipalities were classified based

on the elevation of their centroid in three classes: 1) below 150m, 2) between 150 and 300m, 3) above 300m. The purpose of this classification was to assess the performance of the hazard assessment at different elevations. The inaccuracies in representing the topography in the 100m DEM due to random noise, speckle effect, or presence of vegetation that decrease its vertical accuracy, ~10m RSME (Sanders, 2007), are more influent in flat areas than in areas with a higher internal relief.

This comparison doesn't have a real spatial meaning because, for each municipality, the assessment was carried out by comparing the sums of the flooded areas for each hazard map (a spatial comparison between the map from ADBPO and the map calculated using EFAS team's methodology will be showed afterwards). It is my belief that, due to the high accuracy of the ADBPO hazard assessment carried out at local scale, only a spatial comparison with the EFAS hazard maps at European scale couldn't provide meaningful information; while in this way, the general weak points in the EFAS hazard assessment can be more easily pointed out. In annex B the results of the comparison for the main municipalities is shown in detail.

The results of this comparison are summarized: in table 4.3 for the EFAS-SRTM 100m flood hazard map, and in table 4.4 for the EFAS-SRTM 100m flood hazard map with the introduction of the protection measures.

Tab. 4.3: Results of comparison between ADBPO 100years return period flood extent map and EFAS 100years return period flood extent map in Ha.

Ha	SUM ADBPO food extent	SUM EFAS flood extent	DIFFERENCE (EFAS – ADBPO)	Percentage of ADBPO detected by EFAS
Overall	197434	323427	125993	164%
Below 150m	143987	275107	121120	191%
150 – 300m	39312	36228	-3084	92%
Above 300m	14135	13953	-182	99%

Tab. 4.4: Results of comparison between ADBPO 100years return period flood extent map and EFAS 100years return period flood extent map with introduction of the protection measures in Ha.

Ha	SUM ADBPO food extent	SUM EFAS flood extent	DIFFERENCE (EFAS – ADBPO)	Percentage of ADBPO detected by EFAS
Overall	197434	159414	-38020	81%
Below 150m	143987	109233	-34754	76%
150 – 300m	39312	34467	-4845	88%
Above 300m	14135	12853	-1282	91%

Successively, a spatial comparison was performed between the ADBPO hazard map, and the two EFAS-SRTM 100m hazard maps calculated without and with the introduction of the defence measures for the common area. The comparison was carried out by classifying, in turn, the two maps into Boolean maps (ADBPO: 0 = non-flooded, 1 = flooded; EFAS: 0 = non-flooded, 2 = flooded). In fig.

4.1 the spatial comparison between ADBPO map and EFAS map without defences is shown. The sum of the classified maps is a map with 0,1,2,3 values; 1 stands for the areas underestimated by EFAS hazard maps, 2 represents the overestimations of EFAS hazard maps, and 3 is the matching part.

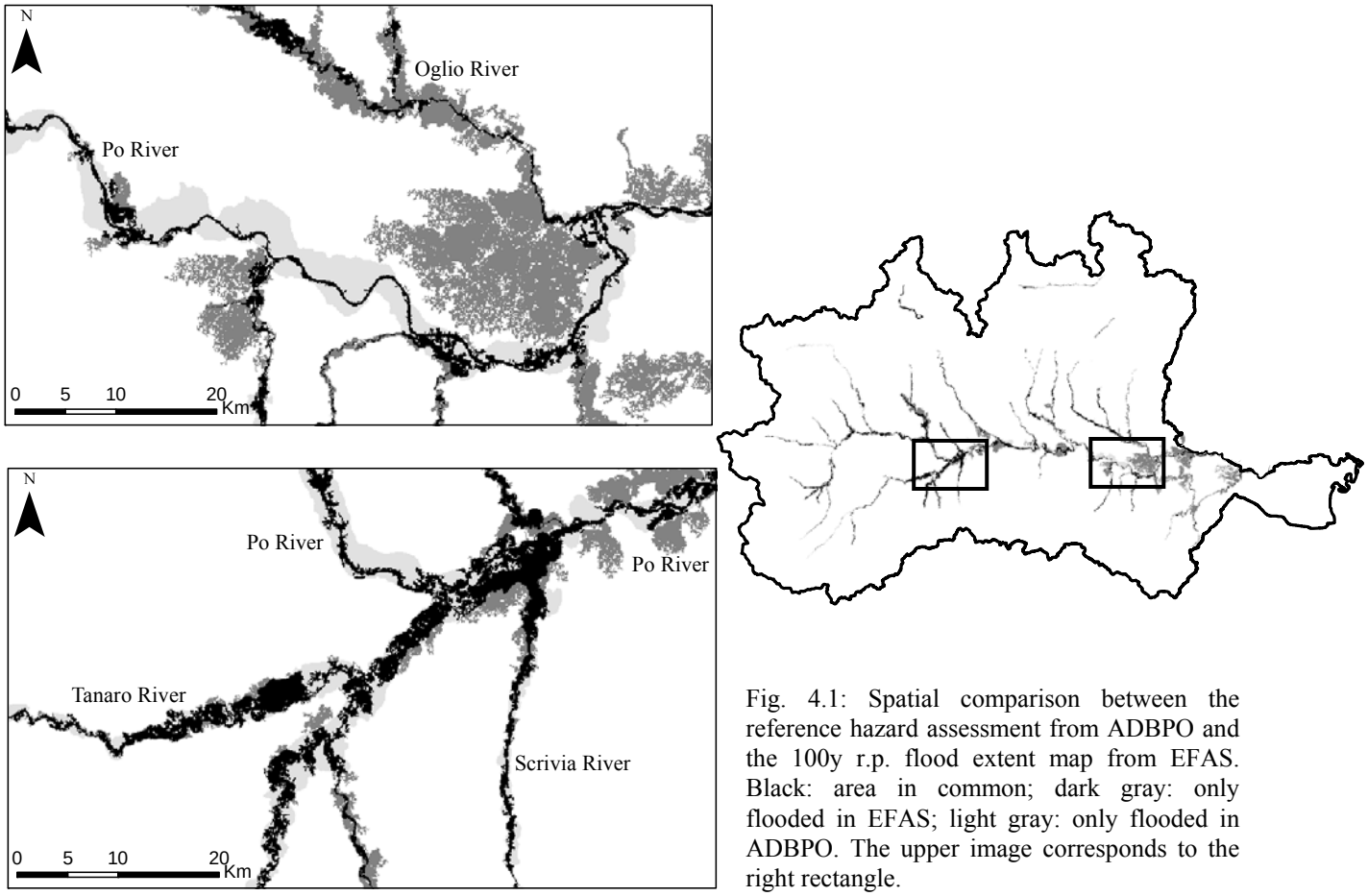

Fig. 4.1: Spatial comparison between the reference hazard assessment from ADBPO and the 100y r.p. flood extent map from EFAS. Black: area in common; dark gray: only flooded in EFAS; light gray: only flooded in ADBPO. The upper image corresponds to the right rectangle.

The formula showed in section 3.4.3 was used to measure the fit of EFAS flood extent maps with the ADBPO map. In tab. 4.5 the results are listed for the assessment of EFAS-SRTM 100m flood extent map without measures and in tab. 4.6 for EFAS-SRTM 100m flood extent map with measures.

Tab. 4.5: results of spatial comparison between ADBPO map and EFAS map without defences in Ha.

(Ha)	Not Flooded in EFAS	Flooded in EFAS
Not flooded in ADBPO	7309950	2) 217412
Flooded in ADBPO	1) 91388	3) 106046

$$Fit(\%) = \frac{IA_{ref} \cap IA_{calc}}{IA_{ref} \cup IA_{calc}} X100 = \frac{3)}{1) + 2) + 3)} X100 = 25{,}6\%$$

Tab. 4.6: results of spatial comparison between ADBPO map and EFAS map with defences in Ha.

(Ha)	Not Flooded in EFAS	Flooded in EFAS
Not flooded in ADBPO	7478101	2) 49261
Flooded in ADBPO	1) 93243	3) 104278

$$Fit(\%) = \frac{IA_{ref} \cap IA_{calc}}{IA_{ref} \cup IA_{calc}} X100 = \frac{3)}{1) + 2) + 3)} X100 = 43{,}0\%$$

The tables 4.5 and 4.6 have some inconsistencies. The purpose of the introduction of the protection measures was to remove the flooded areas in EFAS-SRTM 100m flood hazard map protected by the levees; therefore the only changing value in the tables should have been number 2. If the tables are carefully analyzed, the areas flooded in ADBPO and not flooded in EFAS-SRTM 100m hazard map increased, and the areas where both the maps were flooded slightly decreased. The explanation for these errors is the following: when the levees dataset was rasterized with a resolution of 100m, obviously all the cells corresponding to the levees in the flood extent map were considered not flooded. The assumption that the levees were at least as wide as one cell (100m) produced the above mentioned errors.

The results in tabs 4.5 and 4.6 clearly show the improvement introduced by the simulation of the protection structures. Those improvements came from the exclusion of the areas which were flooded in EFAS-SRTM 100m flood hazard map and not in ADBPO (the areas outside the levees active for a 100 years return period flood event). The matches (tabs 4.5, 4.6) calculated in this way does not show if the low accuracy depends on a general overestimation or underestimation by the flood extent map calculated.

If the results from the spatial comparison (tabs. 4.5 and 4.6) are analyzed together with the results of the comparison at municipality level carried out in the first part of this section (tabs. 4.3 and 4.4), more aspect can be discussed. The EFAS original flood map highly overestimated the flooded areas in lowland (tab. 4.3, 191%). When the defence measures were applied, the EFAS flood hazard map underestimated the flooded areas in lowland (tab. 4.4, 76%). In upstream areas (>150m), the estimation was acceptable; the simulation of the defence structures introduced very small changes in the estimation of flood extent in upper areas (from 92% to 88% for areas in between 150 and 300m; from 99% to 91% for areas with elevation higher than 300m). The main conclusion form the data evaluated is that the methodology developed by EFAS team has the main problems in flat areas where the overestimation of the flood extent was produced by the unexpected spread of floods in certain areas caused by the absence of existing defences (see fig 4.1, upper image). When the defences were applied, and therefore those unexpected errors were excluded in the areas protected by defences systems, the EFAS methodology seemed to underestimate the flooded areas.

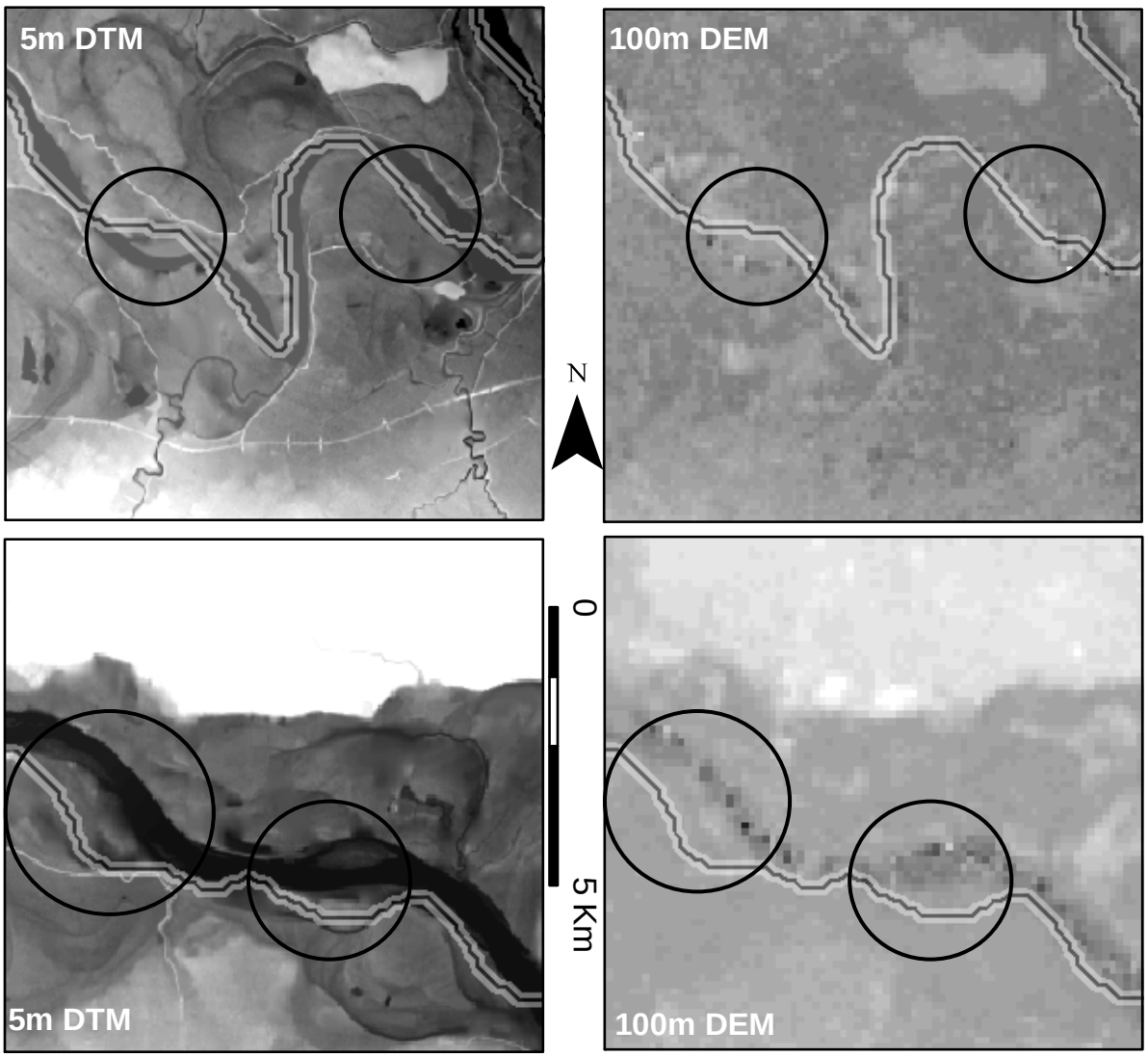

Fig. 4.2: Two subsets of the PO River. The black line represents the CCM2 river network while the black circles show where the river network does not fit with the 5m DTM and the 100m DEM.

In the last analysis, in the upstream areas the simulation of the flood extent has good results (see tab. 4.3); the scale at which the calculation of the flood extent and depth map is carried out (it is calculated by EFAS team for all the Europe at once!) widely justifies the differences between the reference map and the map calculated through EFAS team's methodology In downstream areas (especially the last 350 kilometres of the Po river and the Ticino River) the quantity of water, according to the 100 flood simulation calculated through the EFAS team methodology, seems to be not sufficient to produce a flood with the extent comparable to the reference map (ADBPO) in large parts of the main watercourses. As explained in section 3.2.3, the calculation was based on the assumption that, due to the low resolution of the SRTM-DEM, the rivers were not really visible, and therefore the elevation at the location of the rivers was the floodplain height. The assumption is valid for the majority of the streams in the catchment; but the Po and the Ticino watercourses are carved out in the SRTM-DEM due to their dimension (see fig. 4.2 and 4.3). The level of the rivers in this case is lower than the floodplain, therefore the assumption leaded to underestimations described before.

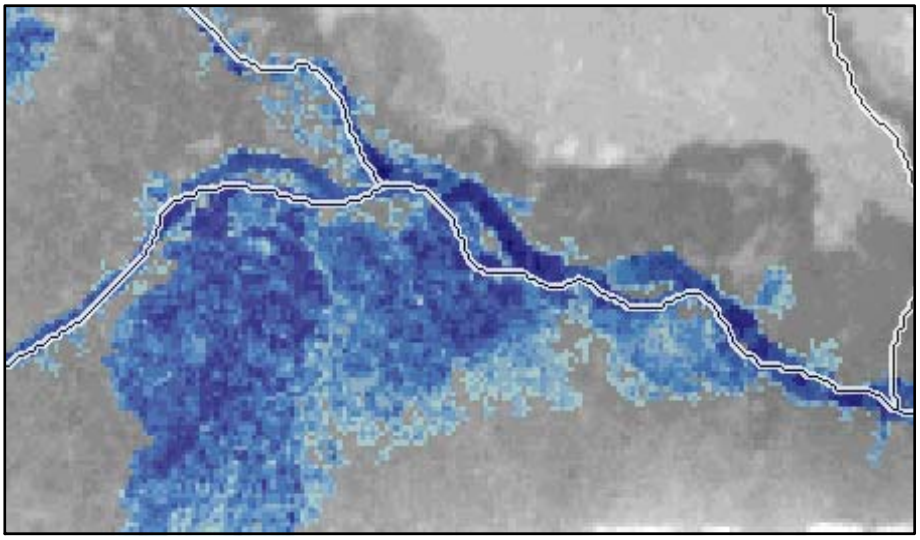

Fig 4.3: Effect of the inaccuracies of the CCM2 river network on the calculation of flood extent and depth (junction between Po and Ticino Rivers.

But in the same downstream areas, the flood spreads over wide areas in such way that the overall estimation of the flooded regions in those areas is exaggerated. One of the causes of the wrong estimations highlighted is related to the the inaccuracies in the CCM2 river network database. In fig. 4.2 two subsets of the Po River (in the areas covered by the DTMs) show the relations between the CCM2 river network and the two elevation models. The CCM2 river network seems to divert from the real river when the river itself generates secondary streams next to the main one. The CCM2 was produced on the basis of the same 100m DEM with the introduction of ancillary data (like different river networks), those data were probably enough accurate to represent also those secondary streams and therefore, when introduced in the extraction of the river network, they drove the procedure to calculate the CCM2 European river network through those small streams instead of through the main river. EFAS team introduced in the methodology, corrections for errors produced by those kinds of inaccuracies as explained in section3.2. According to this correction, the errors produced by the non-fit of the river network with the river in the SRTM DEM were corrected only if they exceeded the threshold of 5m. If such errors are less than 5 meters, the resulting flood extent is miscalculated. Moreover, even if this correction provides a right value for the waterdepth, this waterdepth is applied in a wrong place like is shown in figure 4.3.

4.1.2. Landcover analysis in flooded areas

The 100m mosaic DEM used in the calculation of the flood extent and depth map is produced on the basis of the 3-arcsec SRTM DEM. In vegetated areas, the surface reproduced in the DEM is the canopy surface. (Bourgine and Baghdadi, 2005) stated that for sparse vegetated areas the bias of 3-arcsec SRTM DEMs is 2.3m while for dense vegetated areas the bias rises up to 8m compared to the canopy top from LiDAR data in dense equatorial forests. Those possible biases summed to the height of the vegetation can lead to important errors in case of flood hazard assessment with SRTM based DEMs. Due to this reason an analysis of the land covers in the flooded areas was carried out; the two maps considered in the analysis were the reference 100 years return period flood extent map from the

Po Basin Authority (ADBPO) and the 100 years return period EFAS-SRTM 100m flood extent map without the simulation of defence measures. The analysis of the landcover was carried out on the basis of CORINE (Coordination of Information on the Environment) landcover dataset (De Lima, 2005). This part of the study wanted to assess which are the most predominant land covers in flooded areas. The diagram in figure 4.4 shows the distribution of different land covers for the selected maps related to the lowland areas (lowest municipalities' class). The graphs show how 25% of the reference flood extent map from ADBPO is covered by broad – leaved forests (according to the CORINE codes) and the 13% of the landcover is represented by shrubs and herbaceous vegetation. In the EFAS-SRTM 100m flood extent map, the forested regions cover only the 5% of the entire flooded area, while the shrubs are the 4%. The fact is visually shown if the flood extent map is overlapped on the CORINE landcover: within the levees belt, most of the areas next to the river occupied by forest are not flooded. Not enough information lead to state that the wrong representation of forested areas by the DEM produced errors in the flood extent calculation; but it is likely to consider it reliable.

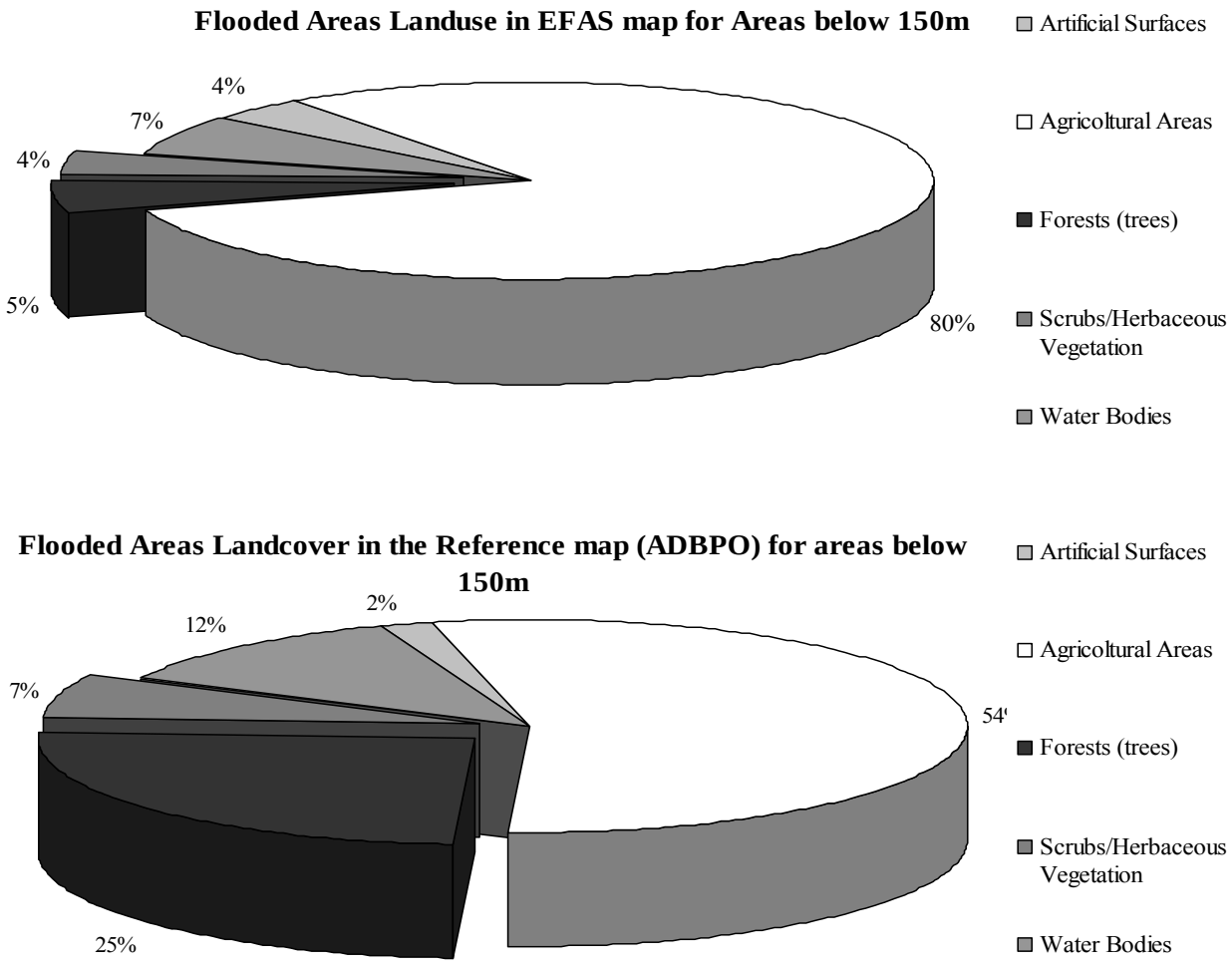

Fig. 4.3: diagrams showing the landcover distribution in the 100 years return period flood extent maps for the lowest municipalities' class.

4.2. Assessment of the DTM based hazard map

The assessment of the 100 years return period flood extent and depth maps calculated using the two 5m resolution DTM subsets provided by Intermap© was carried out by a spatial comparison with the 100 years return period flood extent reference map from Po Basin Authority (ADBPO). The assessment was performed only on water extent, because no information about waterdepth was

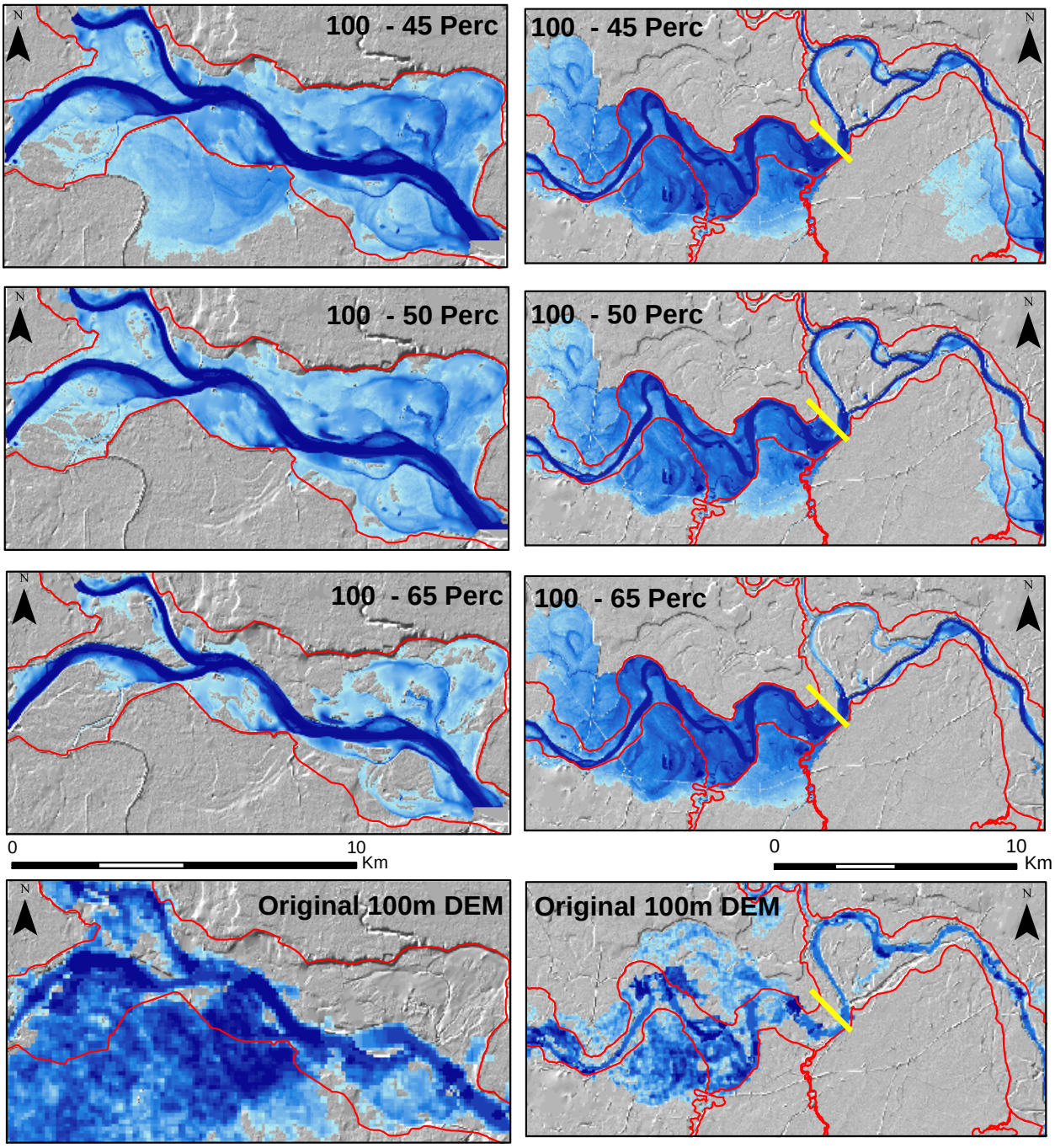

Fig. 4.4: flood extent maps calculated with different waterlevels (100years – 45%; 100years – 50%; 100years – 65%) on the basis of the 5m DTM for the two subsets; the two images in the bottom represent the original flood extent map calculated through the methodology developed by EFAS team on the basis of the 100m DEM. The outline of the 100 years return period flood extent map from ADBPO is shown in red; this was used as validation for the other flood extents. The yellow line represents the position of the hydroelectric power plant in the subset number 2 (right side).

available from the ADBPO reference study. The formula (section3.4.3) was adopted to assess the accuracy of the flood maps from DTM subsets.

For each of the subsets, the flood extent and depth map was calculated using the difference between the 100 years return period waterdepths and, in turn the 40, 45, 50, 60, 65 percentiles waterdepths. The outputs of the comparison is shown in fig. 4.5; in the image, the results from three waterdepth differences (100years – 45%; 100years – 50%; 100years – 65%) are illustrated together with the flood extent previously calculated on the basis of the 100m DEM, representing the original flood extent map from EFAS methodology.

Especially the second subset (right) shows how the ADBPO flood extent map is much more detailed than the flood extent calculated here. In facts in the ADBPO hazard study, the authors evaluated the flood extent also for the three small streams on the right side of the Po River, and for the one on the left side. This aspect has to be taken into consideration when the results will be discussed.

As stated in chapter 3, the best fit for both the subsets was found with the map calculated using the difference between the 100years return period waterdepth and the 50% percentile waterdepth. In tables 4.7 and 4.8 the results of the spatial comparison are shown for the three maps based on the new 5m DTM, and for the original flood extent map calculated using the 100m DEM showed in fig. 4.5.

Tab. 4.7: Spatial comparison for the firs subset (left side of Fig. 4.5)

Waterdepth differences	Flooded in both the Maps (Ha)	Only flooded in the calculated Map (Ha)	Only flooded in ADBPO Map (Ha)	Fit %
100y – 45 Perc.	5389.8	1505.3	975.4	68 %
100y – 50 Perc.	**5233.4**	**47.1**	**1131.7**	**82%**
100y – 65 Perc.	3253.4	2.0	3111.8	51%
Original 100m	3235	2948	2279	38%

Tab. 4.8: Spatial comparison for the second subset (right side of Fig. 4.5)

Waterdepth differences	Flooded in both the Maps (Ha)	Only flooded in the calculated Map (Ha)	Only flooded in ADBPO Map (Ha)	Fit %
100y – 45 Perc.	12132.4	13955.3	6209.3	37%
100y – 50 Perc.	**11526.5**	**10823.5**	**6815.2**	**40%**
100y – 65 Perc.	9920.4	11103.5	8421.3	34%
Original 100m	4978	5086	6208	30%

4.2.1. First subset

The first subset represents a natural floodplain area of the Po River at the junction with the Ticino River, one of the main tributaries in terms of discharge; the hydrology of the area was not disturbed by atrophic interventions apart from the system of levees. The results, showed in tab. 4.7, state that the calculations of 100 years return period flood extent performed well; the fit of the EFAS-DTM 5m flood map calculated using the (100y – 50 percentile) waterdepths difference (second map on the left infig. 4.7) resulted to be 82% with the reference flood map from ADBPO. Moreover, the ADBPO map was drown without considering small areas within the flood extent higher than the waterdepth; the new calculation showed that in the subset some very small areas that emerged from the water in the flood extent (see the light gray spots within the flood extent in fig. 4.4). When the results of the spatial comparison are evaluated this fact has to be considered. The relation between the flood extent calculated using the 5m DTM and the system of levees, illustrated in Fig. 4.5, shows that the effect of those structures is clearly visible. In the Northern – East part of the subset a fluvial terrace delineates the shape of the flood extent; the difference in elevation between the floodplain and the edge of the terrace is almost 20m (ca. 55 in the floodplain and ca. 73 in the terrace); hence floods will never reach the upper terrace part. The southern area is entirely included in the floodplain area; the right side terrace system starts in the south outside the subset. Here a system of levees was raised in order to protect the floodable areas in the South, where various villages and sparse farms are located. The effect of the levees is clear when the flood extent is calculated using the difference with the 45 percentile (first map on the left in fig.4.4). The waterdepth in the river cells calculated with the 50 percentile varies from 8.20 meters in the western part of the subset to 8.04 meters in the Eastern part; the difference with the 45 percentile ranges from 8.65 meters to 8.48. It means a difference in the two flood extent maps of 40-45 centimetres. This difference made the flood to overtake the levees system and to inundate a wide area in the Southern part as visible in the upper image in figure 4.5. This fact enhanced the goodness in detecting main levees structures by the new 5m DTM.

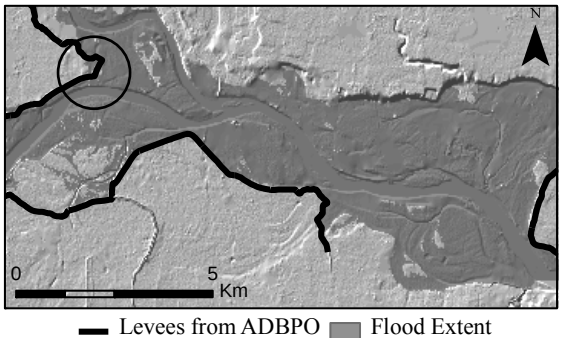

Fig. 4.5: Flood extent from (100y – 50Perc) waterlevel and its relation with the levees dataset from ADBPO; the water flooded outside only in a very small part (black circle).

The comparison of the EFAS-DTM 5m flood hazard map with the EFAS-SRTM 100m flood hazard map (4th map on the left) provided a quantification of the real improvement achieved with the new 5m DTM. The calculation based on the 100m SRTM did not simulate the effect of the levees and the fit with the reference study was only 38%, while with the new 5m DTM it raised up to 82%. Lastly, fig. 4.5 points out the only place where the water overcame the levees; the DTM, observed in details, showed that the levee in that point was damaged, while it was mapped as “in a good maintenance

state" in the database of the defence structures. The 5m DTM was acquired in the last 2 years and it can provide up-to-date information on the levees conditions.

4.2.2. Second subset

The second subset (right side of the Fig. 4.5) gave worse results than the first one: the best fit was found to be 40%. The hydrologic conditions of the river in the area represented in the subset are affected by the presence of a hydroelectric power plant (see yellow line in fig. 4.5 and fig 4.7). Due to the gradient produced by the dams system, the upstream waterdepth is higher than the waterdepths calculated using LISFLOOD model, while in downstream areas after the plant, the waterdepth is lower than the simulated ones. This difference produced an overestimation of flood extent and depth in the upstream part and an underestimation in the downstream area in respect to the position of the power plant. It is likely to consider that, in case of 100 years return period flood event, the normal discharge rates of the dams will be increased, even before the flood event, in order to limit the impact of the flood wave in the upstream areas in which the waterdepth is high. Obviously the above mentioned aspects of the area's hydrology will never be considered by the LISFLOOD model due to its operational scale. Therefore, if the flood hazard assessment is carried out from the outputs of LISFLOOD, errors related to this kind of situations will be always present. It is interesting to understand the impact of these errors on the final results. The overall accuracy of the simulation compared to the reference map from ADBPO is low: 40%; this is due to the overestimation of the flooded areas in the upstream part, and to the underestimation in the downstream area (clearly visible in the 100y – 50 percentile right image in Fig 4.5). The accuracy of the original map based on the 100m DEM was 30%; therefore the introduction of the 5m DTM improved of 10% the accuracy of the flood extent and flood depth map. It is important to state that the 5m DTM performed better also when clear and not removable inaccuracies in the waterdepth calculations were present.

Fig. 4.6: hydroelectric power plant in the subset two: oblique image

5. Damage Assessment

This chapter regards the loss estimation in flood potential damage assessment. EFAS team developed a strategy to calculate potential damages related to a 100 years return period flood event for European State Members involved in EFAS project, based on the calculation of economic losses. The first part of the chapter is a brief review of concepts and methodologies in hazard risk assessment (5.1); in the second part, the methodology suggested by EFAS team is described (5.2). Afterwards, the technique will be applied to the EFAS-SRTM 100m flood hazard maps (5.3) and to the EFAS-DTM 5m flood hazard maps (5.4). The results will be commented separately (5.4).

5.1. (Flood) Risk Assessment: main concepts

The Potential Flood Damage assessment at European scale is, in first analysis, the estimation in monetary terms of the impact of a flood event (100 years return period event, in this case) on the damageable assets in hazard prone areas for all the State Members involved in the EFAS project.

It is based on the main concept of Risk Assessment, therefore before to discuss in depth the methodology applied, a wider description of the concept of Risk is given.

In general, the perception of Risk Assessment involves two main concepts: the occurrence of a disaster and the consequences of the impact on different aspects of the society. In economics, engineering, social sciences different notions are adopted in order to define risk. Engineering sciences define risk as expected loss and it is determinates through measurements and calculations. Economics sciences approach the Risk as a deviation from an expected value of return and define it as the quantifiable likelihood of loss or the reduction of the expected return value. Social scientists consider Risk as dependant on various aspects of physical and social conditions (Jonkman, 2007). (Velk, 1996) compiled a summary of 11 formal definitions of Risk for social scientist listed in table 5.1.

In Natural Hazards research, the official worldwide accepted definition of the term of Risk was established during an experts meeting organized by the Office of United Nations Disaster and Relief Coordinator (UNDRO, 1979).

"...The term *Risk* refers the expected losses from a given *Hazard* to a given *Element at Risk*, over a specific future time period. According to the way in which the Elements at Risk are defined, the Risk may be measured in terms of expected economic losses or in terms of numbers of lives lost, or the extent to physical damage to properties..."

Tab. 5.1: Formal definitions for Risk in Social sciences (Velk, 1996).

	Formal Deinitions of Risk in Social Sciences
1	Probability of undesired consequence.
2	Seriousness of (maximum) possible undesired consequence.
3	Multi-attribute weighted sum of components of possible undesired consequence.
4	Probability x seriousness of undesired consequence (”expected loss”).
5	Probability-weighted sum of all possible undesired consequences (”average expected loss”).
6	Fitted function through graph of points relating probability to ext ent of undesired consequences.
7	Semivariance of possible undesired consequences about their average.
8	Variance of all possible undesired consequences about mean consequences.
9	Weighted sum of expected value and variance of all possible consequences.
10	Weighted combination of various parameters of the probability distribution of all possible consequences.
11	Weight of possible undesired consequences (”loss”) relative to comparable possible desired consequences (”gain”).

According to this definition, the Risk caused by the impact of a certain natural hazard to the elements at risk located in the affected area is given by the following main function.

$$\text{RISK} = \text{HAZARD} * \text{VULNERABILITY} * \text{ELEMENTS AT RISK}$$

In the equation, the risk is a function of 1) the occurrence probability and the magnitude of a certain natural or human-induced hazard in a certain area, 2) the elements at risk present in such area, and 3) the quantification of the effect of such hazard on each element at risk according to its nature and its location. This identification of the risk has a strict physical meaning; the quantification of the risk in this case is related to the impact of hazards on static elements. Therefore the formula quantifies the risk on the basis of physical characteristics of the elements at risk.

When the risk assessment needs to include the impact of hazards on single individuals, communities or societies, the dynamic behaviour of human beings plays an important role. Reaction mechanisms like evacuation, mutual help, cooperation have to be taken into account

The concept of risk can, therefore, include the different ability of single individuals, communities or societies to react when hit by hazards. The cooping capacity represents the ability of the individuals, communities, societies to overcome the hazard’s impacts and effects with the resources autonomously available. The function that includes this aspect is formulated as follows.

$$\text{RISK} = \text{HAZARD} * \frac{\text{VULNERABILITY}}{\text{CAPACITY}}$$

The meaning behind the last formula is that the cooperation capacity can reduce the vulnerability degree of a community or society that is able to react to the occurrence of a certain hazard with its own economic and social resources.

Considering the risk in the physical sense, the three terms of the main function and their meanings are discussed separately and different definitions are given for each term.

HAZARD

- "...The term Hazard is the chance of a rare or extreme event in the natural or man-made environment that adversely affects human lives, properties or activities to the extent of causing disasters. In a more specific meaning, the terms means the probability of occurrence, within a specified period of time and a given area, of a particular, potential damaging phenomenon of a given magnitude..." (Coburn et al., 1994).
- "...Hazard means a source of potential danger or adverse conditions; it includes naturally occurring event such as flood, earthquake, tornados, tsunami, coastal storm, landslide, wildfire, etc.that strikes the populated areas. A natural event becomes a Hazard when it has the potential to harm people or properties..." (FEMA, 2001).

The Hazard related study is called Hazard assessment and it involves the analysis of the physical aspects of the phenomenon through the collection of historical records, the interpretation of topographical, geological, hydrological information to provide the estimation of the temporal and spatial probability of occurrence and the magnitude of the hazardous events.

VULNERABILITY

- "...Vulnerability represents, in its general meaning, the degree to which a community, structures, services or a geographic area are likely to be damaged by the impact of a certain disaster, on account of their nature, construction, and proximity to hazardous regions or disaster-prone areas. More in details for scientific purposes: vulnerability is a mathematical function that expresses the degree of losses to a given element at risk expected from the impact of a hazard of a certain magnitude. It is specific to a particular kind of structure or, in general, category of elements at risk expressed through a value ranging from 0 (no damage\destruction\loss) to 1(total damage\destruction\loss)..." (Coburn et al., 1994).
- "...Vulnerability describes how exposed or susceptible to damage an asset is. It depends on the asset's construction, contents and economic value. Like indirect damages, vulnerability of a community, or one of its members, is related to the vulnerability of another community or member..." (FEMA, 2001).

– "...Vulnerability is a reflection of the state of the individual and collective physical, social, economic and environmental conditions at hand. These are shaped continually by attitudinal, behavioural, cultural, socio-economic and political influences on individuals, families, communities and countries..." (UN\ISDR, 2004).

To assess Vulnerability related to physical elements at risk, historical data related to hazards induced damages are combined to theoretical and empirical analysis on the impact of a certain phenomenon on a certain type of structure. For societal Vulnerability, the principal elements in a society, like physical, social, economic aspects are considered in both short-term and long-term in order to understand if the essential services and coping mechanisms are able to maintain their functions.

ELEMENTS AT RISK

Elements at Risk represent in the function the estimation of the physical, economical or societal entities present in a hazardous area prone to a disaster. The quantification of such exposed assets or people is carried out based on information from cadastral data, landuse data, census data or other sources of statistic information related to constructions, economic services or population. Regarding structures and economically evaluable assets, the estimation of the elements at risk can include also the economic evaluation of different aspects of the assets, like the damaged value, replacement value or the intrinsic value. The elements at risk are also referred as Exposures and they often are represented through information at aggregated areal unit levels with a coarser spatial resolution than the information provided for the hazard assessment; therefore they represent in many cases a big source of inaccuracies (Thieken et al., 2006).

The Risk provides an expression (evaluation or estimation) of the potential losses in a certain flood prone area due to a hazardous phenomenon with a given occurrence probability and a given magnitude. The term loss includes a wide variety of damages. They are dependent on the nature of the hazard and on the nature of the elements at risk present in the disaster-prone area. Dutta et al. (2003) schematized the possible damages caused by flood events into categories and loss examples showed in table 5.2.

Tab. 5.2: Flood damage categories and loss examples (Dutta et al., 2003).

Category	Tangible				Intangible
	Direct		Indirect		
	Primary	Secondary	Primary	Secondary	
Examples	Buildings, Sructures, Contents, Agriculture	Land and Environment Recovery	Business Interruption	Impact on Regional and National economy	Health, psychological damages

Regarding flood damage assessment, the losses can be divided into two main categories. The tangible losses can be expressed in monetary terms and they are divided into two sub-classes, direct and indirect, and further subdivided into primary and secondary. The intangible losses are not describable in monetary terms and they are extremely difficult to understand and model (Dutta et al., 2003).

To finalize the loss estimation, three main directions can be followed, according to the purpose, the data availability and the scale of observation: Qualitative, Semi-Quantitative and Quantitative loss estimation.

The qualitative loss estimation is the simplest approach and involves different techniques. The simple matrix approach is based on the combination of the hazard spatial information with the vulnerability of the elements at risk and on the classification into different risk classes (low, moderate, high risk level).

Different kinds of Risk indices are available nowadays for qualitative loss estimation; such indices aim at measuring risk and/or vulnerability at a national scale and they were designed to allow comparison at international and global scale. Examples of this kind of approach are the Disaster Risk Index (DRI from United Nation Development Programme) based on mortality data which are comparable among different hazards and different countries; the Hot Spot Project (from World Bank and other institutes) where the risk is a product of hazard frequency and consequences; the Americas Indexing Program (from the Institute of Environmental Studies, Colombia – Manizales University) that includes a set of four main indices: Disaster Deficit Index (DDI), Local Disaster Index (LDI), Prevalent Vulnerability Index (PVI), Risk Management Index (RMI); the Community-Based Risk Index (developed by GTZ and partners from communities in Indonesia) that aims at identifying the main risk characteristics within a community and at allowing comparisons among different communities. For a wider description of the list of Indices see Birkmann (2007).

The semi-quantitative loss estimation is mainly based on the main formula that defines Risk (R=H*V*El at R); it involves quantification in monetary terms of the assets and the quantification of their vulnerability degree (from 0 to 1). Usually the vulnerability and the value of the elements at risk are calculated through different levels of aggregation (Kleist et al., 2006; Thieken et al., 2006). In this approach only direct primary losses are considered. It can be based on scenario-based loss estimations or on probabilistic loss estimations.

The quantitative loss estimation theoretically should represent the evaluation of the vulnerability for each flood parameter (water level, velocity, duration, sediment load, etc.) for each asset, and the estimation of the exact value for each element at risk. Single buildings have different behaviours when hit by the flood and, at some point, a certain generalization level is needed according to the scale of observation. Therefore a fully quantitative loss estimation technique is not likely to exist, due to the enormous variety among the elements at risk, their structural and economic characteristics and their vulnerability related to flood events.

5.2. A Semi-Quantitative Approach to Flood Potential Damage Assessment

In this section the EFAS team approach to flood potential damage assessment at European scale is explained.

According to (Messner et al., 2007), in the last years the direction of flood protection went through the management of flood risk, which is seen as one of the several risk sources for societies. In this prospective, flood risk is perceived as expected flood damage for a given return period, i.e. expected losses estimated before a flood event. But flood risk can also be seen from a different prospective; EFAS team aimed at assessing flood risk as the flood damage potential: they studied ex-ante the maximum flood damage in flood prone areas without considering defence measures; therefore, in developing their methodology, the flood damage potential was considered as an abstraction for mapping flood risk zones (Barredo et al., 2008).

The methodology is based on a semi-quantitative approach of loss estimation in monetary terms where only direct primary losses were estimated; secondary losses like environmental damages, indirect losses like business interruption, health damage or other intangible losses were not taken into account (see tab. 5.2). The approach follows the main risk equation showed in the first part of this chapter. The three parameters of the equation are: Hazard, Exposure (or elements at risk) and Vulnerability.

- Hazard: it is represented by a flood event with an occurrence probability of 1 into 100 years; the hazard related parameters were calculated in the previous steps of this research following the methodology developed by EFAS team; in particular the loss estimation is carried out through one single flood parameter: the flood water level.
- Exposure: to estimate the assets in the flood prone areas, a homogeneous dataset covering the entire Europe was required; thus the exposure was economically estimated on the basis of the CORINE Landover dataset.
- Vulnerability: it is, in general, the degree of the damage to the exposure when it enters in contact with the water. In this approach, the vulnerability is dependant on the "water level" parameter through functions that relate a certain degree of damage at a given water level for each of the 44 landcover classes of CORINE dataset; Such functions are denominated Flood – Damage Functions. Being a source of homogeneous landcover information at a reasonable resolution (100m), CORINE is the most suitable dataset at the project scale and it has been already used for regionalization of assets value in risk assessment (Thieken et al., 2006).

The methodology to extract the hazard related information was already widely discussed in chapters 3 and 4 of the present study; therefore there is no need of further explanations. The only aspect that has still to be discussed is the limitation in flood parameters availability to carry out the damage potential assessment. In the methodology developed by EFAS, flood depth is the unique parameter used to estimate potential economic losses. The quantification of damaged due to floods is strictly related to different flood characteristics like depth, velocity, rising time, flood duration, sediment load. From the

primary parameters, other parameters can be extracted to express flood behaviour like the flood impulse, which is given by the multiplication of the waterdepth and the velocity (Alkema et al., 2007). Limiting the flood description to only one parameter (water level) includes obviously abstractions in the damage assessment. On the other hand, (Thieken et al., 2005) carried out a study on the factors that mostly influenced flood damage to private houses after the 2002 flood events. The conclusions achieved stated that the most relevant parameters were water level, flood duration and contamination. Furthermore, on the basis of a survey in United Kingdom to assess the impact of six different flood parameters on flood damage assessment, the engineers concluded that the flood velocity was the less influencing factor (Soetanto and Proverbs, 2004). As final conclusion, it is reasonable to consider only flood depth for potential damage assessment at European scale, based on previous results of studies on flood influencing factors.

The exposure is represented by the monetary evaluation of the landcover classes of CORINE, and the vulnerability is expressed as a function of the water level. Both, exposure and vulnerability are included in the depth-damage functions applied in the flood potential damage assessment: for different water levels, the functions provide the final damage expressed in monetary terms of each landcover class. For this reason vulnerability assessment and exposure estimation will be discussed together in the description of the depth-damage functions.

5.2.1. Depth – Damage Functions

Stage – damage functions represent the most effective solution in relating flood parameters to damage in flood damage assessment models (Krzysztofowicz and Davis, 1983). According to (Dutta et al., 2003), the stage – damage functions can be extracted following two different strategies. The first consists of calculating the functions on the basis of historical flood damages data. The second is the calculation of functions from analysis based on landcover/landuse classes, assets classes, questionnaire surveys, expert knowledge based estimations etc. In this case they are called synthetic stage – damage functions.

When related to the water level parameter, the stage – damage functions are known as depth – damage functions. For the purpose of EFAS team, synthetic depth – damage functions were applied. The extraction of such functions for the 27 State Members of the European Union and for Norway, Switzerland, Croatia and Turkey was performed by the HKV CONSULTANTS© (http://www.hkv.nl/), an independent consulting company providing consultancy and research services in the field of water management.

The methodology was based on a preliminary phase of data collection, in which all the available data related to flood damage and to stage – damage functions were collected for European countries. No information related to flood risk assessment were collected for Italy. A series of questionnaires was sent to the authors of the inventories and documents for clarifications. The second step was the comparison of economic characteristics of the different countries through statistical indices like:

- GDP (gross domestic product): total economic product for the region or per capita
- GPD-PPS (purchasing power standard): an artificial currency that considers differences in national price levels
- GDP-PPP (purchasing power parity): it is the GDP converted into international dollars using purchasing parities rates: an international dollar has the same purchasing power of the dollar in United States. For more in-depth description of the meaning of PPP see (Van Vuuren and Alfsen, 2006).

Based on historical data and literature review, the landcover classes that mostly contributed to the flood damages were defined; 14 classes were excluded because considered irrelevant (23, 24, 25, 29, 30, 31, 33, 34, 36, 38, 39, 41, 42 and 44). For each of the other classes the maximum damage values were calculated based on historical data; this value was corrected using the above mentioned indices in order to consider the inflation rates, and harmonized to allow comparisons among countries with different economic characteristics.

The HKV experts collected the depth – damage functions found in literature and they extracted harmonized depth – damage functions for each landuse class on the basis of "visual averaging". The resulting new "average" functions related nine depths (0, 0.5, 1, 1.5, 2, 3, 4, 5, and 6 or more meters) to the corresponding damage rates (from 0 to 1) for each of the considered exposure classes (see fig. 5.1). The final step was the application of the maximum damage values calculated for each landcover class, for each country. In this way the vulnerability assessment is represented by the construction of the "average" functions ranging from 0 to 1 and the elements at risk were represented by the maximum damage values for each class. The most influencing classes resulted to be: residential areas and contents, commerce and industry and their contents, infrastructure road, and agriculture.

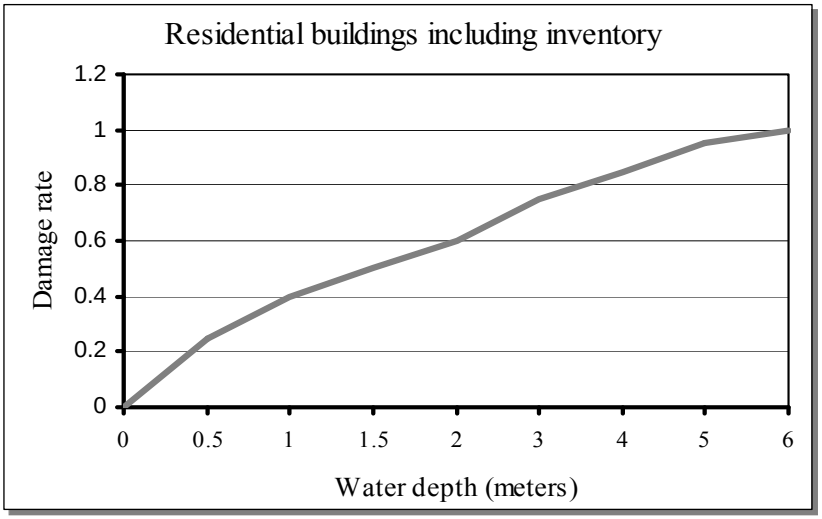

Fig. 5.1: Example of "average" depth – damage function for residential buildings and inventory

The final results are represented by depth – damage functions expressing the damage in terms of Euros in purchasing power parities. For each of the 31 countries involved, 30 functions were provided according to the most relevant CORINE lancover classes. In each class the damage was expressed in Euros Purchasing Power Parities per square meter.

5.2.2. Input Data and Methodology

For the purpose of this study, the 30 depth – damage functions for Italy were provided by EFAS team. The functions for main artificial and agricultural classes are shown in fig. 5.2.The depth – damage functions represent the firs input in flood potential damage assessment methodology.

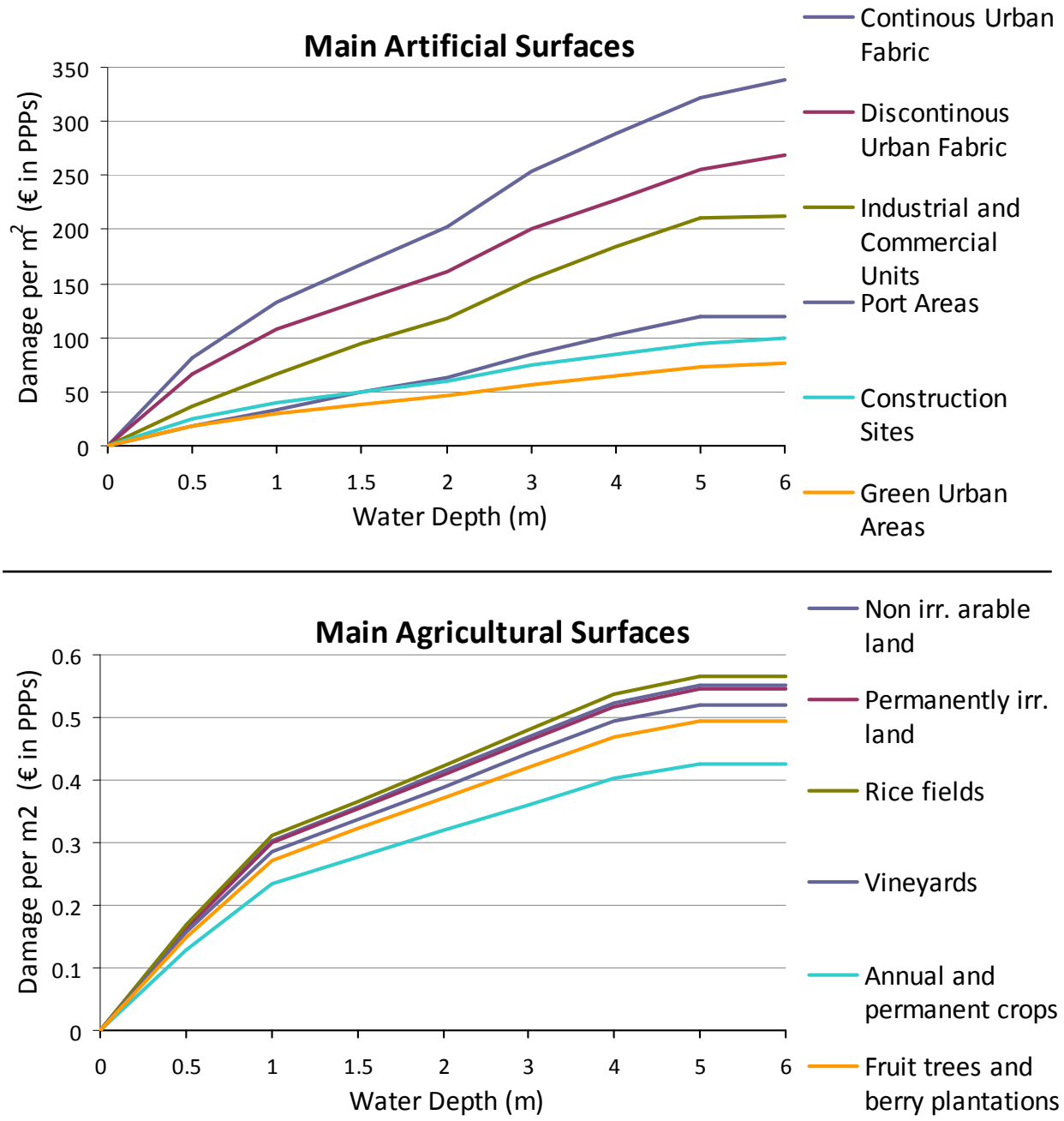

Fig. 5.2: Depth-damage functions of main artificial and agricultural landcover classes for Italy.

As mentioned before the second input was represented by the hazard maps extracted in the first part of the study. The flood potential damage assessment was performed on the basis of: 1) 100 years return period EFAS-SRTM (100m) flood hazard map, for the entire Po basin; 2) 100 years return period EFAS-SRTM (100m) flood hazard map with simulation of protection measures, for the entire Po

basin; 3) 100 years return period EFAS-DTM (5m) flood hazard map, for the first subset (junction between Po River and Ticino River, see section 3.4.1).

The third and last output is the CORINE 2000 Landcover dataset. CORINE (Co-ordination of Information on the Environment) project started in 1985 when the three main guidelines were drawn. The project was carried out at a 1:10.000 mapping scale; the mapping accuracy was set at 100m for the entire European territory. The minimum unit for inventory was set at 25 Ha, while the minimum width for unit at 100m. CORINE classification was based on a hierarchical nomenclature, including 44 classes at the third level, 15 at the second level and 4 at the first level. The classification was performed on the basis of Landsat ETM+ satellite images at 12.5 m resolution integrated by orthorectified aerial photographs and ancillary data. The images collection was realized through a separate project called IMAGE2000 (De Lima, 2005; EEA, 1993). The classification was carried out through three hierarchical levels; the three categories with explanations are listed in Annex C. A subset for the area of interest was extracted. The calculation was carried out using the open source R software, a language and environment for statistical computing and graphic applications similar to the S language (Venables and Smith, 2008). The three inputs, hazard maps, CORINE map, and depth – damage functions, were converted into text (.TXT) files. The maps were imported in R software as matrices without the original headers and with exactly the same numbers of columns and rows (4674x2683 for the EFAS-100mSRTM flood hazard maps; 3138x1716 for the EFAS-5mDTM hazard map). The depth – damage functions were expressed through a matrix with 44 columns and 10 rows; the 44 columns represented all the CORINE landcover classes; in each column, the first number was the landcover class code, the other nine numbers represented the damage in € (PPP)/m^2, for each of the depth steps. For the 14 landcover classes without functions, 0 value vas used in the column. For the waterdepth values in between two steps (between 0.5 m and 1.0m, for instance), the damage value was extracted through linear interpolation between the two closest damage values. For each cell the damage was calculated and the results were stored in a matrix (stored in a .TXT file) with the same dimension of the input maps. Finally the original header was added again and the text file was converted into ArcGIS raster format. The procedure developed by EFAS team provided also the calculation of two other output files:

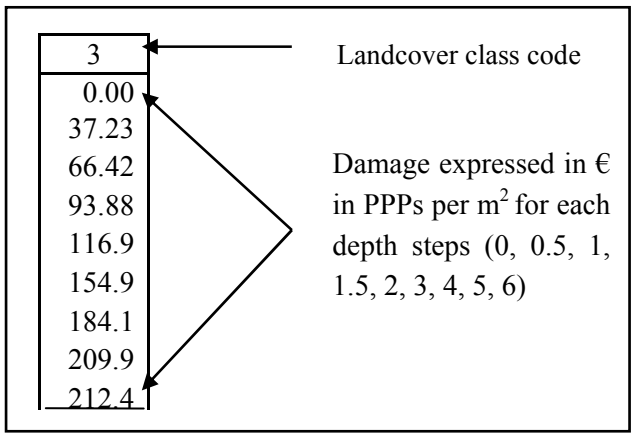

Fig. 5.3: representation of one column of the depth – damage functions matrix in R software.

- losses_x_lu: a text file with the total losses divided per landcover class;
- total_losses: a text file with the overall loss;

The results for the different outputs are discussed separately in the next section.

5.3. Results from 100m SRTM-DEM based Hazard Maps

Firstly, the potential damage assessment was carried out using the EFAS-SRTM100m flood hazard map calculated in session 3.2. The resulting map, representing the total losses for the Po area, is shown in figure 5.4.

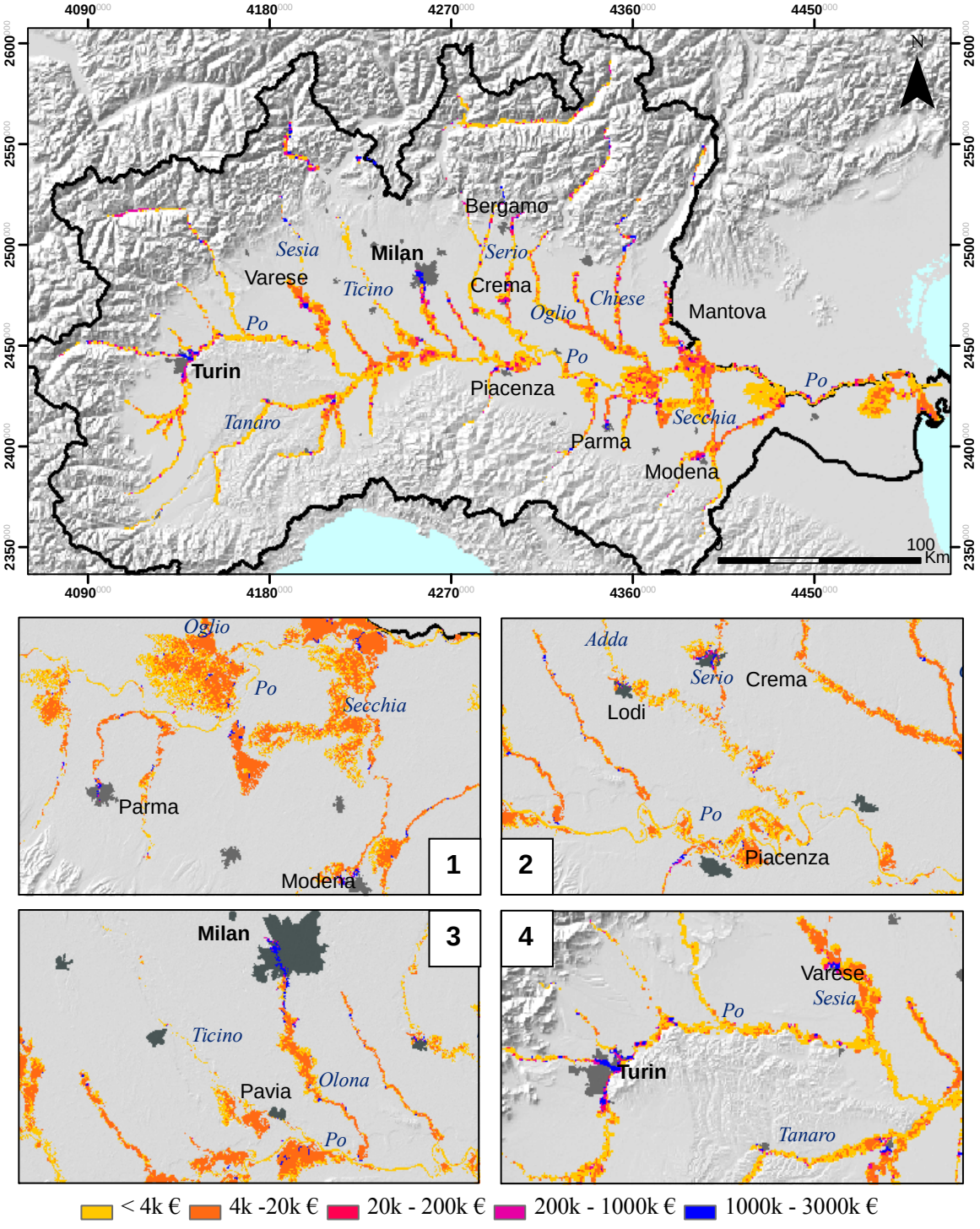

Fig. 5.4: Potential damage assessment map based on EFAS-SRTM100m flood hazard map; the four subsets represent in detail the most sensible areas; the damage is expressed in thousands Euros.

The two classes in the map with highest losses values (blue and purple) represent the damages to the three landcover classes with the highest damageable values: continuous urban fabric, discontinuous urban fabric, industrial or commercial units. The total damage is mainly due to the damage caused by the flood to these classes. The yellow and orange colours are mainly related to the damages to landcover classes with lower values like arable land. In table 5.3, the losses per landcover class are summarized.

Tab. 5.3: Potential losses for each CORINE lancover class from EFAS-SRTM-100m flood hazard map.

Code	Landuse Description	Losses by Landuse
1	Continuous urban fabric	€ 1,003,975,002
2	Discontinuous urban fabric	€ 15,336,324,407
3	Industrial or commercial units	€ 3,309,778,100
4	Road and rail networks and associated land	€ 13,169,054
6	Airports	€ 5,170,198
7	Mineral extraction sites	€ 483,783
8	Dump sites	€ 176,076
9	Construction sites	€ 126,782,426
10	Green urban areas	€ 193,970,265
11	Sport and leisure facilities	€ 94,710,304
12	Non-irrigated arable land	€ 859,833,135
14	Rice fields	€ 121,324,506
15	Vineyards	€ 939,365
16	Fruit trees and berry plantations	€ 2,339,869
18	Pastures	€ 15,094,941
20	Complex cultivation patterns	€ 39,722,412
21	Land occupied by agriculture, with areas of natural vegetation	€ 30,567,868
26	Natural grasslands	€ 137,907
27	Moors and heathland	€ 7,872,797
32	Sparsely vegetated areas	€ 251
35	Inland marshes	€ 1,290,434
37	Salt marshes	€ 162,209
40	Water courses	€ 36,248,216
	TOTAL	**€ 21,200,073,525**

The most affected areas are the city of Turin (subset 4 in fig.5.4), and the surrounding of Milan (subset 3). Turin is built around the junction between Po and Dora Baltea Rivers, the watercourses cross the city, therefore floods caused by these rivers involve large urban areas. In the province of Milan the losses are caused by the flood of Olona River. In the region between the Po River and the cities of Parma and Modena (subset 1), the flood caused by the Po and the Secchia Rivers spreads over a wide area occupied mainly by agricultural areas; the main damages are related to the small urban centres located in the flood extent. The subset 2 represents the flood damages caused to the cities of Cremona and Lodi, which suffer big losses.

The second step was the calculation of the losses on the basis of the EFAS-SRTM100m flood hazard map with the simulation of defence structures carried out in section 3.3. The Potential damage assessment was defined as the total losses in case of 100 years return period flood event without considering the effects of protection structures (Barredo et Al, 2008). With the simulation of such structure, the losses estimation can be referred as a damage assessment of a flood event with a probability of 1 into 100 years. The results are illustrated in figure 5.5.

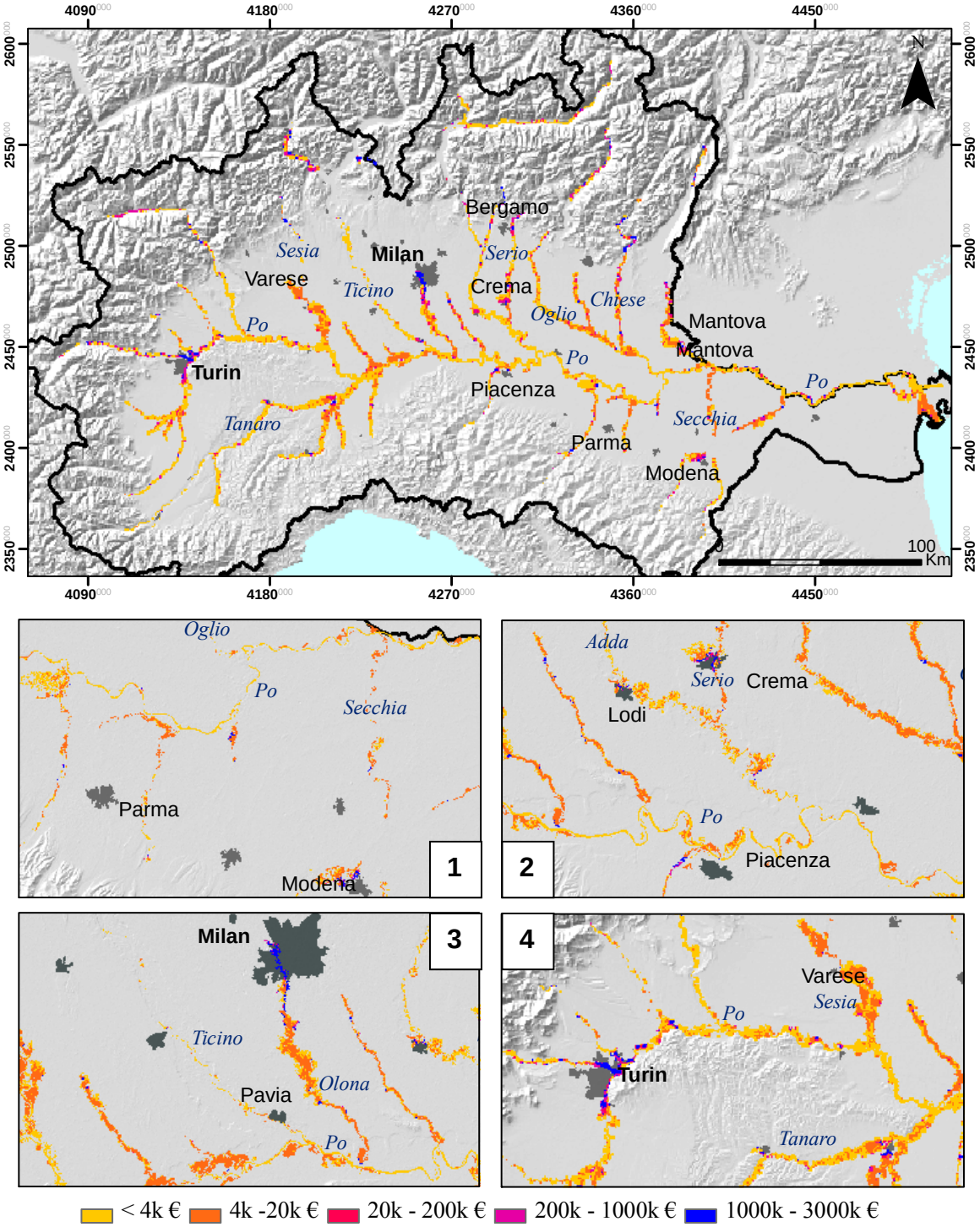

Fig. 5.5: Damage assessment based on the EFAS-SRTM100m flood hazard map with the simulation of protection measures.

To better estimate the impact of the protection structures on the damage calculation, table 5.5 illustrates the losses per landcover class.

Tab. 5.4: Potential losses for each CORINE lancover class from EFAS-SRTM-100m flood hazard map with the simulation of defence measures.

Code	Landuse Description	Losses by Landuse
1	Continuous urban fabric	€ 874,852,898
2	Discontinuous urban fabric	€ 9,749,642,919
3	Industrial or commercial units	€ 2,088,385,211
4	Road and rail networks and associated land	€ 12,694,711
6	Airports	€ 5,170,198
7	Mineral extraction sites	€ 404,562
8	Dump sites	€ 140,834
9	Construction sites	€ 120,236,709
10	Green urban areas	€ 190,707,641
11	Sport and leisure facilities	€ 93,609,921
12	Non-irrigated arable land	€ 302,454,371
14	Rice fields	€ 65,896,880
15	Vineyards	€ 690,219
16	Fruit trees and berry plantations	€ 1,206,293
18	Pastures	€ 14,687,693
20	Complex cultivation patterns	€ 22,447,820
21	Land occupied by agriculture, with areas of natural vegetation	€ 29,364,580
26	Natural grasslands	€ 137,140
27	Moors and heath land	€ 7,872
32	Sparsely vegetated areas	€ 251
35	Inland marshes	€ 1,259,076
37	Salt marshes	€ 134,537
40	Water courses	€ 34,478,845
	TOTAL	**€ 13,608,611,181**

It has to be stated that no validation could be performed on results of the damage assessment due to the absence of similar studies carried out for the Po basin.

The effect of the levees is clearly visible though the visual comparison of the two maps. In the region of Parma and Modena (subset 1 in figs. 5.4 and 5.5) the Parma and Secchia Rivers were bordered by levees for their entire length; the protections avoided the losses in the area. In the surroundings of Pavia and Piacenza (subset 2) the damages were reduced by the levees built on the Po and Ticino rivers. Around the city of Mantova (main map in fig 5.5) the flood damages caused by the Oglio River were heavily reduced by the introduction of the protection measures. Regarding the cities of Milan and Turin (subsets 3 and 4 in the figures 5.4 and 5.5), the dataset of the defence measures did not include protections for these areas; therefore the damage was not changed; even if is unlikely to believe that

any levees system didn't exist for the two metropolises. Moreover, the damages related to the continuous urban fabric landcover class were mainly located in the two metropolises; this is the reason why the damages relate to such class did not sensibly change with the introduction of the levees. The fact is highlighted when the difference between the damages without and with levees are compared (see table 5.5 and fig. 5.6). To better understand the values, the four most affected landcover classes were showed separately, the others were grouped together.

Tab. 5.5: comparison between potential losses without defences and losses with defences.

Landuse Class	Without Defenses	With Defenses	Difference
	Milion Euro	(PPPs)	
Cont. Urban Fabric	1004	875	129
Disc. Urban Fabric	15336	9750	5587
Industrial Areas	3310	2088	1221
Non-Irrigated Arable Land	860	302	557
Sum of minor landuses	690	593	97
TOTAL	**21200**	**13609**	**7591**

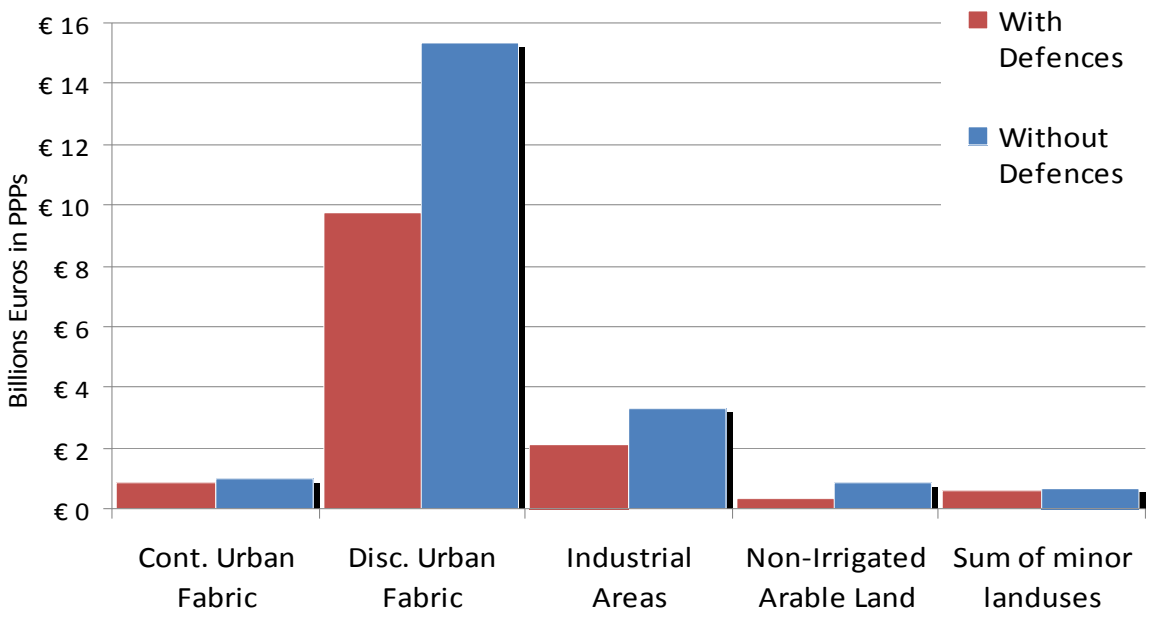

Fig. 5.6: Differences in potential damage between simulation with and without defence structures.

The main differences regard the discontinuous and continuous urban fabric, industrial areas and agricultural areas, which are the classes that mostly contribute to the total losses. The high rate of damage caused by these classes can be explained with the fact that the levees were built in order to protect the most vulnerable areas; or better, the most vulnerable elements at risk like urban areas and industrial sites, were built in areas under the protection of levees. Discontinuous urban areas provided the highest difference. As explained before the class includes villages, small cities and the peripheries of the main cities.

The main changes, produced with the introduction of the levees in the hazard map calculation, regarded spots where the flood spread unexpectedly on large areas. Such areas were mainly agricultural, and the urban centres consisted in farms, villages and small cities, mapped in CORINE as discontinuous urban fabric. Moreover most of the villages and the cities present in those areas have their own industrial/commercial sites; therefore the difference in the losses for the industrial and commercial units is directly connected to the discontinuous urban fabric.

It is interesting to see the relation between the areas occupied by the different landcover classes and the related damages; in tab. 5.5, the surface was calculated for each class in the flooded areas.

Tab. 5.6: comparison between landcover areas without defences and with defences (in Ha).

Landuse Description	Without Defenses	With Defenses	Difference
		(Ha)	
Cont. Urban Fabric	479	400	79
Disc. Urban Fabric	10827	6723	4104
Industrial Areas	3190	2009	1181
Non-Irrigated Arable Land	225273	79432	145841
Sum of minor landuses	128071	108982	19089
TOTAL	**367840**	**197546**	**170294**

Considering the potential loss estimation from flood hazard map without defences, the area occupied by the first three classes (cont./disc. urban and industrial areas) represent the 4% of the total flooded classes. This area contributes for the 93% to the total losses. The arable land cover the 61% of the flooded area and the losses are the 4% of the total. For the loss estimation with the simulation of the defence measures, the first three classes cover the 4.6% of the area with a contribution in the losses of the 86%; Arable land cover 40% of the flooded area producing the 2.2% of the total losses. Those values are similar to the estimations found in literature for areas with same characteristics in Germany (Thieken et Al, 2006).

Finally, due to the underestimation that affected the EFAS-SRTM100m flood hazard map with the simulation of defences (see section 4.1.1), the results from that map can be considered underestimated as well. On the other hand, the areas underestimated were mainly located in between the levees belt along the Po River; therefore the landcover classes were mainly forested areas or similar; the damage assessment for such landcover classes is irrelevant for the total losses estimation. It can be concluded that the damage assessment carried out through the simulation of the defence measure is closer to the reality than the potential damage assessment.

5.4. Results from 5m DTM based Hazard Map

The final step of the calculations related to the damage assessment part was the loss estimation on the basis of the EFAS-DTM 5m flood hazard maps. The flood depth maps were available for the subsets 1

and 2 described in the previous chapters. The damage assessment was carried out only on the first subset, because it is representative of the main part of the Po basin, where the river flows in natural environment without artificial structures affecting the water course. The second subset represented a particular condition; in the area covered by the 5m DTM, an electrical hydropower plant was located (see section 4.2.2); the results of the hazard assessment were only 10% higher than the 100m SRTM, due to the effects of the dams system of the plant. The subset is representative of very few areas in which this kind of structures heavily influence the behaviour of the rivers.

Once decided which hazard map should have been used, the same methodology described before was applied. The depth – damage functions are expressed in loss in Euro per square meter; the only change in the procedure was to set the script in R software in such way that it multiplies by 25 (5m x 5m: the resolution of the DTM) the damage value for each cell instead of 10.000 (100 x 100, resolution of the SRTM).

The main problem related to the loss estimation was the different resolution of the input maps. The flood depth map has a resolution of 5 meters while the CLC (CORINE landcover) has a resolution of 100 meters. Some aspects related to the input data were taken into account in order to find different solutions to perform the calculations.

The information in CORINE landcover is represented by discrete data (or categorical, discontinuous, thematic): the different objects (landcover classes) have defined boundaries, and, inside each class, the values stored in the raster cells are homogenous. Therefore, no information is lost if the CORINE dataset is resampled at 5m resolution.

On the other hand, the flood depth map corresponds to a continuous field: a continuous surface (or field) represents, at each cell, the measurement of a quantifiable characteristic of the field (in this case the waterdepth; it could be elevation, concentration etc.) that continuously changes along the surface; therefore the values progressively vary in the raster grid. If the flood depth map based on the 5m DTM is resampled to 100m resolution, a considerable amount of information is lost due to the fact that 20 x 20 cells with an area of 25 m^2 each will be converted to 1 cell with an area of 100m^2.

Regarding the entire procedure of damage assessment (hazard assessment + loss estimation) the loss estimation was the most time-consuming, due to the slowness of R software in calculating losses.

Taking into account those considerations, two possible solutions were applied.

- The CORINE landcover dataset was resampled at 5m resolution and it was combined with the flood depth map from the 5m DTM. The resampling method chosen was nearest neighbour, where the value for the output cell is taken from the closest cell's centroid in the input map to the cell's centroid of the output map. This operation produced an output with a finer resolution (5m) than the input map, but the accuracy did not change (100m).

– The flood depth map from the 5m DTM was resampled at 100m resolution and it was combined with CORINE to calculate flood damage. This operation basically consisted in transforming 400 cells at 5m resolution into 1 at 100m resolution. None of the commonly resampling methods was suitable; the nearest neighbour considers only the value of one cell; in the bilinear interpolation method, the output cell value is calculated using the weighted average of the 4 closest cells in the input map; the cubic convolution is the same of the previous but the closest 16 cells are considered. It is obvious that 16 cells over 400 give a wrong estimation of the water level in the output 100m cell. Thus the resampling was carried out through the *"Spatial Analyst"* tool in ArcGIS. By applying the function *"neighbourhood statistics"*, the mean of the input cells was calculated with a resolution of 100m. The output's resolution was set at 100m; in each output cell the mean of the area corresponding to that particular cell in the input map was stored.

Finally the damage assessment was carried out using the following two combinations:

– EFAS-DTM flood depth map and CORINE landcover map both at 5m resolution

– EFAS-DTM flood depth map and CORINE landcover map both at 100m resolution.

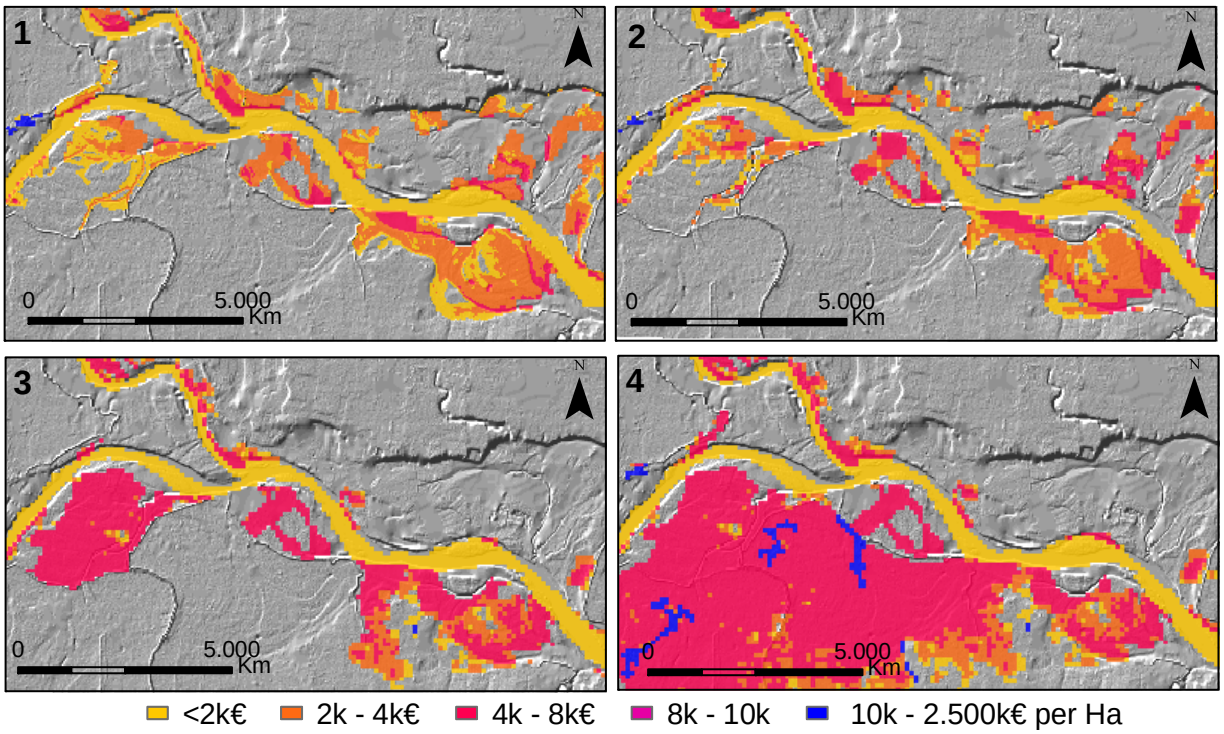

Fig. 5.7: Results of the damage assessment for the first subset area on the basis of: 1) flood depth at 5m from 5m DTM; 2) flood depth at 100m from 5m DTM; 3) flood depth at 100m from SRTM with protection measures; 4) flood dept at 100m from SRTM without protections. Damage is expressed in thousands Euro

The results are shown in fig 5.7 and visually compared, in turn, with the damage assessment carried out with both EFAS-SRTM 100m flood depth maps, and EFAS-SRTM100m map with simulation of defence measures. In the image the first four classes of the legend range from 2,000€ to 10,000€ while

the last class contains values from 10,000€ to 2.5 Million €; the values were stretched in this way to allow a visual interpretation of the maps. In fact the damages over 10,000€ regard built-up areas only.

The quantitative comparison of the results is shown in table 5.7, where the losses per landcover are given for the four maps of fig. 5.7. In fig 5.8, the CORINE landcover classes for the subset are shown. The green colour represents broad-leaved forests; this class (code 20) has no value in loss estimation because such natural areas are not supposed to need any recovery plan after flood events. That's why the losses maps have a discontinuous pattern. In CORINE, the red areas represent the discontinuous urban fabric class (2), which is the class with the highest value. The non irrigated arable land (13) is indicated with beige colour, while the sum of the other agricultural areas present in the subset have yellow colour. Finally the blue cells represent the water courses (class 40); this class was considered damageable by the HKV engineers, therefore a depth-damage function was calculated. The image highlights, in the small rectangle, a spot where the mismatch between urban area (red) in CORINE, and the levee mapped in the 5m DTM is visible. All the four maps will be commented, bearing on mind that the damage is proportional to the landcover class and to the water depth.

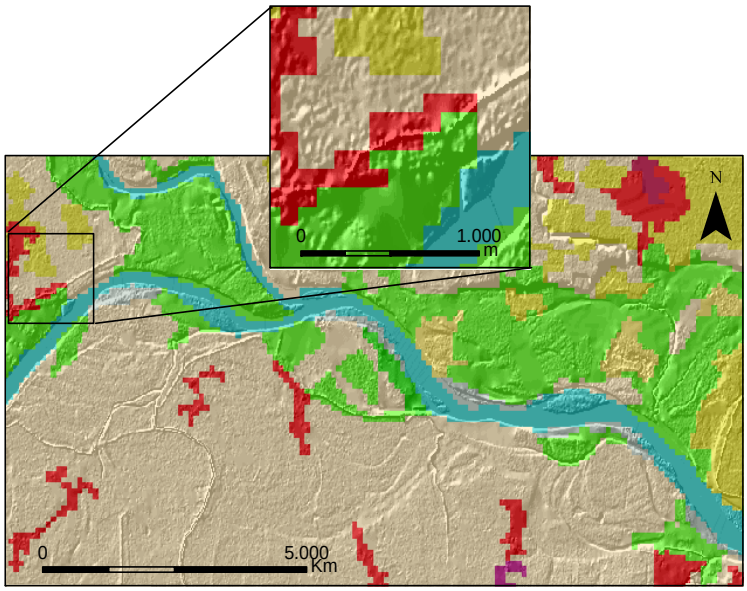

Fig. 5.8: CORINE landuse of the subset; the small rectangle highlights the relation between the levee in the 5mDTM and the settlement in CORINE classification

Tab. 5.7: Losses per landcover class for maps in fig. 5.7; the numbers in the upper left corner refer to the maps.

Landcover class	1) 5mDTM	2) 5mDTM resampled at 100m	3) 100m DEM with defenses	4) 100m DEM without defenses
		Euro (PPPs)		
Discontinuous urban fabric	5556238	4094983	160824	272513419
Non-irr. Arable land	4057733	4040112	6908480	19351989
Other agric. classes	1084898	1080605	243296	369757
Water courses	1232525	1235649	1208764	1204393
TOTAL	**11931393**	**10451339**	**8521364**	**293439557**

The map number 1 (fig. 5.7) represents the loss estimation with DTM based flood depth map and CORINE map at 5m resolution. The 50% of the damage is due a group of cells with high damage (blue

cells in map number 1) on the western part of the subset, representing the flooded area of the village *Travaco'*. The other 50% is mainly due to the inundation of arable land. The total loss estimated is 12 Million Euro. The village should have been protected by the levees, which, in reality, were able to contain the flood. The problem was that few cells of CORINE mapped as urban area were outside the protected area of the levees, due to the large difference in the resolution of the datasets (see zoom in fig. 5.8).

The map number 2 shows the loss estimation calculated using the EFAS 5m DTM flood depth map resampled at 100m. The total loss is more than 10 Million Euro, and the difference of loss with the first map is less than 1.5 Million Euro; in fact, the flooded built-up area of *Travaco'* village was smaller than in the previous map. The difference was caused by the fact that some cells in the flooded built-up area of the map 1 were not represented in map 2, due to the coarser resolution at which the analysis was carried out.. The losses for the other landcover classes are basically the same. The losses calculation with the flood depth map resampled at 100m resolution gave results very close to the calculation at the resolution of 5m. The overall difference between the two loss estimations is basically due to the difference in a few cells.

The map number 3 represents the loss estimation from the 100m flood depth map calculated with the simulation of the protection measures. The value of total loss is the smallest over the four maps: 8.5 Million Euros. In this map the loss related to the built-up areas represents only the 2% of the total loss; the urban area described before corresponding to *Travaco'* village is no more flooded. When the protection measure were introduced in the 100m SRTM DEM (see section 3.3), the vector dataset representing the levees was converted into a raster dataset with 100m resolution according to the DEM. The levee fell exactly on the flooded urban areas that produced the major losses in maps 1 and 2. The addition of the levees automatically removed such cells from the flooded areas. At the same time another built-up area was flooded in the south – eastern part of the subset (the only blue pixel in map 3).

Map number 4 is the loss estimation from the flood depth map calculated using the 100m SRTM DEM without defence measures (it represents the original flood map by EFAS team used in the potential damage assessment). The total loss estimation is 293 Million Euros, and it is the highest over the four maps. The losses in the built-up areas are 272 Million Euros. By comparing this map with the map 1 and 3, the effect of the levees is clear either when they are well represented in the 5m DTM (map 1), or when they were artificially introduced in the 100m DEM (map 3). In the map 4, the flood simulation inundated the four villages present in the southern area due to the absence of levees.

Unfortunately the results of the damage assessment from the different input data could not be validated, because similar information is not available for the subset area and for the entire Po basin. At the same time, the application of the methodology developed by EFAS team to the flood hazard maps from the new DTM showed that the good results achieved in the hazard assessment with the new DTM don't necessarily mean good results in the damage assessment. The coarser resolution of

CORINE compared to the one of the 5m DTM produced unexpected errors. Those errors regard just a few cells in the entire map; but when the cells belong to a landcover class with a very high value (i.e. discontinuous urban fabric, like in this case) they trigger wrong estimations of loss.

5.5. Comparison of the results

The comparison for the entire Po area pointed out the large difference between the potential damage assessment carried out without considering protections and the damage assessment carried out taking into account the protections. Such difference is even enhanced when particular locations are observed, like the subset examined in the previous section. The fact suggests that the exaggerations of the total losses due to the absence of the protection structures are not homogeneously distributed but they affect much more certain areas than others: for the entire Po area the losses without and with defences have a relation of 1 to 1.6; while in the subset area they have a relation of 1 to 25.

One important overall achievement was that some large inaccuracies found in the hazard assessment methodology didn't necessary cause wrong calculations in the damage assessment. For instance, the analysis of the landuse carried out in the section 4.1.2 showed how the SRTM based flood hazard map heavily underestimated the forested areas; in this part it was demonstrated that errors in forested areas are totally negligible for loss estimation because those area did not produce any losses when flooded.

On the other hand, the results of the hazard assessment carried out with the new DTM data were really promising because they provided very good fits according to the hazard maps from the Po Basin Authority (ADBPO). When the loss estimation was carried out, they showed unexpected inaccuracies caused by the resampling procedures, and by the difference in resolution with CORINE dataset.

6. Life Loss Estimation

This chapter aims at providing a brief overview of models and methods for life loss estimation in flood risk assessment. The different methods will be described and a preliminary feasibility analysis will be carried out in order to assess their suitability in this case.

Another aspect of the damage caused by floods more important than economic losses is the impact on the population. In 1953, the Zuiderzee region in the Netherlands was affected by a coastal flood that caused the death of ca. 2000 people. In Romania, the Danube flood of 1926 caused ca. 1000 victims. In Italy the Po flood in Polesine area was the event that caused the larger amount of casualties exceeding the 100 deths. These data come from one of the main sources of worldwide information freely available nowadays on disasters, the EM-DAT database (see below). In the last few years big efforts were put into the collection, standardization and distribution of information on disasters. The two main sources for disaster data freely accessible are:

- EM-DAT, Emergency Events Database, from a collaboration between the Centre of Research on Epidemiology of Disasters (CRED, Brussels) and the United States Office for Foreign Disasters (USAID-UOFD). It contains data on occurrence and effects of worldwide disasters from 1900 up to present exceeding one of the four thresholds: more than 10 casualties, more than 100 affected people, declaration of state of emergency, call for international assistance. The data are collected from various sources, including UN agencies, non-governmental organizations, insurance companies, research institutes and press agencies. It is freely available at http://www.em-dat.net/.
- NATAN, (Natural Hazard Assessment Network) from MunichRe: it is a global database of main disasters, it includes georeferenced datasets and loss rates for each disaster. It is available at http://www.munichre.com/.

Compared to the economic loss estimation, the casualties estimation due to flood needs a wider range of information related to the flood parameters and to the characteristics of the “elements at risk” represented by the human lives.

In-depth studies were carried out in the last decade with the goal to find the triggering factors that cause lives loss in flood events (Jonkman, 2005; Jonkman, 2007; Jonkman and Kelman, 2005; Jonkman and Vrijling, 2008; Parker et al., 2007; Tapsell, 2007).

Jonkman and Kelman (2005) carried out a statistic study on flood damage data from EM-DAT and on previous literature; he finally compiled a list of the major influencing factors contributing to the mortality rate resumed in table 5.8; the mortality rate is defined as the number of casualties divided by the number of affected people. The list takes into account both the physical event parameters and the social and environmental characteristics of the area prone to flood. Many of the fatalities happened when the event was unexpected.

Tab. 6.1: Overview of relevant factors for the estimation of loss of life for floods (from Jonkman, 2007).

Factor	Exposure
Water depth	Important as deeper water gives less possibilities for shelter. It will also influence collapse of buildings
Rise rate of water	Determines the possibility for shelter and influences collapse of buildings
Flow velocity	High flow velocities can cause instability of people and collapse of buildings
Arrival time	mainly determines the time available for evacuation
Occurrence(night/day)	It influences the predictability, preparedness and possibilities for warning and shelter
Day/week/year	It influences the presence of population in an area and the possibilities for warning
Debris	Floodwaters carrying debris present greater threat to people and buildings
Water temperature	Determines the survival chances of people in water.
Waves	Can damage buildings (could be relevant for coastal floods)
Flood duration	Could influence mortality of people stuck in homes, less relevant for direct fatalities
Water quality	Can lead to injuries and illnesses but less relevant for direct mortality
Infrastructure capacity	determines the time required for evacuation
Shelters	can prevent or reduce exposure to floodwater
Buildings quality	Determines the possibility of collapse of buildings and consequent loss of shelter
Early warning	Essential for evacuation, also important for possibilities to find shelter.
Evacuation plans	These can fasten decision-making, warning and evacuation progress
People vulnerability	Important for individual survival, might be less relevant for larger 'average' populations
Reaction/behaviour	Important for evacuation, and survival chances during the flood.
Rescue actions	Remove people from dangerous locations (water, buildings, trees)

The casualties were higher when the event happened during night-time than during the day, due to the fact that warning people during night results more difficult than during the day. Evacuation plans combined to early warning systems proved to sensibly decrease the number of casualties. The presence of shelters plays an important role in reducing the lives loss. Buildings and any other structure higher than the flood water depth could represent a shelter. The benefit of shelters was directly related to the warning time. Collapse of buildings used as shelters was state to be one of the major causes of deaths during large flood events. From historic data Jonkman (2007) stated that, in the areas where the quality of buildings was lower, the casualties resulted very high. Among the society's characteristics, age and gender are related to the mortality rate. Young children and elder people resulted statistically more exposed to death. Casualties among males were much more numerous than females. In relation to the hazard part, the most influencing flood parameters were found to be three: 1) the water depth could reduce the possible shelters available in the flooded areas; 1) the raising rate of the water could hardly affect the warning time, and therefore higher rates triggered more casualties; 3) water velocity was relevant for the behaviour of the people in the flooded areas (they could walk/swim or not). In her research in the framework of the FLOODsite Project (Integrated Project in the Global Change and Eco-systems Sub-Priority, co-funded by the European Community Sixth Framework Program for

European Research and Technological Development, 2002-2006; http://www.floodsite.net/), Tapsell (2007) stated that the casualties in floods were mainly caused by different groups of characteristics:

- Area characteristics (exposure, type and structure of buildings, flood warning)
- Flood characteristics (depth, velocity, debris, raising speed, time of day/year)
- Population characteristics (age, prior health, disability, language constrains, presence of tourists, behaviour)
- Institutional response (evacuation, rescue etc.)

In relation to the flood characteristics, during their study on more than 700 worldwide major flood events, Jonkman and Vrijling (2005) pointed out that the mortality rate is strongly dependant on the type of flood event. They took in consideration four different flood types. Coastal Floods (or storm surges) are related to sea or big lakes rising water due to storms and cyclones. Flash floods generally occur in mountainous areas after heavy rainfall, they have very short warning time, high flow velocity, and therefore they have a high rate of mortality. River floods regard large floodplains; they include also the floods caused by dams or dikes breaches, in this case they have more similarities with flash floods. Drainage problems: they are caused by high precipitation levels that cannot be handled by regular drainage systems. This type of flood poses a limited threat to life due to limited water levels and causes mainly economic damage.

After statistical studies, the resulting mortality average rates were:

- For Drainage floods: $5{,}3 \times 10^{-4}$
- For Riverine floods: $4{,}9 \times 10^{-3}$
- For Flash floods: 3.6×10^{-2}
- For Coastal floods: $\approx 10^{-2}$

The big uncertainty in describing the mortality in floods is even enhanced if the mortality is related to the geographical location. For the flash floods the mortality rate strongly varies among continents: Africa, 0.042; Asia, 0.032; Americas, 0.027; Europe, 0.056 (Jonkman and Kelman, 2005).

6.1. Existing Methods

Many researches put their effort into building models to estimate lives loss in flood risk assessment. Jonkman (2007) compiled an exhaustive review of the models found in literature. The main restriction of the available models is that they limit themselves in taking into account a few of the characteristics listed in table 5.7. The majority of them is based on the calculation of casualties through a uniform mortality rate applied to the population affected (Tapsell, 2007). A list of some of the methodologies reviewed by Jonkman or available in literature is provided.

The "*Risk to people*" Project was developed by DEFRA (Department for Environment, Food and Rural Affairs, England) Flood Management Unit (Ramsbottom et al., 2003). In this project, the fatalities for a particular flood event were expressed as functions of injuries, estimated according to the

characteristics of the area and population. In detail, the number of injuries ($N_{(I)}$)was calculated through the formula:

$$N_{(I)} = 2Nz \times (HR \times Area\ Vulnerability)/100 \times People\ Vulnerability$$

Where Nz was the population affected; HR was a function of flood depth, velocity, and debris factor. Area vulnerability represented the structural characteristics of the area, like warning systems, buildings types etc. People vulnerability was a percentage value expressing the numbers of old people and disable or seriously sick people over the entire population. The total lives losses were calculated afterwards with the formula:

$$Fatalities = 2\ N_{(I)} \times HR/100$$

The model gave reasonable results regarding the UK while it showed week result when applied to events in Europe; hence it was subsequently adapted for application at European level (Tapsell, 2007).

Another existing model was elaborated by Jonkman (2008, 2007). The methodology was developed for low-lying areas protected by flood defenses, especially in the case of floods caused by levees breaches. The model is based on three main steps, briefly described.

The first step consists in the analysis of flood parameters: flood depth, velocity, rise rate, and arrival time. The author suggests their estimation through simulations with 2D models. The second step is the calculation of the affected population. In this part, the effects of shelters, early warning, evacuation plans are taken into account. The third step regards the calculation of deaths through defined mortalities rates. These rates are provided through two stage-damage functions that relate the mortality to the water depth; one function is for the areas with rapidly rising water, and the other is for the remaining areas. Finally the entire flooded area has to be divided into different sectors according to the flood parameters calculated in the first step in order to chose which of the two functions has to be applied.

Other approaches based on statistic calculations were reviewed by Jonkman (2007). In the Netherland a model was developed by Waarts on the basis of the coastal flood disaster in 1953.

$$FD\ (H) = 6.65\ x10^{-3} e^{1.16\ h} \quad With\ (FD)H<1$$

Where h is flood depth and FD is mortality.The formula was successively modified by introducing the water velocity: two different formulas were extracted for slow and fast flowing water.

Jonkman (2007) developed a basic formula for sea and river floods taking into account water depth, flow velocity and evacuation plans, on the basis of the data from the same flood event of 1953 in the Netherlands. The references for the mentioned methods were not found therefore they are referred to the review contained in the PhD thesis of Jonkman (2007).

6.2. Possible applicability of the existing methods

The main limitation in the application of the mentioned method in the case study is the lack of information. Regarding the hazard assessment, the only information available is the water depth; no

data related to the velocity, rising time, or debris content was extracted, and it is reasonable to consider that such parameters will not be available at European scale. The aspect related to the population vulnerability is even more difficult to be studied. Data related to, age, gender, characteristics of buildings, could be available; but other information, like warnings, presence of shelters, evacuation, behaviour of the population in reacting to flood are, and will not be available at European scale.

The only compatible method with the available data, so far, was the formula developed by Waarts in 1992, showed in the previous section. It requires a flood depth map and a map with the spatial distribution of the affected population. A dataset of homogeneous population density was available at JRC. The dataset was calculated through the combination of data at municipality level from NUTS/LAU (Luck and Knors, 2007), CORINE Landcover 2000 and point survey data from LUCAS (Landuse/Cover area frame Survey) (Gallego, 2007). The map has a horizontal resolution of 100m, and it shows the population density expressed in inhabitants per square kilometre.

Two outputs of the hazard assessment, 100 years return period EFAS 100m SRTM flood hazard map, and the 100 years return period EFAS 100m SRTM flood hazard map with protection measures, were considered. The population density was extracted for the flooded areas in the map and the affected population was calculated. The mortality rate from the formula was estimated based on the flood water depth maps and it was combined to the map of the population affected. The lives loss estimation is shown in table 5.8.

Tab. 6.2:Calculation of casualties on the basis of Waart's formula.

	100 y ret period without def.	**100 years ret. period with def.**
Affected population	588155	407162
Lives loss	24117	13811
Averaged Mortality	4%	3%

The results are exaggeratedly high and unacceptable, due to the fact that the formula was extracted from the coastal flood of 1953 in the Netherlands. In fact, according to Jonkman, the mortality for coastal floods is of the order of 1% and the results are not distant.

6.3. A simple life loss evaluation based on statistics of casualties in Europe

After having stated that none of the methodologies described in the previous section was applicable on the available data, a very simple statistic calculation was carried out to evaluate a generalized value for the mortality due to floods in Europe.

In order to achieve that goal, historical data were collected; The EM-DAT database was used to extract the flood events from 1900 up to present. According to the terminology used in the database, a flood is described as "*...Significant raise of water in rivers, lakes, reservoirs or coastal regions*". In EM-DAT, flood events are classified into flash floods and general floods. Flash floods are defined as

"*rapid intense floods due to intense rainfall; in sloped terrains the water flows rapidly with high destruction potential...*". The term general floods is described as "*...gradually raising inland floods due to high total depth of rainfall or snowmelt...*"

The flood records collected for Europe between 1900 and 2008 were 429. Since 1900 to present flood events caused in Europe 8,121 kills over 13,317,000 people affected (source: EM-DAT). Over 429 records, 169 events with information on, both, affected people and casualties were extracted; 92 since 2000 to present, 49 in the 90's, and 28 from 1950 to 1989. The total amount was composed by 115 general floods, 20 flash floods, and 31 unknown floods. In Annex D, the entire list of the events is shown. Three records were excluded because related to coastal events. Following the methodology of Jonkman (2008), the records were plotted on a log-log scale graphic (see fig. 5.9).

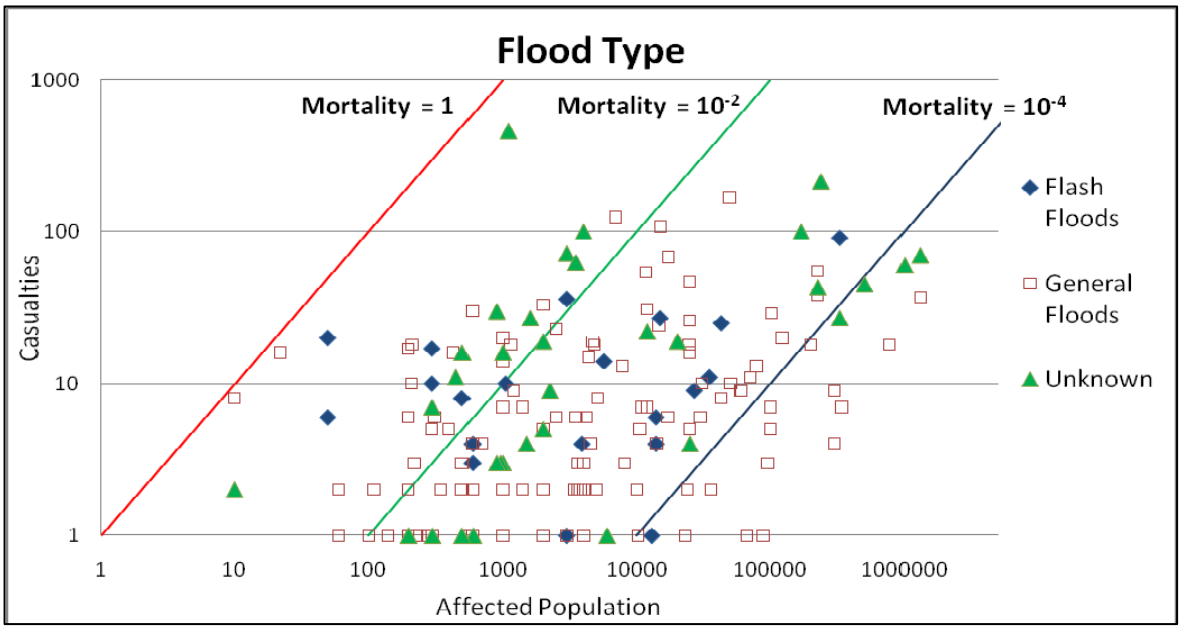

Fig. 6.1: Number of fatalities and people exposed for European floods.

A linear fit was performed for the two flood types. The results are:

$Y = 3*10^{-4}X$ for flash floods

$Y = 4*10^{-5}X$ for riverine floods

The values are different from the ones suggested by Jonkman (2007). Such difference is due to different causes. The calculation carried on is based on a linear fit that doesn't take into account the large variability of the dataset; due to the lack of time, no further statistical analysis could be applied, the function was chosen in order to have a value of the mortality comparable with the ones found in literature. Jonkman (2007) approximated the mortality with a (modified) lognormal distribution, with the following function.

$$F = a + (1-a)LOGN(F_{(D)}, \mu, \sigma)$$

Where *a* is a constant representing the probability mass of *F(D)* =0; μ, σ are respectively the average and the standard deviation of the lognormal distribution. The mortality should have been calculated following the same procedure; but, the procedure was not completely followed. The result achieved can have still a meaning; if the graphic is carefully observed, the line calculated can represent the lower boundary; therefore the minimum number of losses expected evaluated from historical events. Secondly, the source of the data (EM-DAT) is not fully reliable: in fact various records showed strange amount of casualties compared to the affected population (for instance the 1979 flash flood in Spain caused 20 fatalities over 60 affected people; in Portugal in 1967 a flood killed 462 persons over 1100 people affected). Finally, the dataset contained 92 records for the last eight years. It is possible that the mortality in Europe can be lower than developing countries where huge floods happen like India or Bangladesh, due to the improvement of early warning systems like EFAS.

Tab. 6.3: Calculation of fatalities through general statistical evaluations of mortality.

	100 y ret period without def.	**100 years ret. period with def.**
(Jonkman, 2008) $4{,}9 \times 10^{-3}$	2880	1995
Linear fit 4×10^{-5}	25	16
Population affected	588155	407162

Compared to the records, the estimations from the mortality rate calculated by Jonkman are more reliable. These approaches (even with the mortality rate from the literature) don't have any physical meaning. The lives loss estimation is a very difficult field and even the results of complex models (like "risk for people" described before) don't give results comparable to the reality. The literature review and the basic approach applied enhanced the unpredictability of lives loss in flood risk assessment. Moreover, in this case, none of the existing models can be applied due to the lack of information both in the hazard part and in the part related to the population.

7. Conclusions

This work was focused on the improvement the overall damage assessment methodology applied to the simulation of a 100 years return period flood event at European scale within the EFAS project framework. The damage assessment consists in hazard assessment and loss estimation; the conclusions achieved in the two parts are discussed separately.

7.1. Hazard Assessment

Flood extent and depth were extracted through the intersection of a planar approximation approach of the flood wave with a 100m resolution DEM, on the basis of the waterdepths from LISFLOOD model. A novelty in this work was the fact that, for the first time, flood hazard maps from EFAS could be validated through the comparison with a more accurate hazard study from local Authority used as reference. The comparison pointed out that the EFAS hazard map well estimated the flooded regions in the upstream areas; while in the downstream floodplain areas the estimation showed large differences; ca. 275.000 Ha were flooded in EFAS map against 143.000 in the reference hazard map. The sources of such differences were identified.

- The river network (CCM2) dataset used in the calculation didn't precisely fit with the 100m DEM.
- The low accuracy of the 100m DEM caused wrong estimations of flood extent especially in forested areas.
- The elevation of the rivers in 100m SRTM-DEM was assumed to be the floodplain (due to the fact that the streams were not carved out); the 1 year return period waterdepth was assumed to represent the bankfull conditions, therefore the floodplain elevation. Based on it, to estimate the exceeding waterdepth to add on top of the 100m SRTM DEM, EFAS team adopted the difference between 100 and 1 years return period waterdepths. The method performed well for upstream areas but it introduced unexpected estimations in the wide floodplain areas where the main rivers like the Po were visible in the DEM. The methodology is not improvable because the inaccuracies are strictly related to the SRTM-DEM accuracy.

7.1.1. Defence Measures

The first sub-objective of the thesis was *the introduction of protection measures in the methodology and the assessment of the improvements achieved.* Three research questions were related to the sub-objective.

- *Which kinds of information are available about defence structures and which ones have to be considered in order to include the effect of defence structures in the hazard assessment?*

The available information was provided by the major inter-regional water management authority in the area (ADBPO). It regarded only the spatial location of the defence structures for the entire Po basin area. Authorities that deal with water management at inter-regional or national scale for main rivers catchments represent the best sources of homogeneous data related to defence measures. Information regarding the height of the levees in respect to the river should be available to better simulate their capacity in containing the flood. Such kind of records is often not available for large areas, like in this case. To overcome this problem, the defences were classified through the analysis of their relations with flood extents for different return periods that have to be provided by the same source (ADBPO).

– *What could be an adequate strategy to calculate the effect of the structures in the flood extent simulation?*

The structures were introduced directly into the DEM by assuming a standard height according to their classification. The main problems were caused by the difference in the resolution of the DEM and the original defences' dataset. The method suggested was tested only on the Po River basin with a single source of data. The application of the same methodology at European scale has to involve a strategy for collecting information on defences that provides a final dataset as much as possible homogeneous. The advantage of this method is that it overcomes the frequent absence of height information related to the defences.

– *Once the structures have been introduced, is there any significant improvement on the outputs compared with the originals?*

The introduction of defences doubled the accuracy of the hazard map when it was compared to the reference study (from 23% to almost 50%). The improvement rate is not as high as expected. The dataset was not 100% representative of the conditions in reality (according to personal knowledge on the Ticino River, few areas were not well mapped in the dataset). On the other hand, the data availability for the Po basin is likely to be representative of the average situation in the entire Europe. The introduction of the defences had the added value to point out further inaccuracies in the EFAS hazard map without defences, like the errors in forested areas and the underestimation of the flood in various areas.

7.1.2. New 5m DTM

Once stated that the 100m SRTM DEM was one of the major causes of inaccuracies, the possibility to improve the hazard assessment through the acquisition of new elevation data was evaluated. The second sub-objective of the thesis was *the application and the feasibility study of the methodology developed at IES on a new high resolution elevation dataset*. A new 5m DTM involved the change of the other input maps calculated from the elevation data: the local drainage direction map (LDD), and the river network map. Being the river network a source of errors in the original methodology, the calculation of a new dataset from the high resolution DTM removed such errors. The objective suggested three research questions.

– *Is the same methodology applicable to the new datasets? In detail, can the derived input maps be obtained from the new datasets?*

The methodology developed by EFAS team based on the planar approximation approach of the flood wave well performed with the new datasets and it was even simplified. This was due to the fact that LDD and river network were accurate and the calculation did not require the corrections needed by the 100m SRTM-DEM. Problems in the corners of the subsets were found in flood hazard calculation, but they were related to the dimension of the subsets (500 km^2 in total); they were corrected manually. If the subset would have been larger, those problems didn't have influenced the floodable area. New waterdepths had to be calculated through an empirical method. An important aspect is that LISFLOOD model didn't consider the effects of features like polders, reservoirs, dams or any artificial structure affecting the water flow. The subset represented: a natural area without any feature located on the water course, and an area with a dam system. The results showed that the new DTM had a great impact on the accuracy of the flood hazard map; even in the areas with artificial structures.

– *Can the vertical accuracy of the new datasets replace the absence of information on defence measures?*

The main aspect to be highlighted is that the 5m DTM was able to well represent the levees system in the subset areas. In addition, the images were acquired during the last two years; therefore the information from the DTM on the maintenance conditions of the levees is much more up-to-date than the dataset used in this work. The calculation of the hazard assessment with this kind of dataset avoids any other operation to artificially include the defence measures.

– *Do the results justify the acquisition of those elevation maps?*

In the natural areas, the DTM accuracy was 82% compared to the hazard study from ADBPO. On the other hand the entire dataset is enormously costly; IES team has to judge whether to order it or not on the basis of its application in the European damage assessment project and in other applications; a homogeneous high resolution terrain model can provide the basis for applications in different fields in hazard assessment, like 2D flood modelling, landslides modelling, etc.

In conclusion the methodology based on the 5m DTM provided more accurate results than the previous ones from the 100m SRTM. The added value of this method was that it was able to simulate defence structures without the need to include them in a further step.

7.2. Flood damage assessment

The damage assessment was carried out using the outputs of the hazard assessment part. It was based on the application of depth-damage functions expressing the monetary losses per landcover class related to the water depth. The objective of this part of the research was to evaluate the *applicability of the damage assessment to the new hazard data.* The total loss from the hazard map with defence measures was ca. 13 billion Euro, while the hazard map calculated without defences returned a total

damage of 21 billion Euro. The results achieved were not validated because of the lack of previous similar study for the area. Three research questions followed this objective.

- *Are the improvements of the hazard maps corresponding to more reliable results of the potential damage evaluation? Moreover, which effects have the improvements introduced on the damage assessment?*

Unexpectedly, some inaccuracy in the hazard assessment carried out from the 100m SRTM for the entire Po basin was irrelevant in the damage assessment part: the errors in the forested areas were not included in the total losses because the landcover class was not considered damageable. With the introduction of defence measures, the total losses were reduced from ca. 21 billion Euros to ca. 13 billion Euro. This result is strictly related with the reliability of the defence measures dataset. As stated before, it is unlikely to have reliable and homogeneous information on protection structures at European level; therefore, the damage assessment carried out following this method cannot be representative of the situation in reality. This fact further adds value to the methodology based on the 5m DTM.

In the first subset of the Po basin, the losses estimation with the hazard map from 100m DEM gave unreliable results (293 million Euros for an agricultural area of less than 200Km^2). The damage assessment calculated with the new 5m DTM was ca. 11 million euro; according to the hazard map, the results from the DTM were more accurate and probably closer to the reality.

- *How to best combine the resolution of CORINE (100m) and the resolution of the new elevation models (5m)?*

The problem was faced following two directions: firstly the CORINE was resampled at 5m; then the water depth map was resampled at 100m. The results showed that the difference in the two calculations was negligible. The total losses calculation was the most time-consuming part (the machine works for few hours to process ca. 80.000 Km^2). Therefore the second solution is considered the most suitable in the prospective of a calculation at a larger scale.

7.3. Lives loss estimation

An adjunctive sub-objective of this work was to find an applicable method for life loss estimation. This part aimed at providing a brief introduction of the argument and a feasibility assessment on the available methodologies in literature. Life loss estimation is an uncertain field where the researcher found predictive solutions not yet able to explain the variability of the causes that can trigger such phenomena.

- *Which is the information available for life loss estimation? Which are needed?*

The data available were flood depth, flood extent and population affected. The models available nowadays in literature required great amounts of data. The information related to hazard assessment include, for different models, water depth, velocity, rising time, debris content. The vulnerability of

the population is based on a wide fan of elements, including age, prior health, percentage of disables, individual behaviour, and presence of tourists.

The information is not available at European scale. Moreover the results of the models are not jet satisfying.

- *Which are the suitable methodologies in literature to estimate life losses? Are they applicable in this case?*

None of the complex models found in literature was applicable in this case. A method based on estimations of mortality in relation to the water depth was applied. A very coarse and simple evaluation of life loss was carried out through historic records. In conclusion, life loss estimation due to floods cannot be performed without detailed information on various flood parameters and population characteristics.

7.4. Achievements

EFAS project provided for the first time a hydrological model that is able to give homogeneous discharge data at European scale. Due to the availability of such consistent information EFAS team is interested in evaluating potential damage for the entire Europe based on a general flood event with an occurrence probability of one into 100 years. A sensible part in loss estimation is the calculation of the data related to the hazard. Being the first time that flood hazard data are extracted at this scale, no comparisons were carried out on the outputs since now. One of the achievements of this work is to have, for the first time, evaluated the flood hazard maps from EFAS against reliable official local studies. Through this comparison, the inaccuracies in the input maps and the weak points in the methodology were pointed out.

The introduction of the defence measurements is, for EFAS team, an important step in order to shift from the potential loss estimation to the real loss estimation. Following the definition of Barredo (2008), the potential damage is considered as the total damage in a scenario without defence structures. The simulation of the protection measures in this work pointed out useful tenets for the project proceeding. The simulation of defence measures in the hazard assessment through the construction of a database containing information at European scale cannot give successful results. First of all the procedure is affected by the diversity in accuracy and spatial resolution of the data collected, and the scale at which the calculation is carried out. Secondly this work stated that the low reliability of the defences' dataset collected for the Po area cannot ensure to be representative of the reality. Probably others Members of EFAS have accurate and up-to-date datasets at their disposal; but this condition is, with high probability, not guaranteed by all the States.

An alternative was found through the introduction of a new high resolution elevation model (5m DTM) able to represent the defence measures. This work assessed the validity of the methodology with this new input. According to the results, the acquisition of homogeneous high resolution elevation

data for the entire European territory is the most reliable solution to the introduction of protection measures in a European flood damage assessment project.
The calculation of the damage based on the new DTM pointed out the problems in combining the different resolutions of the input maps. After having stated that the loss calculation is the most time consuming part, this work proposes a solution which is oriented to find the best result according to the prospective of the damage calculation for large areas.

7.5. Limitations

The calculation of waterdepths in LISFLOOD model was not part of this study: therefore the accuracy of the waterdepths was not discussed. The final results are dependant on such inputs. It was assumed that the waterdepths provided were correct, no validation was possible due to the absence of similar data for the study area.
The calculations of waterdepths differences described in section 3.2.3 and 3.4.3 were based on an empirical method. The parameters used were chosen on the basis of the best fit of the resulting flood extent maps with the reference flood hazard map from the local authority. This method did not represent a "scientific" approach to the problem; but it was the only possible solution to that problem.
The entire study is carried out on the simulation of a 100 years return period event for the entire Po basin; therefore the validation of the results from both the hazard and the damage assessments was not possible with historic data. The comparison and the validation of the results were carried out on the basis of the only available hazard assessment study at local scale for the entire study area. It was assumed that the results of such study could be considered reliable due to the source of the study.
The extent of the two DTM subsets was ca. 500 Km^2, while the total flooded areas in the Po areas resulted to be ca. 3,500 Km^2. The results achieved with the subsets regard less than the 20% of the entire area; therefore they cannot be assumed to be valid for the entire study area. Such limitation was imposed by the data availability; in fact the data provider put restrictions on the extent and on the locations of the subsets.
No data related to loss estimation were found for the study area; therefore a validation of the results was not possible.
Due to lack of time, the part related to life loss estimation was carried out superficially without any in-depth statistical calculations. This was dictated also by the general idea that it is impossible an estimation of casualties with the available data.

7.6. Recommendations and Future Work

The hazard assessment carried out using the 100m SRTM DEM, cannot be improved because the errors sources mainly lie in the inputs (waterdepths maps and the DEM itself). The only significant improvement could be a change in the input maps. The main discussion focuses on whether or not to acquire the new 5m DTM. An answer can be found taking into account the potentialities related to the

new product. A high resolution DTM can provide a basis for the application of more accurate simulation models like the 2D LISFLOOD FP model. A potential solution of the problem could be the detection of sensitive areas through the damage assessment carried out at 100m resolution, and the acquisition of the new elevation data only for those areas, where a study with more accurate models will be performed. Another approach can be the evaluation of flood-prone areas through the simulation of an extreme event (> 500 years return period) using the original set up (LISFLOOD waterdepths combined with 100m DEM), and the acquisition of the new DTM for such areas. In this case the flood extent and depth can be calculated with the same methodology described in this study, if this methodology is considered reliable by EFAS team. An adjunctive remark to the methodology applied in this study is that the combinations of waterdepths (difference between 100years return period waterdepths and 50 percentles waterdepths) used for the Po basin has to be validated in other catchments.

At the moment, CORINE represents the only available landcover dataset for entire Europe. If the hazard assessment is carried out on the basis of the 5m DTM, the damage estimation should be based on a more accurate landcover dataset. As an example, MOLAND (Monitoring Landcover Dynamics) is a project between JRC and ERA Maptec ltd. based on a similar methodology to CORINE, it uses a minimum mapping unit of 1 Ha in urban areas and 3 Ha in rural areas, against the 25 Ha of CORINE. It covers ca. 50,000 Km2 in Europe. The combination of a 2D flood model with the use of this kind of landuse database, where available, can perform better results in the most sensible areas.

Bibliography

ADBPO, 2006. Caratteristiche del Bacino del Fiume Po e primo esame dell'impatto ambientale delle attivita' umane sulle risorse idriche. . Autorita' di bacino del fiume Po, Parma, ITALY.

AHPS, 2006. Toward a New Advanced Hydrologic Prediction Service (AHPS). The National Academic Press.

Alkema, D., Nieuwenhuis, J.D.p. and de Jong, S.M.p., 2007. Simulating floods: on the application of a 2D hydraulic model for flood hazard and risk assessment, ITC, Enschede, 198 pp.

Annoni, A., Luzet, C., Gulber, E. and Ihde, J., 2001. Map Projection for Europe. Office for Official publications of the European Communities, Luxembourg, EUR 20120 EN.

Austin, G.S., 2002. Advanced Hydrologic Prediction Services Concept of Services and Operations. National Oceanic and Atmospheric Administration (NOAA), National Weather Service, Office of Climate, Water, and Weather Services; Hydrologic Services Division.

Axel, B., 2003. Floods and Climate Change: Interactions and Impacts. Risk Analysis, 23(3): 545-557.

Barredo, J., 2007. Major flood disasters in Europe: 1950–2005. Natural Hazards, 42(1): 125-148.

Barredo, J.I., Salamon, P., Dankers, R., Bodis, K. and De Roo, A., 2008. Flood Damage Potential in Europe. Intitute for Environment and sustainability, Land Management and Natural Hazard Unit, Natural Hazars Action Joint Research Center, Ispra.

Bartholmes and Todini, 2005. Coupling meteorological and hydrological models for flood forecasting. Hydrol. Earth Syst. Sci., 9(4): 333-346.

Bates, P.D. and De Roo, A.P.J., 2000. A simple raster-based model for flood inundation simulation. Journal of Hydrology, 236(1-2): 54-77.

Baudouin, R., 2003. Architecture of the new MARS server. Meteorological Applications ECMWF http://www.ecmwf.int/publications/manuals/mars/server.pdf.

Birkmann, J., 2007. Risk and vulnerability indicators at different scales:: Applicability, usefulness and policy implications. Environmental Hazards, 7(1): 20-31.

Bourgine, B. and Baghdadi, N., 2005. Assessment of C-band SRTM DEM in a dense equatorial forest zone. Comptes Rendus Geosciences, 337(14): 1225-1234.

Chow, V.T., Maidment, D.R. and Mays, L.W., 1988. Applied hydrology. (McGraw-Hill Series in Water Resources and Environmental Engineering). McGraw-Hill, New York etc., 572 pp.

Christensen, J. and Christensen, O., 2007. A summary of the PRUDENCE model projections of changes in European climate by the end of this century. Climatic Change, 81(0): 7-30.

Christensen, O.B. and Christensen, J.H., 2004. Intensification of extreme European summer precipitation in a warmer climate. Global and Planetary Change, 44(1-4): 107-117.

Coburn, A.W., Sspence, R.J.S. and Pomonis, A., 1994. Vulnerability and Risk Assessment. Cambridge Architectural Research Limited. The Oast House, Cambridge, U.K.

Coleman, D., 2001. Radar Revolution: Revealing the Bald Earth, Earth Observation Magazine, November 2001, 30-33.

Coles, S., 2001. An Introduction to Statistical Modeling of Extreme Values. Springer, 228 pp.

Dankers, R. and Feyen, L., 2008. Climate change impact on flood hazard in Europe: An assessment based on high-resolution climate simulations. J. Geophys. Res., 113.

De Jong, K., 2005. PCRaster Version 2 Manual. Department of Physical Geography Faculty of Geosciences, Utrecht University, The Netherlands.

De Lima, N.M.V., 2005. IMAGE2000 and CLC2000 Products and Methods. Joint Research Centre (DG JRC), Institute for Environment and Sustainability (IES), Land Management Unit.

De Roo, A. et al., 2003. Development of a European flood forecasting system. International Journal of River Basin Management 1: 49-59.

De Roo, A. and Maurer, T., 2006. Provision of near real time river discharge and water level data from 35 countries for the European Flood Alert System (EFAS) research project. The European Terrestrial Network for River Discharge (ETN-R), XXII Conference of the Danubian Countries on the hydrological forecasting and hydrological bases of water management Belgrade, Serbia and Montenegro.

De Roo, A. et al., 2006. The Alpine floods of August 2005. What did EFAS forecast, what was observed, which feedback was received from end-users?, Office for Official Publications of the European Communities, Luxembourg.

De Roo, A.P.J., Wesseling, C.G. and Van Deursen, W.P.A., 2000. Physically based river basin modelling within a GIS: the LISFLOOD model. Hydrological Processes, 14(11-12): 1981-1992.

Demeritt, D. et al., 2007. Ensemble predictions and perceptions of risk, uncertainty, and error in flood forecasting. Environmental Hazards, 7(2): 115-127.

Dutta, D., Herath, S. and Musiake, K., 2003. A mathematical model for flood loss estimation. Journal of Hydrology, 277(1-2): 24-49.

DWD, Deutscher Wetterdienst, http://www.dwd.de/, Offenbach, Germany.

ECMWF, European Centre for Medium-Range Weather Forecasts, http://www.ecmwf.int/, Shinfield Park, United Kingdom.

EEA, 1993. CORINE Land Cover - Technical Guide. Office for Official Pubblications of Europeran Communities, Luxembourg.

EUROSTAT, 2005. Guidelines for Geographic Data Intended for the GISCO Reference Database EUROSTAT, EC, Witney, UK.

FEMA, 2001. Mitigation Planning How-To Guide 2, Understanding Your Risk: Identifying Hazards and Estimating Losses. Federal Emergency Management Agency, Washington.

Feyen, L., Dankers, R., Bodis, K., Salamon, P. and Barredo, J., 2008. Climate Warming and Future flood risk in Europe (to be published)

Feyen, L., Vrugt, J.A., Nualláin, B.Ó., van der Knijff, J. and De Roo, A., 2007. Parameter optimisation and uncertainty assessment for large-scale streamflow simulation with the LISFLOOD model. Journal of Hydrology, 332(3-4): 276-289.

Gallego, F.J., 2007. Downscaling population density in the European Union with a land cover map and point survey, Institute for the Protection and the Security of the Citizen (IPSC), JRC, Ispra, Italy. (not pubblished).

Gouweleeuw, B.T., Thielen, J., Franchello, G., De Roo, A.P.J. and Buizza, R., 2005. Flood forecasting using medium-range probabilistic weather prediction. Hydrol. Earth Syst. Sci., 9(4): 365-380.

GRCD, 1988. Global Runoff Data Centre http://grdc.bafg.de/servlet/is/859/, Federal Institute of Hydrology, Koblenz, Germany.

Hall, J.W., Sayers, P.B. and Dawson, R.J., 2005. National-scale Assessment of Current and Future Flood Risk in England and Wales. Natural Hazards, 36(1): 147-164.

Hey, R.D., Heritage, G.L. and Patterson, M., 1990. Design of Flood Alleviation Schemes: Engineering and the Environment. Ministry of Agriculture, Fishering and Food, London.

Huizinga, H.J., 2007. Flood damage functions for EU member states, HKV Consultant, JRC-Institute for Environment and Sustainability (Internal document)

INSPIRE, 2007. Direfctive 2007/2/EC of the european parliament and of the council of 14 March 2007 establishing an Infrastructure for Spatial Information in the European Community (INSPIRE). Office for Official Publication of the European Communities.

InterMAP©, 2008. Product Sheet DTM v1.0 & DTM v1.5 Providing geospatial professionals worldwide with a choice of reliable 3D digital elevation terrain models (DTMs) to meet a wide variety of application needs, pp. 2.

Jenson, S.K. and Domingue, J.O., 1988. Extracting Topographic Structure from Digital Elevation Data for Geographic Information System Analysis. Photogrammetric Engineering and Remote Sensing, 54(11): 8.

Jonkman, S.N., 2005. Global Perspectives on Loss of Human Life Caused by Floods. Natural Hazards, 34(2): 151-175.

Jonkman, S.N., 2007. Loss of life estimation in flood risk assessment, Theory and applications, PhD thesis, Delft University, Delft.

Jonkman, S.N. and Kelman, I., 2005. An Analysis of the Causes and Circumstances of Flood Disaster Deaths. Disasters, 29(1): 75-97.

Jonkman, S.N. and Vrijling, J.K., 2008. Loss of life due to floods. Journal of Flood Risk Management, 1: 43-56.

Kalas M., Ramos M. H., Thielen J. and Babiakova, G., 2008. Evaluation of the medium-range European flood forecasts for the March–April 2006 flood in the Morava River. J.Hydrol. Hydromech., Vol. 56, No. 2, 2008, p. 116 56(2,2008): 16.

Kimura, R., 2002. Numerical weather prediction. Journal of Wind Engineering and Industrial Aerodynamics, 90(12-15): 1403-1414.

Kleist, L. et al., 2006. Estimation of the regional stock of residential buildings as a basis for a comparative risk assessment in Germany. Natural Hazards and Earth System Sciences, 6(4): 541-552.

Krzysztofowicz, R. and Davis, D.R., 1983. Category-Unit Loss Functions for Flood Forecast-Response System Evaluation. Water Resources Research, 19(6): 1476-1480.

Kundzewicz, Z.W. et al., 2005. Summer Floods in Central Europe – Climate Change Track? Natural Hazards, 36(1): 165-189.

Kwadijk, J., 2003. EFFS – European Flood Forecasting System, Final report of Contract EVG1-CT-1999-00011.

Leutbecher, M. and Palmer, T.N., 2008. Ensemble forecasting. Journal of Computational Physics, 227(7): 3515-3539.

Li, B., Phillips, M. and Fleming, C.A., 2005. Application of 3D hydrodynamic model to flood risk assessment. Water Management, 159(1): 12.

Liu, H.-L., Chen, X., Bao, A.-M. and Wang, L., 2007. Investigation of groundwater response to overland flow and topography using a coupled MIKE SHE/MIKE 11 modeling system for an arid watershed. Journal of Hydrology, 347(3-4): 448-459.

Luck, D. and Knors, N., 2007. The LAU2 Code How to Analyse Regional Differences. Job Mobilities and Family Lives in Europe Modern Mobile Living and its Relation to Quality of Life funded by the European Commission.

Mangelsdorf, J., Scheurmann, K. and Weiss, F.-H., 1990. River morphology : a guide for geoscientists and engineers. Springer series in Physical environment;7. Springer-Verlag, Berlin, 243 pp.

McCuen, R.H., 1982. A Guide to Hydrologic Analysis Using SCS Methods. Prentice-Hall.

Messner, F. et al., 2007. Evaluating flood damages: guidance and recommendations on principles and methods. FLOODsite Project - Integrated Flood Risk Analysis and Management Methodologies T9-06-01.

Mitchell, J.K., 2003. European River Floods in a Changing World. Risk Analysis, 23: 567-574.

Mourier, B., Walter, C. and Merot, P., 2008. Soil distribution in valleys according to stream order. CATENA, 72(3): 395-404.

Munich-Re, 2003. Annual Review: Natural Catastrophes 2002.

Muzik, I., 2002. A first-order analysis of the climate change effect on flood frequencies in a subalpine watershed by means of a hydrological rainfall-runoff model. Journal of Hydrology, 267(1-2): 65-73.

Nicholls, R.J., 2002. Analysis of global impacts of sea-level rise: a case study of flooding. Physics and Chemistry of the Earth, Parts A/B/C, 27(32-34): 1455-1466.

Parker, D., Tapsell, S. and McCarthy, S., 2007. Enhancing the human benefits of flood warnings. Natural Hazards, 43(3): 397-414.

Perry, C., 2000. Significant floods in the United States during the 20th Century – USGS measures a century of floods. US Geological Survey, Fact Sheet 024–00.

Persson, A. and Grazzini, F., 2007. User Guide to ECMWF forecast products, Shinfield Park (UK).

Pimentel, D. and Pimentel, M., 2006. Global environmental resources versus world population growth. Ecological Economics, 59(2): 195-198.

Raghunath, H.M., 1987. Ground Water. New Age International, ISBN 8122419046, 9788122419047.

Ramsbottom, D., Floyd, P. and Penning-Rowsell, E., 2003. Flood Risks to People Phase 1. Final Report Prepared for Defra/Environment Agency Flood and Coastal Defence R&D Programme.

Sadl, K.U., 2005. GISCO Database Manual, Eurostat official Pubblications.

Sanders, B.F., 2007. Evaluation of on-line DEMs for flood inundation modeling. Advances in Water Resources, 30(8): 1831-1843.

Sanders, R., Shaw, F., MacKay, H., Galy, H. and Foote, M., 2005. National flood modelling for insurance purposes: using IFSAR for flood risk estimation in Europe. Hydrol. Earth Syst. Sci., 9(4): 449-456.

Shultz, M.J., Crosby, E.C. and McEnery, J.A., 2008. Kinematic wave technique applied to hydrologic distributed modeling using stationary storm events: an application to synthetic rectangular basins and an actual watershed. Hydrology Days 2008.

Soetanto, R. and Proverbs, D., 2004. Impact of flood characteristics on damage caused to UK domestic properties: the perceptions of building surveyors. Structural Survey, 22(2): 95-104.

Soille, P., 2003. Morphological Image Analysis. 2nd Edition. Berlin, Heidelberg, New York.

Tapsell, S., 2007. Socio-economic and ecological evaluation methodologies, FLOODsite Project, T10-07-13.

Tarboton, D.G., Bras, R.L. and Rodriguez-Iturbe, I., 1991. On the extraction of channel networks from digital elevation data. Hydrological Processes, 5(1): 81-100.

Thieken, A., Muller, M., Kreibich, H. and Merz, B., 2005. Flood damage and influencing factors: New insights from the August 2002 flood in Germany. Water Rsources Research, 41(W12430, doi:10.1029/2005WR004177, 2005): 16.

Thieken, A.H. et al., 2006. Regionalisation of asset values for risk analyses. Natural Hazards and Earth System Sciences, 6(2): 167-178.

Thielen, J., Bartholmes, J., Ramos, M.H. and De Roo, A., 2006. The benefit of probabilistic flood forecasting on European scale - Results of the European Flood Alert System for 2005/2006. Office for Official Publications of the European Communities.

Thielen, J., Bartholmes, J., Ramos, M.H. and de Roo, A., 2008. The European Flood Alert System - Part 1: Concept and development. Hydrol. Earth Syst. Sci. Discuss., 5(1): 257-287.

Thielen, J., de Roo, A. and Schmuck, G., 2003. FIRST LISFLOOD ALERT WORKSHOP - Practical benefit from European Research, Institute for Environment and Sustainability, Ispra (IT).

Tighe, M.L., 2003. Topographic Mapping from Interferometric SAR Data is Becoming an Accepted Mapping Technology. In: I. Technologies (Editor), Map Asia 2003, Kula Lumpur, Malayisa.

UN\ISDR, 2004. (United Nations International Strategy for Disaster Reduction), Living with Risk, a Global Review of Disaster Reduction Initiatives, UN Pubblications, Geneva.

UNDRO, 1979. Natural Disaster and Vulnerability Analysis, Office of the United Nations Disaster Relief Coordinator, Report of Expert Group Meeting 9-12 June 1979, UN Pubblications, Geneva.

Usamah, M.B. and Alkema, D., 2006. Integration of GIS and Hydrodynamic Modelling to predict and simulate flood inundation risk in the Lower Bicol Floodplain, the Philippines, T.G.R. Portal.

USGS, 2001 GTOPO30. E.R.O.a.S. http://eros.usgs.gov/products/elevation/gtopo30/html.

Van Der Knijff, J. and De Roo, A., 2008. LISFLOOD – distributed water balance and flood simulation model, (Revised User Manual 2008). European Commission, EN22166.

Van Vuuren, D. and Alfsen, K., 2006. PPP Versus Mer: Searching for Answers in a Multi-Dimensional Debate. Climatic Change, 75(1): 47-57.

Velk, C.A.J., 1996. A multi-level, multi-stage and multi-attribute perspective on risk assessment, decision-making and risk control. Risk Decision and Policy, 1(1): 23.

Venables, W.N. and Smith, D.M., 2008. An Introduction to R Notes on R: A Programming Environment for Data Analysis and Graphics, Version 2.8.1, http://www.r-project.org/.

Vogt, J.V., Colombo, R., Paracchini, M.L., De Jager, A. and Soille, P., 2003. CM River and Catchment Database Version 1.0. Office for Official publications of the European Communities, Luxembourg.

Vogt, J.V. et al., 2007. Developing a pan-European Database of Drainage Networks and Catcment Boudaries from a 100 Metre DEM. Office for Official publications of the European Communities, Luxembourg, EUR 22920 EN.

Zhao, R.J. and Liu, X.R., 1995. The Xinanjiang model. Singh, V.P. Editor, Computer Models of Watershed Hydrology Water Resources Publication, pp. 215-232.

Annexes

Annex A

The methodology explained in section 3.4 was followed to extract the flood extent depth from a 2.5 meters DTM. The DTM represents stream section of the Elbe River with a length of ca. 18 Km. The area is located in between the German cities Wittenberg in the North and Torgau in the South. With this analysis EFAS team aims at assessing the validity of the methodology developed to extract the flood parameters from high resolution DTMs. In the DTM, the bathymetry of the riverbed is represented; therefore the calculation was carried out using the 100 years return period waterlevel from LIFLOOD model without any further correction. In addition, two othr maps were calculated using, in turn, the difference (100y r.p. waterlevel – 40 percentile waterlevel) and the difference (100y r.p. waterlevel – 50percentile waterlevel).

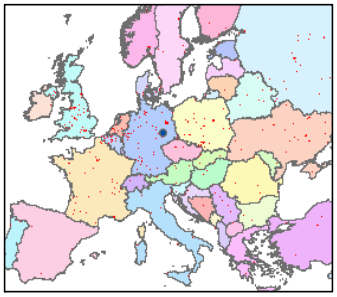

Fig. 1: Location of the Elbe River subset (blue spot in the map)

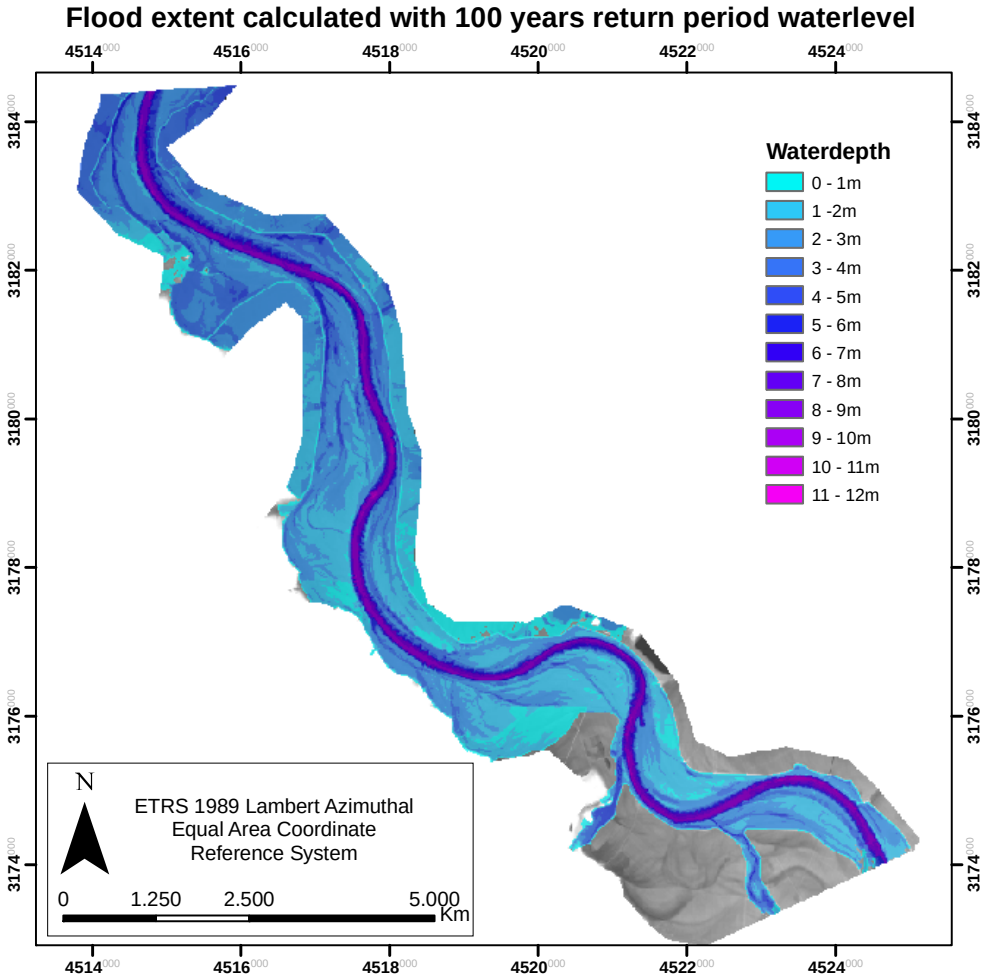

Flood extent calculated with (100 y. r. p.- 40%) waterlevel

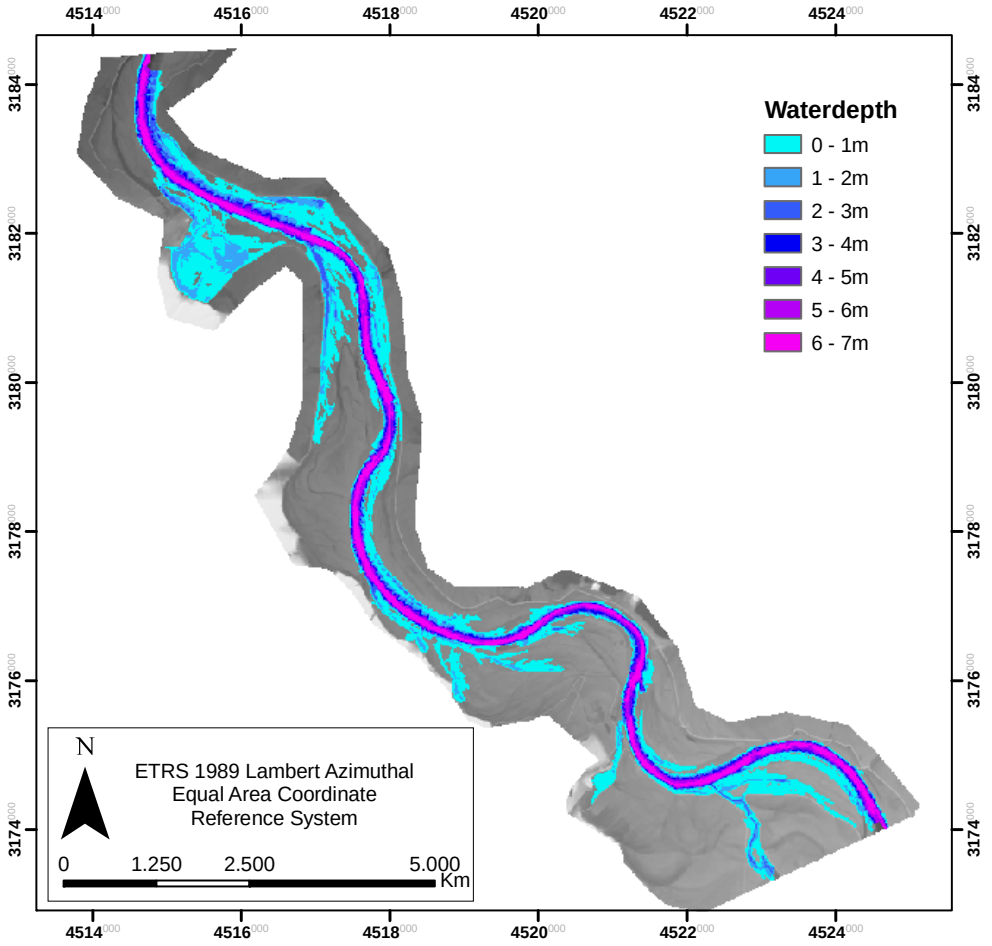

Flood extent calculated with (100 y. r. p.- 50%) waterlevel

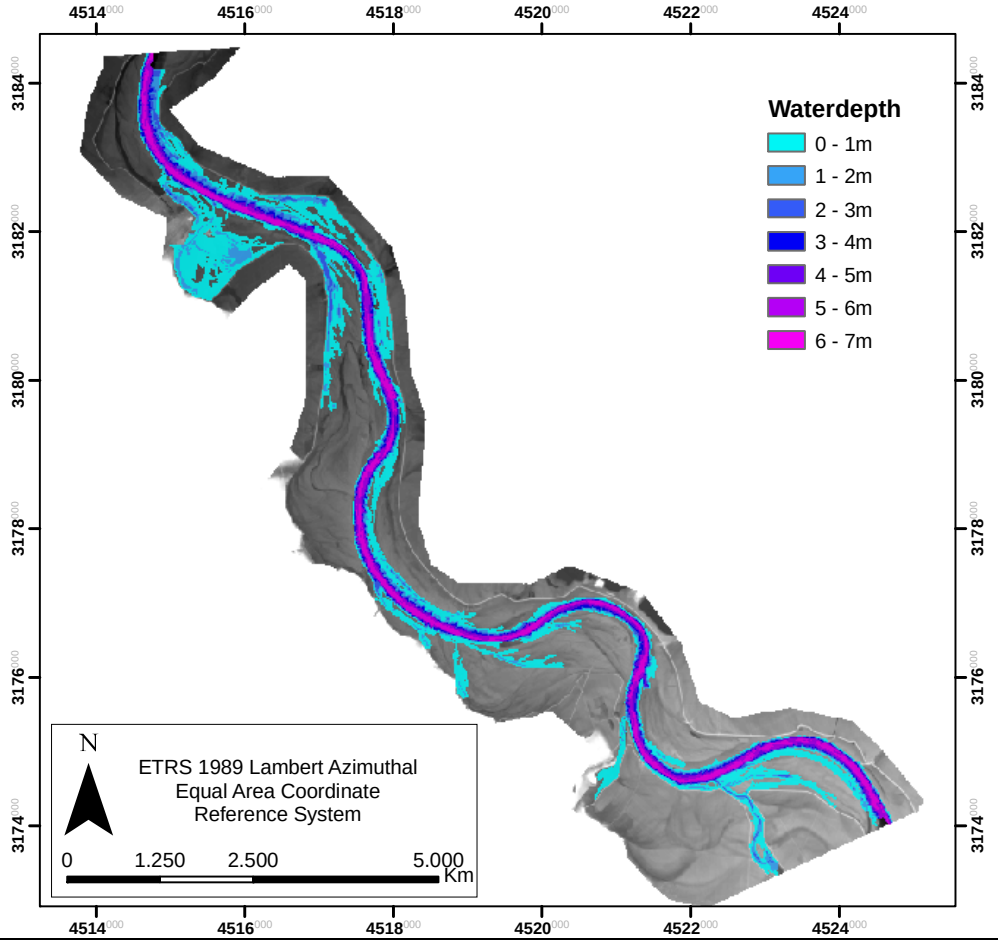

No hazard assessment was available for the subset; hence a validation was not carried out. The EFAS team already studied in depth the area in previous project and therefore they will judge the results according to their knowledge on the basis of the results of previous studies.

Annex B

As explained in section 4.1.1, the comparison between the EFAS-SRTM100m flood hazard map and the reference hazard map from the Po basin Authority (ADBPO) was carried out at municipality level. The boundaries of the various municipalities were extracted from the NUTS\LAU (Nomenclature of Territorial Units for Statistics/Land Administrative Units) European database. The comparison gave the possibility to calculate the flooded areas for each municipality. In the table showed, the main municipalities among the 978 hit by the flood extensions are ranked according to their area.
In the table, the field CMLAD represents the code for the LAU level 2, presenting, for Italy, the municipalities. The field TOPO-CLASS indicates to which topographic class the municipality belongs, according to the classification suggested in section 4.1.1: (0- 150m) 1st class, (150-300m) 2nd class, (over 300m) 3rd class. The flooded areas are expressed in hectares and in percentage of the total municipality area for both the EFAS-SRTM flood hazard map without defence measures and the reference flood hazard map from ADBPO

NAME	CMLACD	AREA (Ha)	TOPO CLASS	FLOODED ADBPO (Ha)	Perc. (ADBPO)	FLOODED EFAS (Ha)	Perc (EFAS)
FERRARA	IT40600008	40611	1	654	2%	999	2%
PARMA	IT40200027	26055	1	1540	6%	1392	5%
ALESSANDRIA	IT11800003	20396	1	5814	29%	3980	20%
MODENA	IT40400023	18363	1	714	4%	3547	19%
MILANO	IT20500357	18226	1	506	3%	0	0%
BONDENO	IT40600003	17488	1	638	4%	8162	47%
ASTI	IT11700005	15196	2	799	5%	764	5%
MIRANDOLA	IT40400022	13764	1	0	0%	386	3%
CARPI	IT40400005	13168	1	86	1%	1843	14%
FOSSANO	IT11600279	13131	3	232	2%	145	1%
TORINO	IT11100272	13029	2	719	6%	1662	13%
CUNEO	IT11600268	12004	3	170	1%	260	2%
PIACENZA	IT40100032	11850	1	1871	16%	3339	28%
TEGLIO	IT20400314	11519	3	371	3%	278	2%
SAVIGLIANO	IT11600405	11021	3	1031	9%	612	6%
FINALE EMILIA	IT40400012	10494	1	131	1%	3090	29%
CASTELFRANCO EMILIA	IT40400006	10302	1	62	1%	200	2%
VIADANA	IT20B00066	10268	1	2750	27%	6816	66%
CREVALCORE	IT40500024	10254	1	21	0%	349	3%
TORTONA	IT11800174	9803	1	1319	13%	774	8%
CARMAGNOLA	IT11100059	9674	2	529	5%	801	8%
FIDENZA	IT40200014	9454	1	249	3%	0	0%
BRESCIA	IT20700219	9062	1	58	1%	0	0%
MARCARIA	IT20B00031	9051	1	566	6%	1154	13%
MEDESANO	IT40200020	8879	2	642	7%	96	1%
CASALE MONFERRATO	IT11800039	8633	1	1270	15%	1318	15%
MONTECRESTESE	IT11400296	8415	3	16	0%	24	0%
BARGE	IT11600202	8364	3	61	1%	1	0%
VERCELLI	IT11200158	8040	1	1132	14%	3128	39%
MONTICHIARI	IT20700303	8037	1	90	1%	627	8%
CHERASCO	IT11600257	8010	2	570	7%	416	5%
NOCETO	IT40200025	7870	1	223	3%	2	0%

VIGEVANO	IT20800292	7789	1	935	12%	457	6%
BUSSETO	IT40200007	7650	1	75	1%	1	0%
SALUZZO	IT11600393	7644	3	1108	14%	5	0%
ASOLA	IT20B00002	7367	1	300	4%	704	10%
SOLIGNANO	IT40200035	7281	3	0	0%	2	0%
CREMONA	IT20A00036	7116	1	427	6%	132	2%
PIATEDA	IT20400298	7088	3	33	0%	64	1%
TRINO	IT11200148	7055	1	732	10%	349	5%
LANGHIRANO	IT40200018	7004	3	48	1%	0	0%
FENIS	IT12000027	6947	3	32	0%	28	0%
SAN BENEDETTO PO	IT20B00055	6907	1	953	14%	5430	79%
CONDOVE	IT11100093	6876	3	60	1%	92	1%
CURTATONE	IT20B00021	6732	1	0	0%	796	12%
PONTE IN VALTELLINA	IT20400301	6617	3	10	0%	16	0%
CASALMAGGIORE	IT20A00021	6517	1	917	14%	3236	50%
CENTO	IT40600004	6499	1	0	0%	37	1%
VARANO DEMELEGARI	IT40200045	6450	2	10	0%	14	0%
VOGHERA	IT20800297	6434	1	0	0%	529	8%
BUSCA	IT11600224	6410	3	66	1%	206	3%
MANTOVA	IT20B00030	6398	1	0	0%	120	2%
PAVIA	IT20800225	6277	1	1021	16%	400	6%
CARPANETO PIAC.	IT40100011	6256	1	58	1%	0	0%
QUART	IT12000054	6196	3	83	1%	31	1%
SUZZARA	IT20B00065	6083	1	1097	18%	296	5%
FIORENZUOLA DARDA	IT40100021	6049	1	182	3%	0	0%
BRA	IT11600219	6023	2	62	1%	12	0%
DRONERO	IT11600272	5940	3	15	0%	29	0%
NOVELLARA	IT40300028	5884	1	0	0%	2557	43%
COLLECCHIO	IT40200009	5867	1	771	13%	512	9%
CASTELLARANO	IT40300014	5822	2	42	1%	7	0%
LENO	IT20700278	5821	1	176	3%	265	5%
FORNOVO DI TARO	IT40200017	5734	2	212	4%	179	3%
SERMIDE	IT20B00061	5697	1	416	7%	1544	27%
TRONTANO	IT11400318	5682	3	139	2%	96	2%
NOVI LIGURE	IT11800114	5598	2	172	3%	100	2%
NUS	IT12000045	5597	3	24	0%	25	0%
ALSENO	IT40100002	5529	1	247	4%	0	0%
LUGAGNANO VAL DARDA	IT40100026	5476	3	55	1%	0	0%
NONANTOLA	IT40400027	5459	1	69	1%	223	4%
ALBA	IT11600193	5450	2	454	8%	385	7%
GAMBOLO	IT20800183	5426	1	439	8%	37	1%

Annex C

The damage assessment model developed by EFAS team is based on the loss calculation through depth-damage functions for each class of CORINE LandCover (CLC) dataset. CLC consist of a hierarchical classification of the landcover carried out through image interpretation techniques. In the table below, the three levels are shown as they appear in the dataset.

LABEL1	LABEL2	LABEL3	GRID_CODE
Artificial surfaces	Urban fabric	Continuous urban fabric	1
		Discontinuous urban fabric	2
	Industrial, commercial and transport units	Industrial or commercial units	3
		Road and rail networks and associated land	4
		Port areas	5
		Airports	6
	Mine, dump and construction sites	Mineral extraction sites	7
		Dump sites	8
		Construction sites	9
	Artificial, non-agricultural vegetated areas	Green urban areas	10
		Sport and leisure facilities	11
Agricultural areas	Arable land	Non-irrigated arable land	12
		Permanently irrigated land	13
		Rice fields	14
	Permanent crops	Vineyards	15
		Fruit trees and berry plantations	16
		Olive groves	17
	Pastures	Pastures	18
	Heterogeneous agricultural areas	Annual crops associated with permanent crops	19
		Complex cultivation patterns	20
		Land principally occupied by agriculture, with significant areas of natural vegetation	21
		Agro-forestry areas	22
Forest and semi natural areas	Forests	Broad-leaved forest	23
		Coniferous forest	24
		Mixed forest	25
	Scrub and/or herbaceous vegetation associations	Natural grasslands	26
		Moors and heathland	27
		Sclerophyllous vegetation	28
		Transitional woodland-shrub	29
	Open spaces with little or no vegetation	Beaches, dunes, sands	30
		Bare rocks	31
		Sparsely vegetated areas	32
		Burnt areas	33
		Glaciers and perpetual snow	34
Wetlands	Inland wetlands	Inland marshes	35
		Peat bogs	36
	Maritime wetlands	Salt marshes	37
		Salines	38
		Intertidal flats	39
Water bodies	Inland waters	Water courses	40
		Water bodies	41
	Marine waters	Coastal lagoons	42
		Estuaries	43
		Sea and ocean	44
NODATA	NODATA	NODATA	48
UNCLASSIFIED	UNCLASSIFIED LAND SURFACE	UNCLASSIFIED LAND SURFACE	49
	UNCLASSIFIED WATER BODIES	UNCLASSIFIED WATER BODIES	50

Annex D

The statistics shown in section 6.3, a statistic review on flood disasters in Europe was shown. The graphic in fig.6.1 the flood events happened since 1900 to present were plotted. The information source is the EM-DAT (Emergency events databases) free database. The events recorded have to fulfil one of the following requisites: 10 or more casualties; 100 or more affected people; declaration of state of emergency, call for international aid. The records available were 429; The statistics were calculated only among those events with records for both casualties and affected people. The 169 events are listed in the table below. For each record, the mortality rate is calculated as the casualties divided by the affected people.

2000-2008							
Start Date	End Date	Country	Location	Subtype	Killed	Tot Affected	Mortality
30/11/2005	03/12/2005	ALB	Vlora, Fie, Gjirokaster, ...	General flood	3	500	6,00E-03
21/09/2002	10/10/2002	ALB	Lezha, Shkoder regions (N ...	General flood	1	66884	1,50E-05
12/08/2002	20/08/2002	AUS	All	General flood	9	60000	1,50E-04
16/11/2007	21/11/2007	BUL	Radnevo, Galabovo, Tsarev ...	General flood	2	60	3,33E-02
04/08/2007	07/08/2007	BUL	Rouss?, Tsar-Kaloyan (Nor ...	General flood	8	10	8,00E-01
22/05/2007	06/06/2007	BUL	Plovdiv, Lovech, Gabrovo, ...	General flood	2	1000	2,00E-03
04/08/2005	11/08/2005	BUL	Pazardzhik, Smolyan, Vrat ...	General flood	7	12000	5,83E-04
02/07/2005	06/07/2005	BUL	Shoumen, Stara Zagora, Ta ...	General flood	17	200	8,50E-02
31/03/2002	02/04/2002	CIS	North Santa Cruz de Tener ...	General flood	16	430	3,72E-02
20/11/2001	20/11/2001	CIS	La Palma (Isl.), Grand Ca ...		7	300	2,33E-02
28/03/2006	17/04/2006	CZE	Ostrava, Prague, Vestec, ...	General flood	6	4200	1,43E-03
07/08/2002	28/08/2002	CZE	Prague, Bohemia, Plzen, K ...	General flood	18	200000	9,00E-05
15/11/2005	17/11/2005	FRA	Perpignan area	General flood	2	1000	2,00E-03
07/09/2005	09/09/2005	FRA	H?rault, Alpes-Maritimes, ...	Flash flood	1	3000	3,33E-04
02/12/2003	03/12/2003	FRA	Herault, Gard, Bouches-du ...	Flash flood	9	27000	3,33E-04
08/09/2002	12/09/2002	FRA	Gard, H?rault, Vaucluse, ...	General flood	23	2500	9,20E-03
21/03/2001	28/03/2001	FRA	Calvados and Seine-Mariti ...	General flood	3	8100	3,70E-04
00/11/2000	00/11/2000	FRA	C?te d'Azur (Alpes-Mariti ...		1	302	3,31E-03
10/07/2000	10/07/2000	FRA	Epaux-B?zu, Coincy (Aisne ...		1	600	1,67E-03
00/05/2000	00/05/2000	FRA	Seine-Maritime		2	10	2,00E-01
10/06/2000	10/06/2000	FRA	Haute-Garonne, Tar-et-Gar ...		1	200	5,00E-03
11/08/2002	20/08/2002	GER	Basse-Saxe, Saxe-Anhalt, ...		27	330108	8,18E-05
16/11/2007	02/12/2007	GRE	Evros region, Eastern Mac ...	General flood	2	600	3,33E-03
08/10/2006	12/10/2006	GRE	Thessaloniki, Halkidiki, ...	General flood	1	3000	3,33E-04
00/01/2001	00/01/2001	GRE	Athens, Corinth, Cape Sou ...		11	450	2,44E-02
19/11/2000	19/11/2000	GRE	Ath?nes, Corinthe		1	6000	1,67E-04
06/04/2000	01/05/2000	HUN	Boka Borsod-Abauj-Zemplen .	General flood	1	2000	5,00E-04
13/11/2004	14/11/2004	ITA	Toscane, Ombrie, Molise	General flood	2	200	1,00E-02
29/08/2003	31/08/2003	ITA	Udine province, Frioul-V? ...	General flood	2	350	5,71E-03
25/01/2003	27/01/2003	ITA	Abuzzo, Puglia, Molise, B ...	General flood	1	1000	1,00E-03
22/11/2002	03/12/2002	ITA	Liguria, Emilia Romagna, ...	General flood	2	10000	2,00E-04
20/11/2000	20/11/2000	ITA	Tuscan, Lombardy, Friuli, ...		5	2000	2,50E-03
14/10/2000	22/10/2000	ITA	Pi?mont, Val d'Aoste, Li ...	Flash flood	25	43000	5,81E-04
10/09/2000	10/09/2000	ITA	Soverato (Near Catanzaro, ...	General flood	16	22	7,27E-01
08/01/2003	10/01/2003	MAC	Kumanovo region, Orizare, ...	General flood	2	4000	5,00E-04
26/07/2008	27/07/2008	MOL	Riscani, Glodeni, Falesti ...	General flood	3	4000	7,50E-04
00/06/2002	00/06/2002	MOL	Tighina, Lapushna, Gagauz ...		1	500	2,00E-03
17/03/2005	26/03/2005	POL	Lower Silesia, northern M ...	General flood	2	3600	5,56E-04
20/07/2001	03/08/2001	POL	Malopolskie, Swietokrzysk ...	Flash flood	27	15000	1,80E-03
18/02/2008	18/02/2008	POR	Loures, Sacavem, Setubal ...	General flood	2	110	1,82E-02
26/12/2002	26/12/2002	POR	North	General flood	1	60	1,67E-02
26/01/2001	29/01/2001	POR	Mesao Frio region (north) ...	General flood	6	200	3,00E-02
00/08/2008	00/08/2008	ROM	North East	General flood	5	10520	4,75E-04
05/09/2007	11/09/2007	ROM	Galati, Vrancea, Vaslui, ...	General flood	7	1400	5,00E-03
25/08/2007	26/08/2007	ROM	Brasov county, Moldovita ...	General flood	2	1400	1,43E-03
07/08/2007	07/08/2007	ROM	Constanta, Suceava depart ...		3	960	3,13E-03
30/06/2006	03/07/2006	ROM	Arbore (Suceava), Bistrit ...	General flood	30	600	5,00E-02
19/06/2006	19/06/2006	ROM	Cotrsti (Centre), Mures (...	General flood	1	600	1,67E-03
20/06/2006	26/06/2006	ROM	Bistrita Nasaud, Maramure ...	Flash flood	14	5712	2,45E-03
13/03/2006	07/04/2006	ROM	Dolj, Alba, Arad, Botosan ...	General flood	6	17071	3,51E-04
21/09/2005	23/09/2005	ROM	Costinesti, Tuzla, Consta ...	General flood	10	30800	3,25E-04
14/08/2005	25/08/2005	ROM	Harghita, Mures, Dolj, Ba ...	General flood	33	2000	1,65E-02
16/08/2005	17/08/2005	ROM		General flood	18	1140	1,58E-02
12/07/2005	28/07/2005	ROM	Alba, Tulcea, Giurgiu, Vr ...	General flood	24	14669	1,64E-03
02/07/2005	03/07/2005	ROM	Olt department, Hunedoara ...	General flood	8	5102	1,57E-03
21/04/2005	15/05/2005	ROM	Arad, Mehedinti, Timis, C ...	General flood	2	3400	5,88E-04

17/03/2005	25/03/2005	ROM	Mures department	General flood	2	600	3,33E-03
27/08/2004	27/08/2004	ROM	Constanta, Vaslui, Bacau	Flash flood	6	14000	4,29E-04
28/07/2004	01/08/2004	ROM	Brasov, Buzau, Iasi, Baca ...	General flood	4	14128	2,83E-04
02/01/2003	02/01/2003	ROM		Flash flood	3	600	5,00E-03
06/08/2002	07/08/2002	ROM	Ciaoara, Baia de Aries , ...	General flood	1	301	3,32E-03
00/08/2002	00/08/2002	ROM	East, Center, Sud-East	Flash flood	4	3900	1,03E-03
19/07/2002	23/07/2002	ROM	Constanta, Suceava, Praho ...	General flood	4	4500	8,89E-04
19/06/2001	22/06/2001	ROM	Central Transylvania So ...	General flood	7	10803	6,48E-04
05/04/2000	25/04/2000	ROM	Alba, Arad, Bihor, Bistri ...	General flood	9	60431	1,49E-04
00/04/2005	00/04/2005	RUS	Patrikha, Krasno?arsk (Si ...	General flood	3	222	1,35E-02
14/04/2004	18/05/2004	RUS	Krapivino (Kemerovo regio ...	General flood	18	4800	3,75E-03
08/08/2002	18/08/2002	RUS	Novorossiisk (Krasnodar r ...	General flood	167	49500	3,37E-03
19/06/2002	01/07/2002	RUS	Stavropol, Krasnodar, Kar ...	Flash flood	91	330613	2,75E-04
06/01/2002	23/01/2002	RUS	Krasnodar, Temryuk, Anapa ...	General flood	1	3000	3,33E-04
06/08/2001	12/08/2001	RUS	Vladivostok region	General flood	16	25000	6,40E-04
07/07/2001	13/07/2001	RUS	Buryata, Irkutz (Siberia) ...	Coastal flood	11	300000	3,67E-05
12/05/2001	27/05/2001	RUS	Yakutia, Bashkiria, Tuva ...	General flood	10	50305	1,99E-04
30/07/2000	06/08/2000	RUS	Primoriye, Khabarovosk, S ...	General flood	2	24000	8,33E-05
14/04/2000	14/04/2000	RUS	Kurgan, Orenburg (Cheliab ...	General flood	1	23000	4,35E-05
20/04/2005	20/04/2005	S_M	Jasa Tomic, Plandiste, Ve ...	General flood	2	3790	5,28E-04
27/07/2004	02/08/2004	SLO	Spisska Nova Ves, Gelnica ...	General flood	1	230	4,35E-03
12/10/2007	18/10/2007	SPA	Alicante, Valencia areas, ...	General flood	3	3600	8,33E-04
23/05/2007	26/05/2007	SPA	Madrid area (Central Spai ...	General flood	1	550	1,82E-03
03/04/2007	05/04/2007	SPA	Aragonia, Navarra, Caralo ...	General flood	1	280	3,57E-03
31/03/2002	01/04/2002	SPA	Santa Cruz	Flash flood	6	50	1,20E-01
20/10/2000	26/10/2000	SPA	Catalonia, Valencia, Muri ...	Flash flood	8	500	1,60E-02
10/06/2000	10/06/2000	SPA	North-East		16	500	3,20E-02
08/08/2007	12/08/2007	SWI	Alpes	General flood	1	101	9,90E-03
21/08/2005	26/08/2005	SWI	Bern, Brienz, Lucerne, Sc ...	General flood	6	2500	2,40E-03
26/07/2008	27/07/2008	UKR	Ivano-Frankivsk, Chernvit ...	General flood	38	224725	1,69E-04
02/07/2006	03/07/2006	UKR	Belogorsky district, Lviv ...	General flood	2	5000	4,00E-04
04/03/2001	17/03/2001	UKR	Zakarpatian Oblast, Trans ...	General flood	9	300000	3,00E-05
06/09/2008	08/09/2008	U K	Wales, Northern, Western	General flood	6	200	3,00E-02
20/07/2007	24/07/2007	U K	Gloucestershire, Worceste ...	General flood	7	340000	2,06E-05
25/06/2007	03/07/2007	U K	Yorkshire, Lincolnshire, ...	General flood	6	30000	2,00E-04
15/06/2007	21/06/2007	U K	Yorkshire, Leeds, Wakefie ...	General flood	1	200	5,00E-03
20/07/2002	20/07/2002	U K	Ecosse, West Yorkshire, C ...		1	200	5,00E-03

1990-1999

20/09/1995	20/09/1995	ALB	Laci, Rrogozhina, Lushnja ...		4	1500	2,67E-03
17/11/1992	19/11/1992	ALB	Kruja, Lac, Lezha, Shkdor ...	Flash flood	11	35000	3,14E-04
07/03/1999	10/04/1999	BEA	Brest,Gomel and Minsk reg ...	General flood	2	2000	1,00E-03
12/09/1998	14/09/1998	BEL	Diest	General flood	1	140	7,14E-03
02/07/1997	24/07/1997	CZE	Moravia, Bohemia regions	General flood	29	102107	2,84E-04
10/05/1996	14/05/1996	CZE	Bruntal, Lichnov (North M ...	General flood	1	60	1,67E-02
12/11/1999	15/11/1999	FRA	Aude, Tarn, Herault, Pyre ...	Flash flood	36	3005	1,20E-02
27/01/1996	30/01/1996	FRA	Beziers, Puisserguier, Ca ...	Flash flood	4	600	6,67E-03
07/01/1994	12/01/1994	FRA	Camargue	General flood	10	210	4,76E-02
11/05/1999	30/06/1999	GER	Bavaria	General flood	7	100000	7,00E-05
21/12/1993	31/12/1993	GER	Saarland, Rheinland-Palat ...	General flood	5	100000	5,00E-05
03/02/1998	03/02/1998	GRE	Levos Isl.		3	900	3,33E-03
24/10/1994	27/10/1994	GRE	Athens, Rhodes Isl., Kard ...	General flood	14	1000	1,40E-02
09/07/1999	16/07/1999	HUN	Heves conty (Nord-Eastern ...	General flood	8	42795	1,87E-04
19/06/1996	21/06/1996	ITA	Tuscany, Lucca, Massa, Ca ...	Flash flood	17	300	5,67E-02
01/11/1994	10/11/1994	ITA	Piemont, Ligura, Cuneo, T ...	General flood	68	17300	3,93E-03
06/07/1997	29/07/1997	MOL			9	2244	4,01E-03
24/08/1994	29/08/1994	MOL	Hancesti, Telenesti, Stra ...	General flood	47	25000	1,88E-03
21/12/1993	31/12/1993	NET	Limburg and Gelderland Pr ...	Flash flood	1	13000	7,69E-05
01/06/1995	14/06/1995	NOR	Lillestroem (Gudbransdal, ...	General flood	1	4000	2,50E-04
23/07/1998	27/07/1998	POL	Kedzko region	General flood	9	1200	7,50E-03
03/07/1997	09/08/1997	POL	Katowice, Opole, Walbrzyc ...	General flood	55	224500	2,45E-04
08/01/1996	08/01/1996	POR	Central and North Regions ...	Flash flood	10	1050	9,52E-03
09/07/1999	16/07/1999	ROM	Northern and western	General flood	15	4362	3,44E-03
22/06/1999	16/07/1999	ROM		General flood	19	4671	4,07E-03
15/06/1998	30/06/1998	ROM	Bacau, Vaslui, Vrancea (N ...	General flood	31	12000	2,58E-03
04/07/1997	09/08/1997	ROM	Alba, Arad, Bihor, Bistri ...	General flood	20	122320	1,64E-04
28/12/1995	07/01/1996	ROM	Transylvania, Moldova, Ma ...	General flood	2	5000	4,00E-04
29/07/1991	30/07/1991	ROM	Bacau, Suceava, Neamt, On .	General flood	108	15000	7,20E-03
18/02/1998	07/03/1998	RUS	Coast of Azov Sea to Kras ...	General flood	1	88000	1,14E-05
16/05/1998	06/06/1998	RUS	Sakha-Yakutia region (Sib ...	General flood	13	78600	1,65E-04
15/04/1997	17/04/1997	RUS	Krasny (Akskaisky region) ...	General flood	2	500	4,00E-03
01/08/1996	25/08/1996	RUS	North Primorye, Southern ...	Flash flood	4	14000	2,86E-04
05/08/1994	08/08/1994	RUS	Bashkortosan (Ural mounta ...	General flood	20	1000	2,00E-02
17/03/1994	22/03/1994	RUS	Volga delta (Kalmykia rep ...	General flood	7	1000	7,00E-03
17/09/1994	26/09/1994	RUS	Olginskiy, Lazovskiy (Pri ...	General flood	18	775429	2,32E-05
01/03/1994	01/03/1994	RUS	Kurgan, Belozyorsk (Urals ...	General flood	1	10204	9,80E-05

00/12/1993	00/12/1993	RUS		General flood	13	7800	1,67E-03
13/06/1993	17/06/1993	RUS	Districts of Serov and Kr ...	General flood	125	6953	1,80E-02
00/07/1999	00/07/1999	S_M	Belgrade, Podunavlje, Sum ...	General flood	11	70678	1,56E-04
22/06/1999	01/07/1999	SLO	Southwest, Northern and C ...	General flood	2	36148	5,53E-05
20/07/1998	24/07/1998	SLO	Sabinov, Presov districts ...	General flood	54	11667	4,63E-03
28/09/1997	01/10/1997	SPA	Alicante, Almeria, Murcia ...	General flood	5	400	1,25E-02
22/12/1996	24/12/1996	SPA	Huelva, Matalascanas, Sev ...	General flood	1	4000	2,50E-04
08/11/1998	08/11/1998	UKR	Tyachev, Rahi, Vinogradi, ...	General flood	18	24570	7,33E-04
20/12/1993	24/12/1993	UKR	Zakarpattya oblast (Tyach ...	General flood	5	25000	2,00E-04
25/07/1993	12/08/1993	UKR	Thearea, Rovno (Northern ...	General flood	4	300000	1,33E-05
09/04/1998	10/04/1998	U K	Norhtampton, Worcestershi ...	General flood	5	300	1,67E-02
07/12/1994	12/12/1994	U K	Glasgow , Scotland	General flood	4	700	5,71E-03
20/12/1993	31/12/1993	U K		General flood	4	600	6,67E-03
1980-1989							
03/10/1988	03/10/1988	FRA	Nimes (Gard)	Flash flood	10	300	3,33E-02
00/03/1983	00/05/1983	FRA	North, East	General flood	18	212	8,49E-02
21/09/1980	21/09/1980	FRA	Central Region	General flood	6	313	1,92E-02
26/03/1988	26/03/1988	GFR	Bavaria	General flood	6	3500	1,71E-03
18/11/1983	18/11/1983	POR	Lisbon, Louros, Cascais r ...		19	2000	9,50E-03
29/12/1981	29/12/1981	POR	Lisbon		30	900	3,33E-02
04/11/1987	04/11/1987	SPA	Valencia, Murcia	General flood	5	2000	2,50E-03
25/08/1983	25/08/1983	SPA	Bilbao, Pays Basques, Nor ...		45	506000	8,89E-05
19/10/1982	19/10/1982	SPA	Valencia, Alicante		43	226600	1,90E-04
1970-1979							
00/01/1978	00/01/1978	FRA	Marseilles		3	1000	3,00E-03
08/07/1977	08/07/1977	FRA	Gers (S-west)	General flood	26	25000	1,04E-03
01/10/1977	30/11/1977	GRE	Piraeus, Athens		27	1600	1,69E-02
00/10/1977	00/10/1977	ITA	North (Po plain		16	1000	1,60E-02
07/10/1970	07/10/1970	ITA	Genoa prov.	General flood	37	1301650	2,84E-05
00/02/1979	00/02/1979	POR	N-Coast Central		4	25000	1,60E-04
00/01/1979	00/01/1979	POR	Madeira Island		19	20220	9,40E-04
00/07/1975	00/07/1975	ROM	South, N-East,		60	1000000	6,00E-05
11/05/1970	11/05/1970	ROM	East		215	238755	9,01E-04
02/08/1979	02/08/1979	SPA	Valdepenas	Flash flood	20	50	4,00E-01
00/11/1979	00/11/1979	YUG	Montenegro		22	12000	1,83E-03
1960-1969							
02/11/1968	02/11/1968	ITA	Piedmont, Asti, Biella, N ...		72	3000	2,40E-02
03/11/1966	03/11/1966	ITA	Florence, Venice		70	1300000	5,38E-05
26/11/1967	26/11/1967	PORT	Lisbon + 3 other cities		462	1100	4,20E-01
09/05/1965	09/05/1965	YUG		General flood	3	95000	3,16E-05
1950-1959							
31/01/1953	31/01/1953	BEL	Ostende	Coastal flood	11	350	3,14E-02
21/10/1953	21/10/1953	ITA	Catanzaro R. Calabria		100	4000	2,50E-02
16/10/1951	16/10/1951	ITA	Reggio Calabria		63	3500	1,80E-02
14/11/1951	14/11/1951	ITA	Po river Valley,Polesine		100	170000	5,88E-04
31/01/1953	31/01/1953	NET	Zuiderzee area	Coastal flood	2000	300000	6,67E-03